SUMMER RAINS IN NORTHEAST BANGLADESH: Onset and triggering mechanisms

SSEMUJJU MUSA

Thesis for the degree of Masters of Science in Meteorology

GEOPHYSICAL INSTITUTE
UNIVERSITY OF BERGEN
NORWAY

June 2016

My success was due to good luck, hard work, and support and advice from friends and mentors. But most importantly, it depended on me to keep trying after I had failed. —**Mark Warner**

Acknowledgment

بسم الله الرّحمن الرّحيم

First of all, I thank the Almighty Allah for the charitable time and strength, aptitude and persistence for magnificently completing my masters studies at this great institution. I could have done nothing if it was not for His Willpower.

I am indebted to my supervisor Prof. Dr. Thomas Spengler and co-supervisors Dr. Mathew Alexander Stiller-Reeve, and MSc. Aleksi Nummelin for their devoted help and professional advice that enabled me to learn a lot during this project work. Special thanks to Aleksi, who took over the responsibility of helping me when Thomas and Mathew were away for sometime on their sabbatical leave and research issues, respectively. You really did a great job in the time when matlab codes were becoming too complex for me to develop what I wanted to address.

I am grateful to all the academic staff at the Geophysical Institute at University of Bergen for the knowledge I have got from you all through the different lecture sessions and discussions. Special thanks go to Prof. Dr. Joachim Reuder for the parental care and advice you have given to me whenever I approach you. Great thanks to Assoc. Prof. Harald Sodemann and Jan Asle Olseth for always willing to help me whenever I approached you.

I would like to take this opportunity to thank all the TRACKS project Bergen members for sharing with me, and suggesting some of the issues that my thesis work should address in regards to the cores of the project. This gave me a formidable platform on which areas to stick to while working on my thesis for the benefit of the project.

Great thanks are due to my family members and relatives for the moral support, and the Government of Norway through the QUOTA Scheme for their financial support during the entire period of my Master's studies at GFI, UiB..

I wish to humbly acknowledge with sincere gratitude, all my classmates for the wonderful academic environment you shared with me during my study at Geophysical Institute, UiB. Much more thanks to Lars Andreas Selberg for always being next to me, sharing with me all the challenges we have encountered during the two years we have spent together in Bergen, and finally the discussions we have shared during the time of writing our theses in the G-Lab. You are such a good friend to me, in fact I can say that you are one in a million. I acknowledge Ståle Dahl-Eriksen for always making fun while reminding me to learn and speak Norsk. You stand to be remembered for that, Tusen takk.

Lastly, I wish to thank my parents who bore me, raised me, supported me, taught me, and showed me unending love. May the Almighty Allah reward you abundantly. Allahumah Ameen.

Dedicated

to

Hajati Shamim Namutebi Mutesasira and Abdul Mutesasira (Mr)

List of Abbreviations

4D-Var	Four-dimensional variational analysis
ATS	Arc-type precipitation systems
BMD	Bangladesh Meteorological Department
BST	Bangladesh Standard Time
CHT	Chittagong Hill Tracts
CPM	Climatological Pentad Mean
DJF	December-January-February
DRFA	Daily Rainfall Amount
ECMWF	European Centre for Medium-Range Weather Forecasts
Eq	Equation
ERA-15	ECMWF Re-Analysis 15
ERA-40	ECMWF Re-Analysis 40
ERA-Interim	ECMWF Re-Analysis Interim
FGGE	First GARP Global Experiment
GARP	Global Atmospheric Research Program
GCM	Global Circulation Model
GFI	Geophysical Institute
IA	Integrated Approach
IBT	India-Burma Trough
IFS	Integrated Forecast System
IMT	India-Myanmar Trough
IOM	Integrated Onset Matrix
JJAS	June-July-August-September

JP	Julian Pentad
LCL	Lifting Condensation Level
LFC	Level of free convection
LTS	Line type precipitation systems
MAM	March-April-May
MARS	Meteorological Archival and Retrieval System
MC	Monte Carlo
MCS	Mesoscale Convective Systems
OLR	Outgoing Long-wave Radiation
ON	October-November
OVC	Overlap Coefficient
PDF	Probability Density Function
SEAM	Southeast Asian Monsoon
STS	Scattered type precipitation systems
TRACKS	**TRA**nsforming **C**limate **K**nowledge with and for **S**ociety
TWC	Total Water Convergence
UiB	Universitetet i Bergen
USA	United States of America
UTC	Universal Coordinated Time
VarBC	Variational Boundary Condition
VIMFX	Vertically Integrated Moisture Flux

Abstract

The aim of this study is to shed light on convective triggering mechanisms around the onset of the summer rains in Northeast Bangladesh. We want to understand this rainfall since it has a large impact on the local climate, and because 25.3% of the annual rainfall in Northeast Bangladesh falls in Bangladesh summer (March - May). To do this, we first identified the onset of the summer rains for each year using Sylhet station rainfall data with a 11 mm/day pentad rainfall mean threshold and a 6-pentad algorithm developed by Stiller-Reeve et al. [2015]. Then the onset pentads were used to make lead-lag composites from the ERA-Interim reanalysis data to examine the large-scale situation prior to and after the onset. To see if there were any large transitions, we used the Monte Carlo (MC) method and the Overlap Coefficient (OVC) method to test for statistical significance of the composites.

The compositing and OVC results show that there is a large transition in rainfall amount over Northeast Bangladesh at the first pentad after the onset. This rainfall is not a result of the large scale monsoon, because the upper-level winds are westerlies during the onset of summer rains, in contrast to the upper-level easterlies of the large-scale monsoon. Instead, the atmosphere over Northeast Bangladesh is convectively unstable at lower-mid troposphere due to the presence of abundant moisture transported from the Bay of Bengal by the strong low-level winds at pentad +1. Further analysis shows that the heavy precipitation is limited to the southern slope of the windward side of the Meghalaya Plateau where Northeast Bangladesh is situated. Immediately after the onset, a cold pool of air develops over Northeast Bangladesh at 925 hPa. The results further reveal that both the dry-line and the thermal low over India are only confined to the lower troposphere below 600 hPa.

Once we had a better understanding of the large scale conditions, we continued to investigate how the diurnal cycle of several parameters change around the time of the onset. The diurnal cycles of precipitation, low-level winds, and total water convergence over Northeast Bangladesh are similar, increasing from 1800 BST and attaining their peaks between midnight and early morning. However, the diurnal variation of evaporation shows a minimum (maximum) between evening and midnight (early morning and midday), respectively.

Based on our results, we see that the conditions around the onset are favourable for several of the triggering mechanisms previously proposed in the literature: 1) orographic uplifting; 2) the nocturnal low-level jet; 3) convergence with the boundary of the cold pool of air present at 925 hPa after the onset; and 4) the dry-line and associated strong mid-upper level westerly flow. Our results also point to the sea breeze circulation mechanism which is not yet discussed in the literature. Finally, we propose that future work on summer rains over Northeast Bangladesh should be based on numerical modeling with a high resolution to fully investigate the mechanisms influencing the summer rains such that a sounding conclusion can be made about their likely causes.

Contents

Chapter 1

Introduction

Northeast Bangladesh experiences a widespread of convective processes during the summer months of March to May. These convective processes lead to heavy rains that are dominated by nocturnal rainfall [Terao et al., 2008], and show maximum convective activity at late night-early morning [Ohsawa et al., 2001]. The local people deem this rainfall important in a variety of ways among which agriculture is the central point for their livelihood. Although these heavy rains are welcomed by the local community because of their great importance, the mechanisms leading to their formation have left the research community divided. Several theories such as orographic lifting [Sanderson and Ahmed, 1979; Murata et al., 2008; Shahid, 2010; Murata et al., 2011; Fujinami et al., 2014; Hatsuzuka et al., 2014], nocturnal low-level jet [Terao et al., 2006; Sato, 2013; Fujinami et al., 2014; Hatsuzuka et al., 2014], katabatic convergence [Ohsawa et al., 2001; Basu, 2007], cold pool convergence [Kataoka and Satomura, 2005; Murata et al., 2011], dry-line [Weston, 1972; Sanderson and Ahmed, 1979; Lefort, 2013], and the Indian-Burma trough [Wang et al., 2011; Reeve, 2014] have been linked to this summer convection. However, none of these theories has been agreed upon by the research community as the main driving mechanism triggering this summer convection. This disagreement leaves us with a lot of intriguing aspects of this rainfall. It is this disagreement that motivates this research. And as the research community is still with much ambiguity and disagreement, this project comes in as a worthwhile effort to contribute to our understanding of the mechanisms that drive these summer rains in Northeast Bangladesh which are very important to the local people who depend primarily on rain-fed agriculture for food and socio-economic development. We hope this study will help us to come up with a robust description of the convective diurnal cycle in Northeast Bangladesh, which can explain at least one of the mechanisms that could be at play during these heavy rainfall events in this region. Finally, this thesis is part of the research project called '**TRA**nsforming **C**limate **K**nowledge with and for **S**ociety' (TRACKS)[1], which focuses on communities in Northeast Bangladesh, where there is high uncertainty about climate variation particularly associated with monsoon and its impacts on the community.

[1] see: http://www.uib.no/en/rg/tracks

1.1 Large-scale monsoon and summer rainfall in Northeast Bangladesh

Bangladesh ($88.05 - 92.74°$E, $20.67 - 26.63°$N) is found in the southern part of the Asian continent, surrounded mostly by India in the north, west and east, with only its southeastern border shared with Myanmar (Burma), and the Bay of Bengal in the south (Figure 1.1). It straddles the Tropic of Cancer (23.5°N), and this implies that it has a tropical monsoon climate which is characterized by wide seasonal variations in rainfall, temperatures and humidity among others. This makes Bangladesh prone to a number of natural disasters such as floods, tropical cyclones, tornadoes and storm surges that affect the country on a yearly basis. In addition, these disasters may precede further drought, high spread of water-borne diseases or ground water contamination.

Bangladesh is termed as a land of six seasons (Sadartu) namely: Summer (Grisma), Rainy Season (Borsha), Autumn (Sarat), Late Autumn (Hemanta), Winter (Shit), Spring (Basanta) [Islam, 2003]. The summer season is the first and warmest season of the year, with its first day marking the Bengali new year [Islam, 2003]. However, from a climatic point of view, Bangladesh has four distinct seasons and these are: (1) the dry winter season (December-February); (2) the pre-monsoon hot summer season (March-May); (3) the rainy monsoon season (June-September); and (4) the post-monsoon autumn season (October-November) [Shahid, 2010].

1.1.1 Climatology of large-scale monsoon

The word monsoon comes from the Arabic word *mausim* which simply means season. Monsoon is defined as the large-scale wind system that covers most parts of the Indian ocean and the adjoining landmasses, blowing from southwest half the year and from northeast during the other half [Gadgil, 2003]. The seasonal reversal of the wind direction is believed to begin in May and brings moisture from the warm waters of the tropical Indian ocean to the South Asian continent through southwesterlies. The monsoon system is strongly linked to wind and this is why earlier studies such as [Ramage, 1971, 1995] about monsoon considered wind as the only meteorological parameter to describe the monsoon onset. But the definition of monsoon has now somewhat changed, whereby monsoon is widely used to refer to both tropical and subtropical seasonal reversals in atmospheric circulation and its associated precipitation (e.g.,Trenberth et al. [2000]; Trenberth [2011]).

The large-scale monsoon is believed to arise from the annual reversals in the heating and temperature gradients between the continental regions and the adjacent oceans with the progression of the seasons [Webster et al., 1998; Trenberth et al., 2006]. This implies that the major driving mechanism of the large-scale monsoon system is regulated by the differential heating of the land and the adjacent ocean, which results from their widely differing heat capacities. As the latitude of maximum insolation changes meridionally due to earth's rotation, seasonal reversing land-ocean temperature contrasts develop. This

in turn, leads to seasonally reversing meridional temperature gradients and tropospheric circulations, and migration of the large-scale precipitation regions. This same process explains how the large-scale Asian summer monsoon develops, with contrasting temperature gradients between the Asian continental land mass and the oceans to its south.

The summer monsoon is best known for its regular occurrence from June to September every year, southerly/southwesterly low-level flow, mid-upper tropospheric easterlies, and the irregular variations in the mean seasonal rainfall amount on a yearly basis [Lawrence, 1999]. Strong monsoon years are characterised by excess seasonal rainfall which leads to floods, while weak monsoon years are characterised by deficient seasonal rainfall which lead to drought. Even within the monsoon season, there is a considerable variation both in space and time, in the rainfall over the Indian subcontinent. These intraseasonal variations are characterised by the "active" periods of high rainfall and the "break" periods with little or without any rainfall, and each phase lasts for a few days [Lawrence, 1999]. The intraseasonal and interannual variability of the summer monsoon has a tremendous socio-economic impact on the country especially in the fields of agriculture and health, whereby it can lead to low crop yield, drought, floods, high spread of water-borne diseases, and loss of life among others.

Before the large-scale monsoon onset, Bangladesh and entire south Asia is dominated by the dry winter monsoon circulation, which is characterised by low-level Northeasterlies, and upper-level tropospheric westerlies. The lower tropospheric circulation is a result of high surface pressure over the relatively cold Asian land mass and the low pressures over the relatively warm Indian and tropical Pacific oceans, while the upper-level tropospheric circulation is a result of the presence of prevailing north-south thermal gradient through the troposphere. During the large-scale monsoon onset, the low-level circulation reverses to southerly/southwesterly circulation over Bangladesh, and upper-level tropospheric winds reverse from westerlies to easterlies in response to the change in the meridional temperature gradient over the Asian continent [Zhang and Wang, 2008]. Hence, large-scale monsoon low-level winds are southerly/southwesterly from May-September, and reverse direction to northeasterly from November-March.

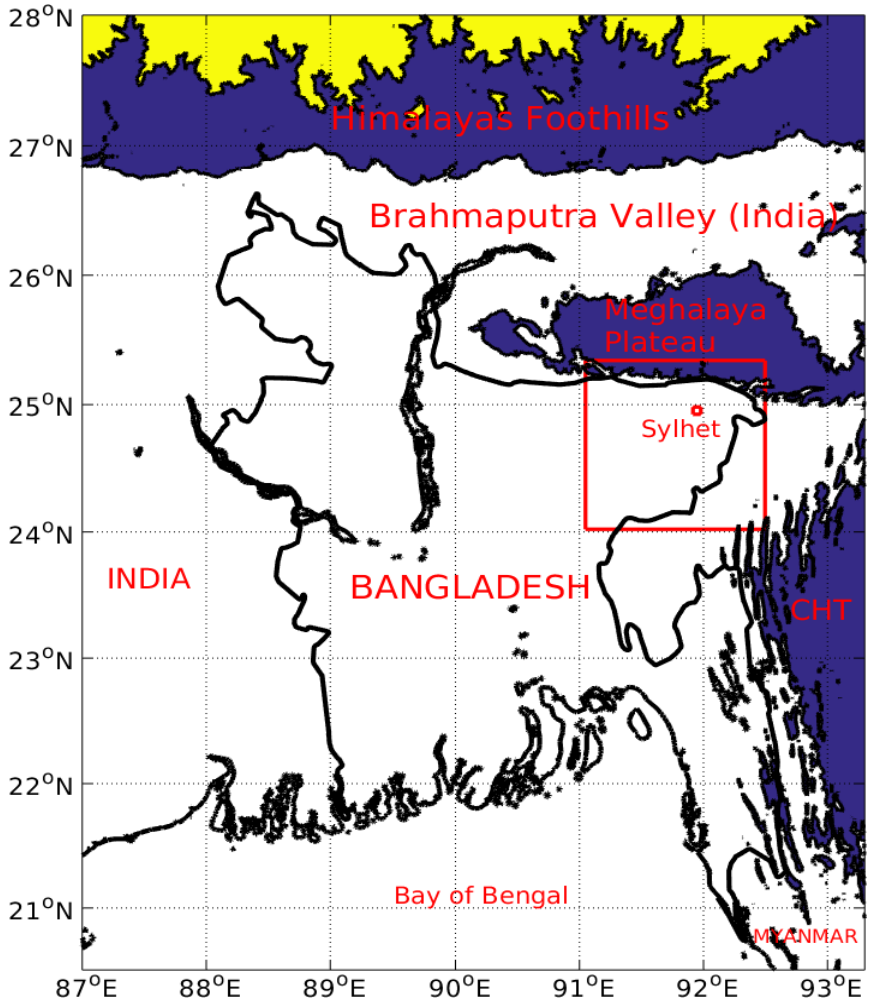

Figure 1.1: Map of Bangladesh and its surrounding geography. The elevation above 500 m is shaded blue, while elevation greater than 3500 m is shaded yellow. The red square box indicates Northeast Bangladesh, while 'CHT' stands for Chittagong Hill Tracts.

1.1.2 Monsoon rainfall over Bangladesh

Bangladesh is one of the rainiest countries in the world [Matsumoto, 1989], and receives approximately 6000 mm of its rainfall during the monsoon months of June-September [Matsumoto et al., 1996]. These monsoon rains received in Bangladesh are caused by weak tropical depressions that are brought from the Bay of Bengal into Bangladesh by the wet monsoon winds [Shahid, 2010]. This huge amount of rainfall in Bangladesh is useful in the formation and maintenance of the strong summer monsoon circulation through the release of latent heat due to condensation[Li and Yanai, 1996; Xie et al., 2006]. The rainy season in Bangladesh is divided into three periods namely: pre-monsoon (March-May), monsoon (June-September), and post-monsoon (October-November) [Islam and Uyeda, 2007; Shahid, 2010]. About 20.0%, 62.4%, 15.5%, and 2.1% of the annual rainfall in Bangladesh occurs during the pre-monsoon, monsoon, post-monsoon, and winter periods, respectively [Islam and Uyeda, 2005]. The pre-monsoon rainfall is characterised by short lifetime and high intensity, while monsoon rains are more continuous but less intensive

[Islam and Uyeda, 2005]. The rainfall over Bangladesh varies both in space and time, and increasing from west to east across the country with the northeastern part receiving the highest rainfall amount annually (Figure.1.2), [Shahid, 2010].

The monsoon precipitation systems in Bangladesh are categorized into three types according to their shape, and these are; arc-type, line type, and scattered type precipitation systems [Rafiuddin et al., 2010]. The arc-type precipitation systems (ATS) are small, fast moving, and dominant in pre-monsoon months over Northeast Bangladesh [Rafiuddin et al., 2010]. They propagate southeastward, and usually mature in Northeast Bangladesh, hence not reaching the southeastern part of the country [Islam and Uyeda, 2007; Rafiuddin et al., 2010]. On the other hand, the scattered type systems (STS) are large stationary or slow moving systems, that dominate over southern, eastern and northern parts of Bangladesh during the monsoon months, with their propagation being northeastward, northwestward, or southeastward [Rafiuddin et al., 2010]. The line type systems (LTS) occur in both pre-monsoon and monsoon months, with their appearance frequency decreasing with the monsoon progression. The above three precipitation systems (i.e., ATS, STS, and LTS) are responsible for the rainfall that is received in Bangladesh. In the monsoon season, the STSs are generated by the abundant moisture supply from the Bay of Bengal that is brought by the low-level southerly/southwesterly monsoon winds and blocked by the Meghalaya Plateau and the high-elevated topography in the eastern part of Bangladesh [Rafiuddin et al., 2010]. On the other hand, the pre-monsoon ATSs are associated with an outburst of severe local convective storms that develop in northwest Bangladesh and propagate eastward [Rafiuddin et al., 2013]. These severe convective storms are called nor'westers (Kal-baishakhi in Bangladeshi) by the local people since they come from northwest [Rafiuddin et al., 2010, 2013]. Such severe storms not only produce thunder, lightning, hail, wind gusts, and tornados, but also produce intense rains over small areas and their consequences range from extensive agricultural and property damage to loss of human life [Rafiuddin et al., 2013].

While most studies on rainfall variability over Bangladesh and entire Indian subcontinent have been centered on the monsoon season, it is important to note that the heavy rains in Northeast Bangladesh begin earlier before the actual monsoon season [Kripalani et al., 1996; Pant and Kumar, 1997]. This season is called the summer season in Bangladesh, or pre-monsoon [Islam and Uyeda, 2007]. The early onset has been seen in a number of publications by several climate scientists (e.g.,Ashfaq et al. [2009]; Matsumoto [1997]), in their attempts to define monsoon onset (see Figure 1.3). In this figure, Matsumoto [1997] found an early onset of the rainy season in Northeast Bangladesh on 8^{th} April than elsewhere in the country, while Ashfaq et al. [2009] who even applied a cut-off date at Julian pentad 28 (around 16-21 May) to imply that no onset date appeared before this date, still found the earliest onset on 21^{st} May over Northeast Bangladesh. And because this rainfall occurs in the summer season before the large-scale monsoon season over Bangladesh starts, we therefore refer to these rains as *summer rains* or *summer rainfall* hereafter.

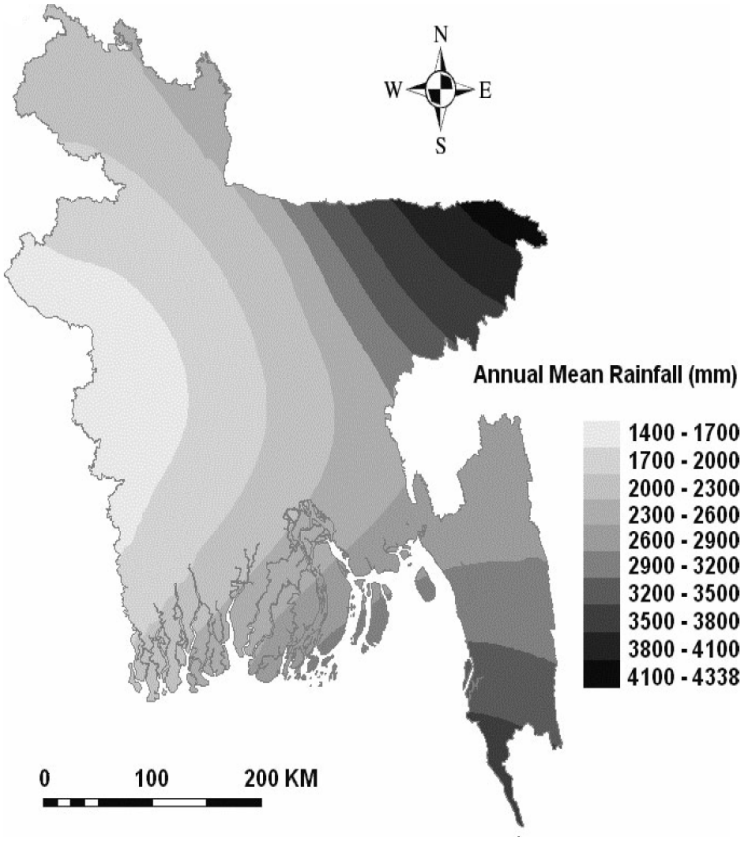

Figure 1.2: Spatial distribution of rainfall in Bangladesh. Adapted from [Shahid, 2010]

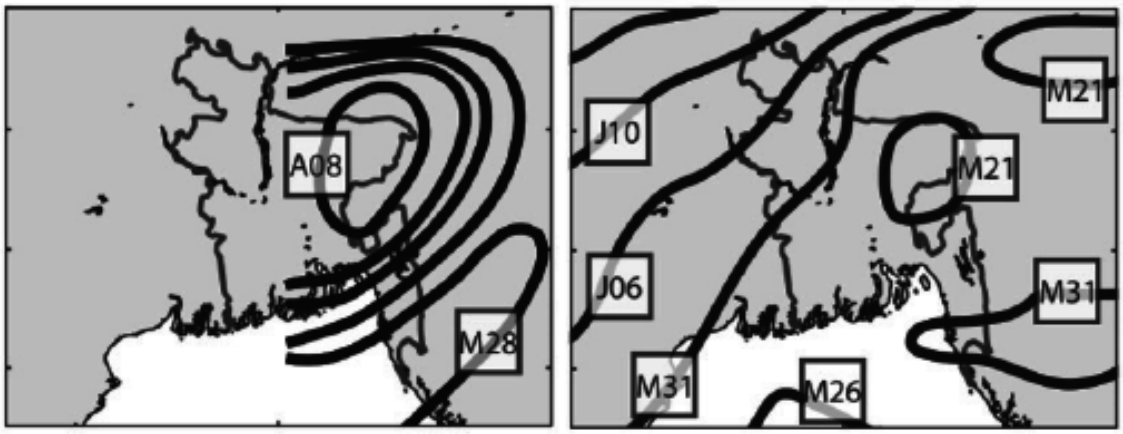

Figure 1.3: Average monsoon onset and its progression across Bangladesh as defined by: (left) Matsumoto [1997], and (right) Ashfaq et al. [2009]. These figures are adapted from Reeve [2014]; with A-April, M-May, J-June, and the number attached to them indicate the date; e.g., A08 indicates 8th April.

Northeast Bangladesh receives plenty of summer rainfall starting from April, and increases within the season until when the large-scale monsoon starts in June all over the country (Figure 1.4). This summer rainfall is estimated to contribute about 20%- 30% of the total rainfall received annually in Bangladesh [Ahmed and Kim, 2003]. On average, observation data from Sylhet station in Northeast Bangladesh shows that the region receives 3916.9 mm of precipitation per year, but the rainfall amount received can be higher than 5000 mm for wet years and lower than 3000 mm for dry years (Figure 1.5). The precipitation

climatology of Northeast Bangladesh shows that on average, the high rainfall amount over the region is received starting from March and increases onwards until June when it peaks up, and thereafter starts to decrease from July to December (Figure1.6). On average, June is the wettest month with 774.8 mm while the least precipitation is received in December with 8.4 mm (Figure 1.6). The analysis further reveals that Sylhet has an average of 149.0 rain days in a year, with the most rain occurring in July (25.0 rain days), and the least rain occurs in December with 1.0 rain day. In terms of temperature, the Sylhet region shows little variance in temperature throughout the year with an average of 23.9°C, with the warmest being August (27.8°C) and coolest being January (17.8°C) on average [http://www.weatherbase.com].

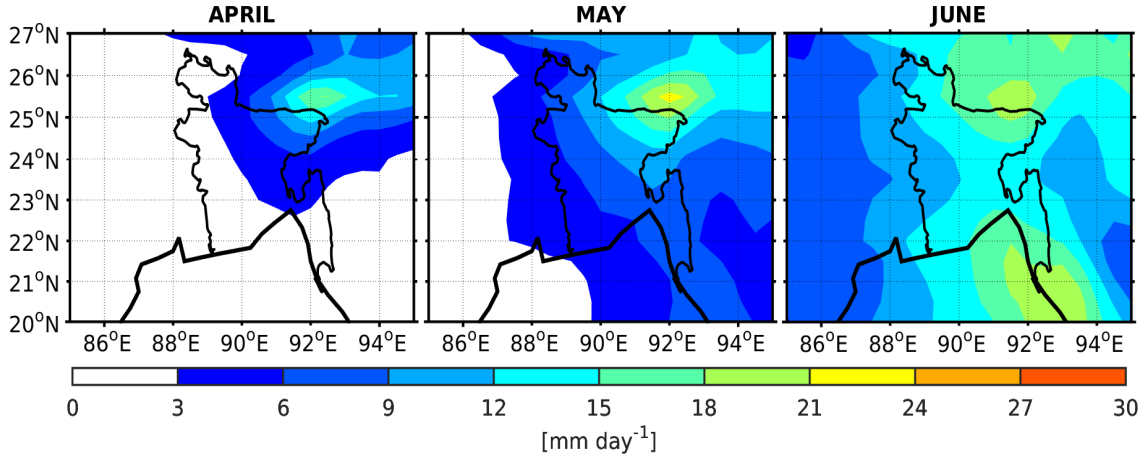

Figure 1.4: Average daily rainfall for April, May, and June (1979-2010) from European Centre for Medium-Range Weather Forecasts (ECMWF) Re-Analysis Interim (ERA-Interim) data set [Dee et al., 2011]. Extensive regions especially northeastern Bangladesh receive rainfall above 9 mm/day from April onwards.

The diurnal variation of precipitation in Northeast Bangladesh is characterised by nocturnal rainfall that peaks during the late night-early morning hours [Ohsawa et al., 2000; Kataoka and Satomura, 2005; Sato, 2013]. The late night-early morning rainfall maximum is believed to be strongly associated with the precipitation systems that are triggered around the southern foot of the Meghalaya Plateau, which later move southwards [Kataoka and Satomura, 2005; Hatsuzuka et al., 2014]. Sato [2013] associated the late night-early morning rainfall maximum to the diurnal cycle of a low-level jet that develops over windward areas of the Meghalaya Plateau during the late night-early morning hours. However, there is no clear conclusion about the causes of the nocturnal rainfall over Northeast Bangladesh. Hence, it remains a point of interest for the research community to understand the processes that lead to the development of the summer rainfall systems in Northeast Bangladesh and their associated characteristics.

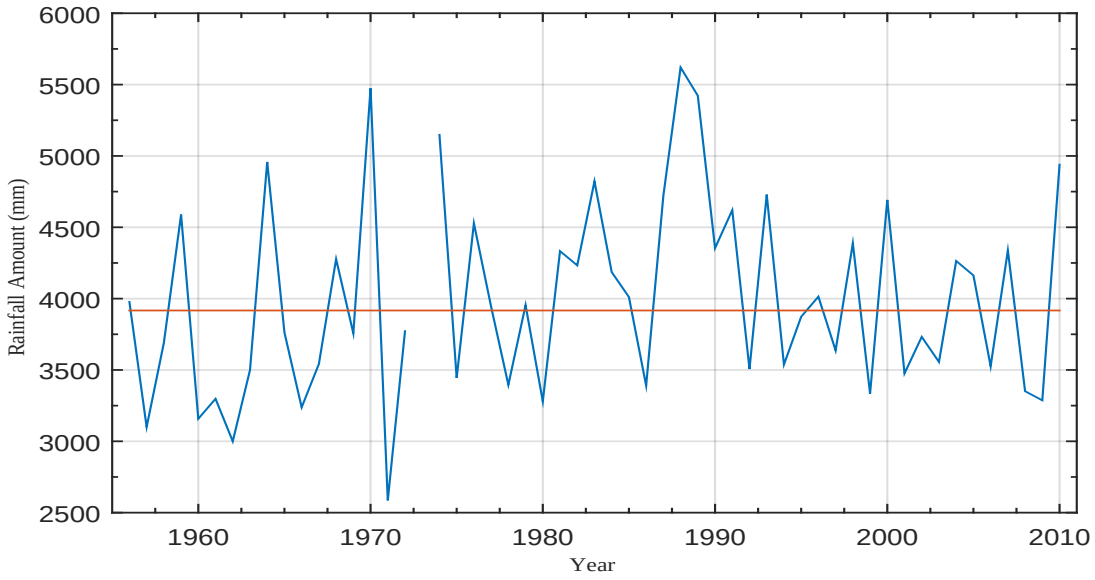

Figure 1.5: Total annual rainfall amount received in Sylhet for the period 1956 - 2010. The reddish-brown line indicate the average annual rainfall for this study period, and the gap indicate missing data for the year 1973.

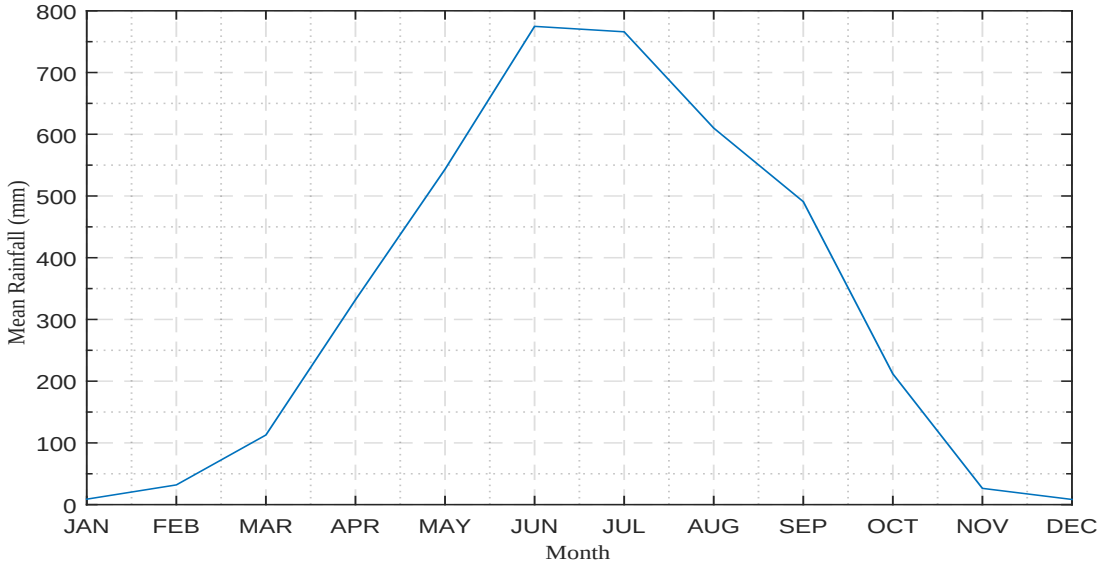

Figure 1.6: Precipitation climatology of Sylhet region (mm month^{-1}) showing the early rainfall onset in March - May for the period 1956-2010.

1.2 Theories of summer rains

A multitude of researchers (e.g., Weston [1972]; Sanderson and Ahmed [1979]; Ohsawa et al. [2001]; Kataoka and Satomura [2005]; Terao et al. [2006]; Murata et al. [2008]; Ghosh et al. [2008]; Murata et al. [2011]; Lefort [2013]) have come up with different theories to explain the likely causes of summer rains in and around Northeast Bangladesh. Most of these theories relate to the orography around Northeast Bangladesh (e.g., Sanderson and Ahmed [1979]; Murata et al. [2008, 2011]). Other theories (e.g., Ohsawa et al. [2001]; Terao

et al. [2006]; Sato [2013]; Hatsuzuka et al. [2014]) try to explain the diurnal convective maximum. In this section, we review these theories in detail.

1.2.1 Orographic lifting

The role played by elevated topography (mountains) in modulating weather and climate of a region is well known, right from the local people living in those vicinities to climate scientists all over the world. This can not be overlooked especially if someone is researching on a weather phenomenon in a region like Northeast Bangladesh, that is surrounded by elevated topography of the Meghalaya Plateau to its north, and the Chittagong Hill Tracts to its east (see Figure 1.1). In the Indian subcontinent, Bangladesh is surrounded by India in its west, north and east, and the effects of elevated topography in south Asia on monsoon is heavily felt. These mountains effectively block the low-level and mid-level atmospheric flow, and hence significantly alter the circulation from its direction it would have taken without mountains present. For example, the large massif of the Himalayas presents a major obstacle to the atmospheric flow, blocking both the prevailing cold and dry westerlies of the extratropics north of the Himalayas and the warm southerly moist flow that comes from the tropics. The influence of topography on summer convection and precipitation was assessed by Xu et al. [2009], and found that both summer convection and precipitation modulate with variations in topography with much precipitation being received in the high terrain and their slopes, while the plains receive less precipitation.

During the Bangladesh summer months of March - May, the elevated topography around northern and northeastern Bangladesh (i.e., the Himalayas and Meghalaya Plateau) are strongly heated by summer insolation, thereby creating a mid-tropospheric heat source. The elevated sensible heat source and the radiative cooling in the surrounding environment (e.g.,Brahmaputra Valley in India and the low-lands in northeast Bangladesh) maintain a strong temperature gradient that may drive a vigorous ascent in the region and a strong descent in the surrounding regions. This local circulation can interact with the convectively-driven circulation in the monsoon region, hence influencing the early onset of the rainy season as well as its development across northeastern Bangladesh.

Hahn and Manabe [1975] simulated the Indain monsoon with a general circulation model (GCM) to investigate the influence of topography on summer convection. They conducted two model experiments; one with a realistic representation of the mountains, and the other without any mountains. They found that the presence of the Himalayan mountains effectively maintains the Asian low pressure system in the summer by allowing warm and moist air from its north to be drawn southwards to fill the low pressure system over south Asia. The net effects were found to strengthen the Indian monsoon and produce high rainfall well into the subcontinent mechanically/dynamically through orographic uplifting of warm moist air to higher altitudes which are colder. Thermodynamically, when the temperatures become colder, air can no longer hold moisture in the clouds, and hence precipitation occurs as the air moves southwards causing the summer rains. Both effects

were also found in a GCM study by Zheng and Liou [1986], verified in an analysis of observations made during the First GARP (Global Atmospheric Research Program) Global Experiment (FGGE) experiment [He et al., 1987], and later using the FGGE data by Yanai and Li [1994]. Model experiments by Kutzbach et al. [1989]; Ruddiman and Kutzbach [1989] also confirmed the role of topography, particularly the elevated heating effect, in changing the climate of south Asia from one with little or no monsoon to one in which a vigorous monsoon occurs each summer as observed today.

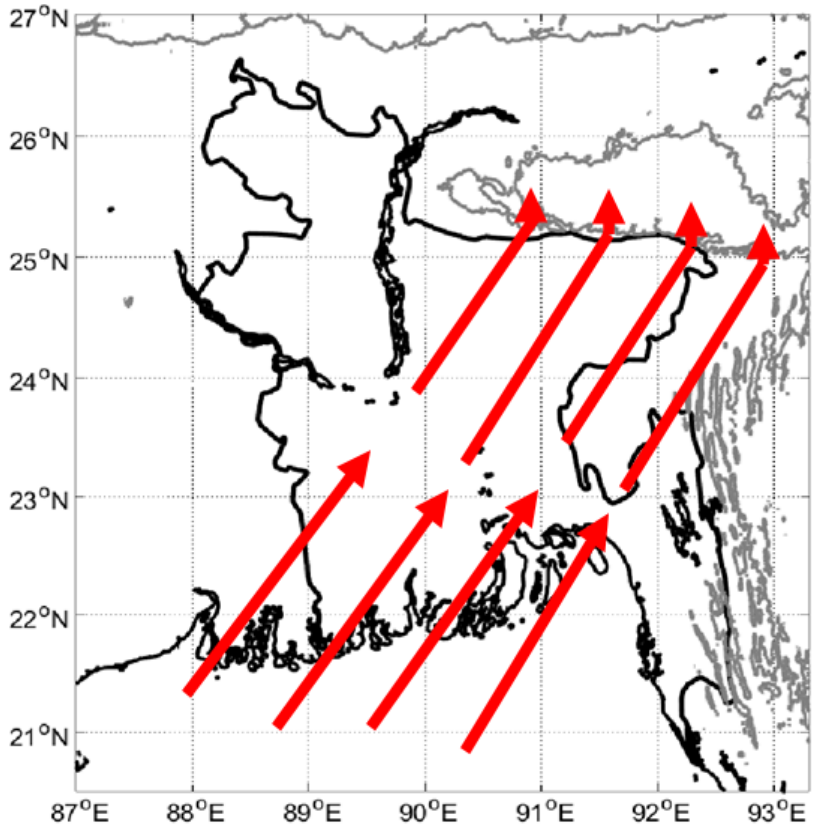

Figure 1.7: Figure illustrating the behavior of the low-level winds across Bangladesh during the summer months. The southerly/southwesterly winds bring warm moisture from the Bay of Bengal towards the Meghalaya Plateau which blocks them and forces them to rise. The Meghalaya plateau and other elevated land above $500m$ is marked with grey contour.

In Bangladesh, the effects of the surrounding elevated topography are received in a similar fashion. There exists a heat low in India just along the western border of Bangladesh which results from strong heating of the land mass during the pre-monsoon months of March-May [Reeve, 2014; Turner and Annamalai, 2012]. This heat low has a strong effect on the circulation over the western coast of the Bay of Bengal and Bangladesh. The winds change direction from northwesterlies to southwesterlies and transport moisture from the western coast of the Bay of Bengal across Bangladesh and towards Northeast Bangladesh. As these warm moist winds reach the Meghalaya Plateau, which is on the northern tip of Northeast Bangladesh, they are blocked and forced to rise over the plateau (Figure 1.7). This uplift by the Meghalaya plateau results in rising moist air triggering convection on the windward side of the mountain where Northeast Bangladesh is located [Hatsuzuka et al., 2014].

While topographic uplifting of the southwesterly flow by the Meghalaya Plateau and other surrounding mountains is considered by many researchers (e.g.,Sanderson and Ahmed [1979]; Murata et al. [2008]; Shahid [2010]; Murata et al. [2011]) as one of the major factors for triggering convection and causing summer season heavy precipitation over Northeast Bangladesh, results from numerical experiments for monsoon heavy precipitation by Kataoka and Satomura [2005] revealed that the katabatic mountain winds do not play a major role in the formation of the nocturnal convective systems over Northeast Bangladesh. This means that this theory alone can not explain the occurrence of nocturnal rainfall which has a late night-early morning maximum. Hence, there must be something else that influences summer season convection over this region.

1.2.2 Nocturnal Low-level Jet

As the strong low-level southerly/southwesterly jet from the Bay of Bengal blows across Bangladesh, its speed may increase or decrease along the way. This in the end may affect the intensity of topographic lifting. The study on diurnal wind variation by Terao et al. [2006] using rawinsonde and pilot balloon observations for 2000 and 2001 showed strong acceleration of low-level winds below 900 hPa from evening to midnight. This strong low-level jet is what is termed as the *nocturnal low-level jet*. It occurs at a time when daytime convection ceases Reeve [2014]. The nighttime lower tropospheric southwesterly jet over Bangladesh was also confirmed by Kataoka and Satomura [2005] during their simulations of the diurnal variation of precipitation over Northeast Bangladesh in the active period of June 1995.

When the low-level jets intersect with fronts or outflow boundaries or even interact with mesoscale convective vortices, they often lead to initiation and sustenance of the long-lived mesoscale convective complexes which are capable of producing overnight heavy rains and flash floods [Markowski and Richardson, 2010]. The nocturnal low-level jet is famous for production of heavy nighttime rainfall maxima during the warm season [Markowski and Richardson, 2010], and indeed this was the case found out by Terao et al. [2006] during their analysis when the increase in the strength of nocturnal low-level jet corresponded with the increase in the intensity of precipitation in northeastern Bangladesh. Thus, Terao et al. [2006] concluded that the nocturnal jet was responsible for the development of the convective systems that cause the late night-early morning rainfall peak in Northeast Bangladesh. However, they also concluded that some other mechanisms could play some role in formation of this convection. Sato [2013], Hatsuzuka et al. [2014], and Fujinami et al. [2014] also confirmed the influence of nocturnal low-level jet on enhancing nocturnal precipitation around the Meghalaya Plateau and Northeast Bangladesh. They found a strong association between the nocturnal low-level jet and the late night-early morning rainfall maximum over Northeast Bangladesh.

1.2.3 Large-scale flow convergence with Katabatic winds

Katabatic winds are dense cool winds that flow downslope of the mountain at night as gravity current. They can also be termed as mountain breezes or nocturnal valley winds because of the strong affection to the mountain at night. During the daytime in the summer months of March-May, the Meghalaya Plateau is heated more by the strong insolation from the sun. And during the night, the slopes of the mountain cool. This cool surface cools the adjacent air over it to become dense. The denser air then flows downslope the mountain as a gravity current. This process results in katabatic winds, which can also be termed as mountain breeze or nocturnal valley winds. Researchers e.g.,Ohsawa et al. [2000, 2001] link katabatic wind flow to midnight-early morning rainfall maximum in Northeast Bangladesh.

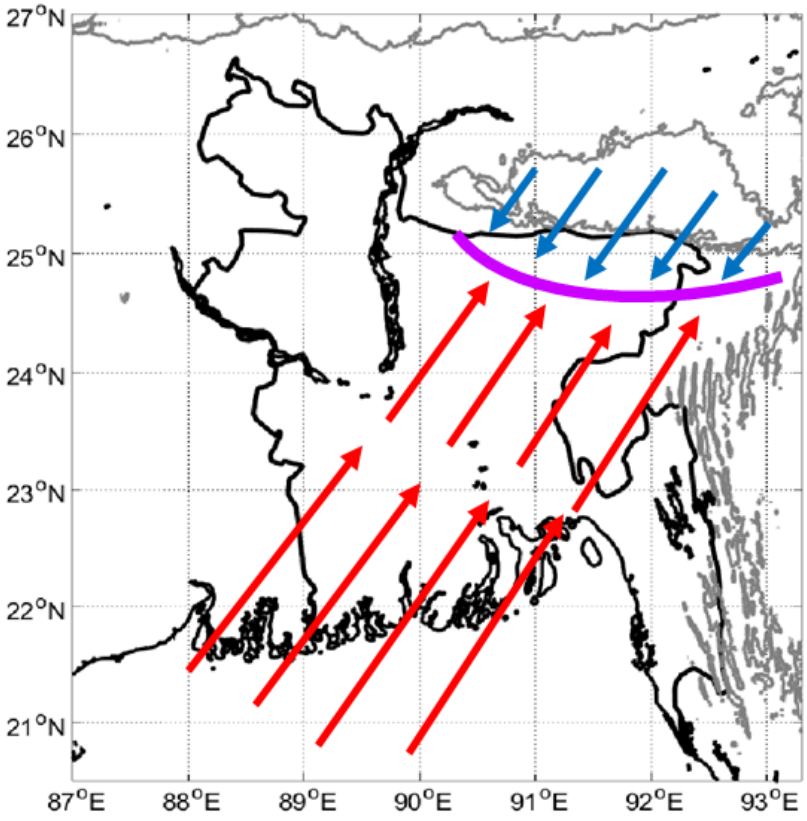

Figure 1.8: Figure illustrating how the warm moist low-level southerly/southwesterly flow (red arrows) from the Bay of Bengal converge with the cooler katabatic winds from the Meghalaya (blue arrows) to trigger nocturnal convection. The magenta line shows the convergence of katabatic and southwesterly winds.

In 1974, Prasad [1974] in his study around the Brahmaputra valley found the existence of late night-early morning rainfall maximum and he attributed this rainfall maxima to low-level convergence of mountain breezes from both sides of the Himalayas (north) and the Meghalaya Plateau (south). Later, Ohsawa et al. [2001] found the late night-early morning rainfall maxima along the foothills of the Himalayas and on the southern side of the Meghalaya Plateau. Their results suggested that mountain breeze from one side was sufficient to cause the low-level convergence during the nighttime, most especially when

the prevailing winds are blowing against the mountain breeze. They later concluded that land and mountain breezes have the possibility to trigger convection during the late night-early morning hours. And this happens to be the case in Northeast Bangladesh, which is located to the south of the Meghalaya plateau. According to Reeve [2014], the late night-early morning convective maximum could be triggered by the convergence of cool nocturnal valley (katabatic) winds on the slopes of Meghalaya (blue arrows in Figure 1.8) and prevailing warm moist monsoon southwesterlies from the Bay of Bengal (red arrows in Figure 1.8).

The combination of Katabatic wind theory and nocturnal low-level jet looks robust in answering the intriguing aspect of summer rains in Northeast Bangladesh as it gives both the location and timing of the convective maximum in the diurnal cycle [Reeve, 2014]. However, after simulating an active precipitation period of 14-21 June 1995 over northeast Bangladesh, Kataoka and Satomura [2005] suggested that the katabatic mountain winds do not play a major role in the formation of the nighttime convective systems over northeast Bangladesh, and instead recommended a further look at the lag of rainfall peak against the lower tropospheric jet maxima. Hence, this leaves the question of what theory completely explains the *summer rains* phenomenon in Northeast Bangladesh still unanswered.

1.2.4 Cold Pool Convergence

A cold pool can be defined in a number of ways and these include: 1) a block/region of cold air, often cooler than the surrounding air that is used to show the stability of air. That is, low-level cold pools are often regions of relatively stable air, while cold pools aloft represent regions of relatively low stability; 2) a topographic depression, such as a valley or basin filled with cold air[2]. That is, the cold air is heavy, and settles at the bottom of the depression which implies that it can remain stagnant, hence being trapped by the surrounding higher terrain which can result into long periods of fog depending on the amount of moisture in the air; and 3) one of the most distinctive features of a well-organized mesoscale convective systems (MCS), that develops at lower levels beneath or just behind the strongest convection [Corfidi, 2003]. Cold pools represent the collective outflow of individual convective cells and the negative buoyancy of parcels within or beneath the convection. The cold pool can be strengthened through sublimation and/or melting and evaporation of precipitation falling through unsaturated air, precipitation drag, and vertical perturbation pressure gradients [Corfidi, 2003]. In the periphery of a cold pool, there is an outflow boundary (gust front) which is marked by low-level convergence and ascent [Corfidi, 2003]. Hence, this results in gust fronts being often suitable for the development of new convective cells.

Most of the above definitions have been applied by researchers to highlight how convection is triggered in Northeast Bangladesh. For example, Kataoka and Satomura [2005]'s simulations of the diurnal cycle of precipitation from June 17, 1995 featured a cold pool that

[2] http://amsglossary.allenpress.com/glossary/search?id=cold-air-pool1

was formed by precipitation on the early morning of June 16 and maintained by daytime evaporative cooling by precipitation in a valley or basin between the Meghalaya Plateau and the eastern mountains. This cold pool lifted the low-level moist southwesterly air mass to a level of free convection (LFC) at about 850 hPa below the height of the Meghalaya Plateau and eventually triggered precipitation over Northeast Bangladesh. Although Kataoka and Satomura [2005]'s simulations were carried out for the monsoon season, Murata et al. [2011] also found the existence of a cold pool over Northeast Bangladesh during daytime in the pre-monsoon month of April 2010. They suggested that this cold pool was a result of the nocturnal precipitation. Recently, Reeve [2014] illustrated by giving an example, how cold pool convergence can trigger convection in Northeast Bangladesh. He showed how the cold air can be trapped over northeastern Bangladesh thereby resulting into an outflow boundary along which the moist southwesterly air mass can be forced to rise and hence, resultant convection (see Figure 1.9).

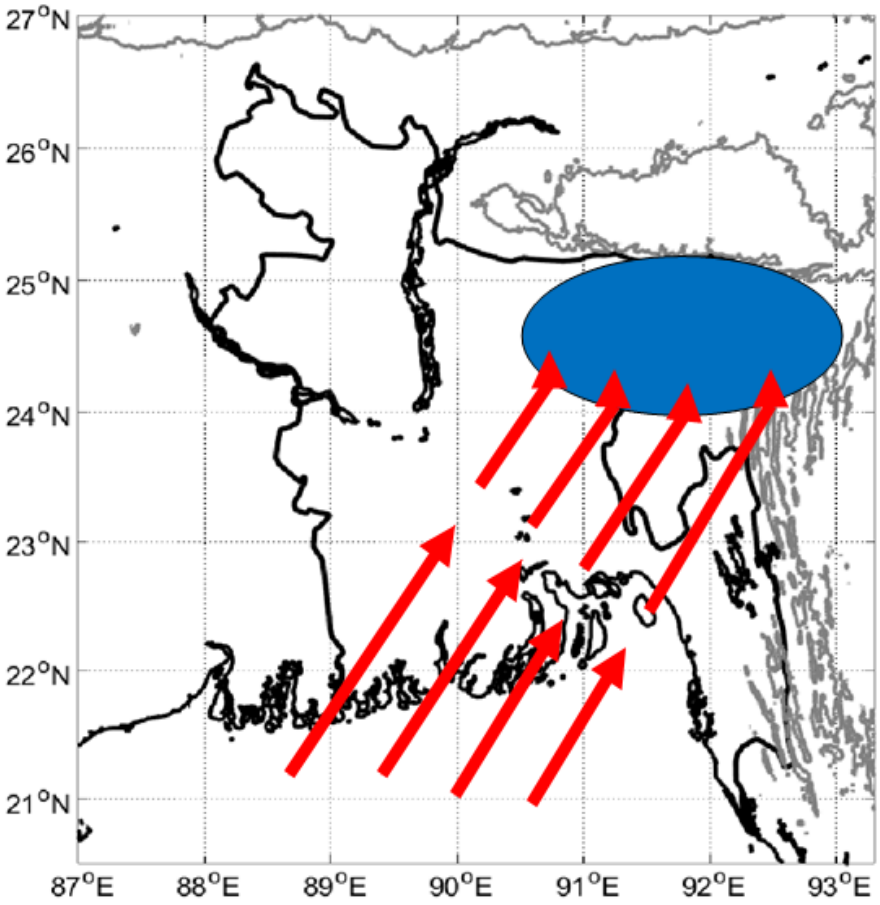

Figure 1.9: The blue shading shows a cold pool that forms over Northeast Bangladesh as a result of topographic depression. The cold pool causes an increase in the low-level pressure. When the warm moist less dense low-level southwesterly air mass (red arrows) converges with the cold denser air mass (blue shading), it is forced to rise, thereby triggering convection

1.2.5 Dry-line convection

Dry-lines are air mass boundaries that separate moist, maritime tropical air from dry, continental tropical air, and are commonly found in the Great Plains region of the United

States of America (USA) during the spring and early summer [Markowski and Richardson, 2010]. Many convective storms are frequently initiated along them during this period. Although we find less work done on them on the Indian subcontinent of which Bangladesh is part, this discontinuity between the warm moist air over Bangladesh and the hot dry air over India manifests during the pre-monsoon months of March-May.

In 1972, Weston [1972] located the dry-line in northeast India just west of Bangladesh during the pre-monsoon months of March-May and even went further to design a dynamical model that illustrated how the circulation within this moist air boundary produced conducive conditions for convection to be initiated near this dry-line. Later, Sanderson and Ahmed [1979] located this dry-line directly across Bangladesh, and most recently Lefort [2013] also recognised this dry-line in an operational forecasting perspective. He pointed out a similar propagation of this dry-line to those discerned in USA.

In a simulation of an arc-shaped convective systems of 26 April 2002 by Rafiuddin et al. [2013], the dry-line kind of structure was evident. This dry-line occurred in India near northwestern Bangladesh and caused convective instabilities that resulted in the development of convective systems, which later moved eastward towards Northeast Bangladesh. Rafiuddin et al. [2013] suggested that the convective instabilities were a result of southerly moist air inflow that was intensified by moderate to strong westerlies in the mid troposphere.

Recently Reeve [2014] illustrated how the dry-line seen over India, near western Bangladesh propagates, and its possibility in triggering convection over Northeast Bangladesh. The propagation of the dry-line is illustrated in Figure 1.10. In this figure, the red line which is the dry-line propagates westward during the night as the low-level flow mostly from the Bay of Bengal (shown with blue arrows) increases, resulting in a decrease of convective mixing. During the daytime the dry-line reverses its direction of propagation eastward as the low-level moist flow from the Bay of Bengal becomes weaker compared to the hot dry continental air mass from India, and hence, a lot of mixing takes place. This implies that the dry-line triggers convection closer to the west of Bangladesh during the late afternoon as suggested by Ghosh et al. [2008]. But this late afternoon convection seems not to explain the midnight-early morning convective maximum that is seen in Northeast Bangladesh and hence, something else might be in play. Usually systems triggered along the dry-line propagate in south-eastward direction [Reeve, 2014], and because they come from northwest, the local people often call them nor'westers (Kal-baishakhi in Bangladeshi). It is believed that these systems reach Northeast Bangladesh towards late-night or early morning [Reeve, 2014], and hence they have an affection to the late night-early morning maximum in Northeast Bangladesh.

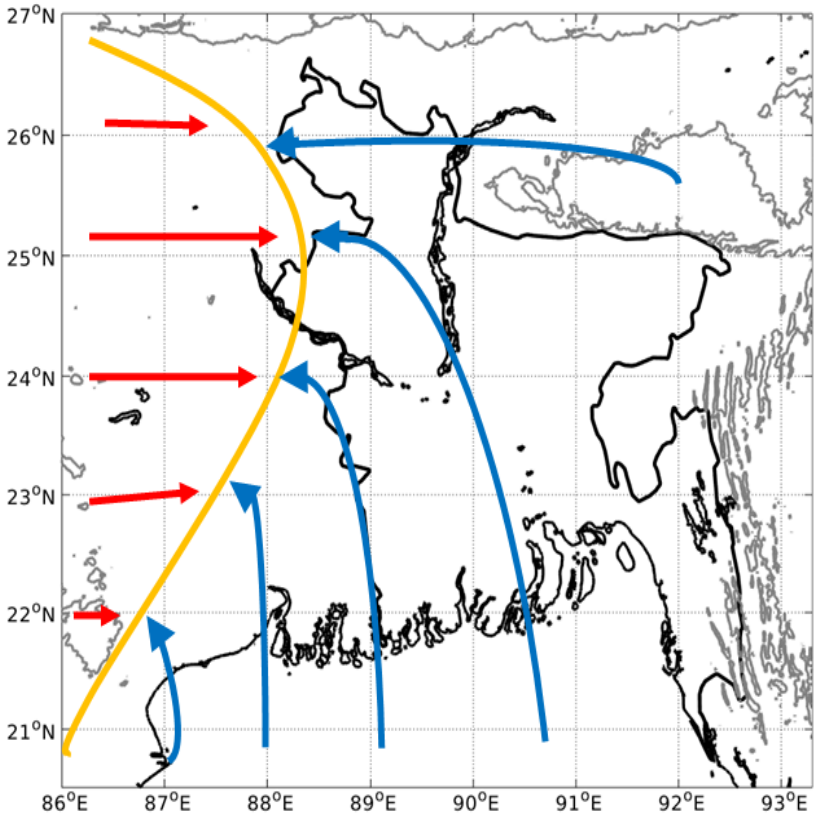

Figure 1.10: The dry-line (yellow line) near western part of Bangladesh showing the discontinuity between the moist low-level inflow (blue arrows) from the Bay of Bengal and the hot dry continental air (red arrows) over India.

1.2.6 India-Myanmar Trough

The India-Myanmar trough (IMT) previously known as the Indian-Burma trough (IBT), appears mainly at lower and mid tropospheric levels and can be seen in a number of meteorological fields [Wang et al., 2011]. These fields include; temperature, specific humidity, vertical velocity, geopotential height, and potential vorticity. It exists all year-round, but it exhibits seasonal variations in its location and strength [Wang et al., 2011]. The IMT is closely related to both the southwesterly monsoon flow and the monsoon trough during the summer monsoon [Wang et al., 2011].

The IMT is considered to be among the important systems that affect weather over southern Asia especially during the summer monsoon [Wang et al., 2011]. It results from the splitting of the tropospheric westerly flow when it meets the Tibetan Plateau [Wang et al., 2011], and the trough is over the region where the subtropical high first breaks up in association with the onset of the monsoon season [Wang and Wan, 2008]. Since Bangladesh is part of southern Asia, this implies that the IMT also has a significant effect on the weather pattern in Bangladesh. Over Bangladesh, the trough can be located around 700 hPa [Wang et al., 2011]. [Wang et al., 2011] assessed the influence of the IMT on the weather of Bangladesh during the December - February period by calculating the IMT index for this period and thereafter, correlating it with rainfall amount received during

the same period. Their results revealed a strong correlation between the IMT and the amount of rainfall received in Bangladesh during that period .

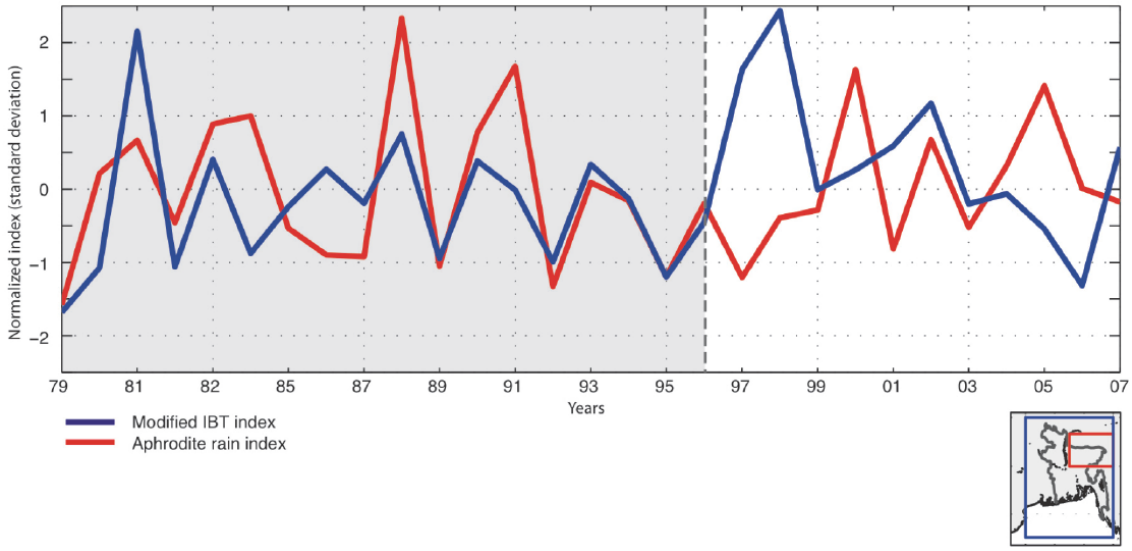

Figure 1.11: Time series of the modified Indian-Myanmar trough (formerly India-Burma trough) index calculated as normalised ERA-Interim potential vorticity at 600 hPa, and the normalised rainfall over Northeast Bangladesh calculated using APHRODITE rainfall data set for the period 1979 - 2007. Figure adapted from Reeve [2014].

Recently, Reeve [2014] calculated the IMT index for the period 1979 - 2007 using ERA-Interim vorticity data [Dee et al., 2011] at 600 hPa, and compared it with the rainfall index for the same period over Northeast Bangladesh for the summer season (March - May). He found a strong correlation between rainfall and IMT for the years between 1979 - 1996, and thereafter the correlation broke down from 1996 - 2007 (Figure 1.11). His conclusion was that the IMT may not trigger rainfall directly, but at least it may play a role in the intensification of the rainfall. He also hinted at the possibility of how the IMT westerlies may influence the intensification of the nighttime convection in Northeast Bangladesh during the summer months.

To conclude this section, the above theories may be thought as the main drivers for the summer rains/summer rainfall in Northeast Bangladesh. However, most of them don't fully explain both the triggering mechanism and the late night-early morning rainfall maximum in Northeast Bangladesh. Thus, a combination of the above processes or some other processes may act to trigger this convection, and this is what the research in this thesis intends to investigate.

1.3 Thesis Objectives

While a multitude of researchers have acquired better understanding of the development mechanisms of the different types of the convective systems in other parts of the world, research on the development mechanism of the summer season convective systems in Northeast Bangladesh has been lacking. This thesis therefore aims at shedding light on the

convective triggering mechanisms that influence summer rains in Northeast Bangladesh as its major objective. The specific objectives of this thesis include;

1. Understanding the climatology of the summer rains/summer rainfall using observations and reanalysis data.
2. Use large scale composites to see if we can draw conclusions about the mechanisms causing the summer rains.
3. To understand the diurnal cycle of precipitation and its effects on summer rainfall in Northeast Bangladesh.

1.4 Thesis overview

This thesis consists of five chapters with the current chapter, chapter 1 giving an overview of the thesis topic, motivation, and thesis objectives. In the later chapters, this thesis is organised as follows. Chapter 2 gives a description of the data used, while chapter 3 presents the methods used in this study. In chapter 4, we present and discuss the results obtained using the data and the methods from the from the previous two chapters. Finally, chapter 5 gives the summary and conclusive remarks on the important findings of this work. It also provides a discussion of the important extensions that can be considered for future research.

Chapter 2

Data

This chapter deals with the data used in this study, giving details of the data used, and why they are chosen. The chapter also explains some manipulations that were done to the data before the analysis could take off. The data used in this study comprises of two data sets namely; Station observation data, and ERA-Interim reanalysis data. Details of these data are given in the subsequent sections below.

2.1 Station observation data

A number of weather fields can be observed from a meteorological weather station. These weather parameters include,among others; daily rainfall, maximum and minimum temperature, dew-point temperature, wet-,and dry-bulb temperature, wind speed and direction, cloud type, base, and height, sunshine hours, and station pressure. Some stations even provide radiosonde data, and in this case the vertical profile of the atmosphere can be assessed. These data are archived in a proper way such that they can be retrieved when need arises. Station observation data can be used to serve many purposes such as forecasting, data assimilation in numerical weather predication models, production of monthly weather bulletins, and research, among others. For our purpose, which is research in this case, daily observation rainfall data for Sylhet station was used. This data was obtained from the Bangladesh Meteorological Department (BMD), and it spanned for a period of 55-years starting from 1956 to 2010. The reason for using station based rainfall data is that it is more precise in obtaining the regional characteristics, and can also strongly elaborate on the field of convective activity. The other reason is that it helps in revealing the association between rainfall and the moisture transport over our region of interest.

2.2 ERA-Interim

ERA-Interim (ERA-I) is a short notation of European Centre for Medium-Range Weather Forecasts (ECMWF) Re-Analysis Interim. It spans from 1st January 1979 to present and

continues to be extended forward in near-real time. But as the name suggests, ERA-Interim was originally planned to be an interim reanalysis while preparing for the next generation of a reanalysis to replace ERA-40 (1957-2002). At first, ERA-interim was from 1st January, 1989 but later in 2011, it was extended a decade back and now it spans from 1st January 1979 to present [Dee et al., 2011].

The ERA-Interim reanalysis is more extensive than all the previous ERA versions such as ERA-40, ERA-15 and others [Berrisford et al., 2011; Dee et al., 2011]. That is, the number of pressure levels increased from ERA-40's 23 to 37 levels and additional cloud parameters are included in ERA-Interim. It also includes several parameters that were not available in ERA-40 and other earlier ERA versions. ERA-Interim represents a third generation reanalysis in which several inaccuracies that existed in ERA-40 such as too strong precipitation over oceans from the early 1990's onwards and a too strong stratospheric circulation were eliminated or significantly reduced [Dee et al., 2011].

The ERA-Interim reanalysis is based on the ECMWF Integrated Forecast System (IFS Cy31r2)[1][Dee et al., 2011]. This atmospheric model has a spectral resolution of T255 (spherical-harmonic representation for the basic dynamical fields), 60 vertical levels with its top at 0.1 hPa (about 64 km), and is based on a reduced Gaussian grid with approximately 79 km uniform spacing for surface and other grid-point fields [Berrisford et al., 2011; Dee et al., 2011]. The atmospheric model uses a hybrid sigma-pressure vertical coordinate, and a semi-Lagrangian semi-implicit time stepping scheme. It is also coupled to an ocean-wave model which resolves 30 wave frequencies and 24 wave directions at the nodes of its reduced 1.0° x 1.0° latitude-longitude grid [Berrisford et al., 2011; Dee et al., 2011].

The ECMWF IFS model uses a 12-hourly four-dimensional variational analysis (4D-Var) for data assimilation, and the benefit of this is that the forecast model can constrain the state evolution within each analysis window [Dee et al., 2011]. The other benefit of using 4D-Var data assimilation is to incorporate the actual observations (from satellite, radar, ship, land surface, balloon) into the model in order to create a unified, complete description of the atmosphere. The version of 4D-Var used for ERA-Interim also updates a set of parameter estimates that define bias corrections needed for the majority of satellite-based radiance observations through Variational Boundary Condition (VarBC) [Dee et al., 2011]. Until 2002, ERA-Interim used input observations that were prepared for ERA-40 in some cases, and thereafter data from ECMWF's operational archive [Dee et al., 2011].

The ERA-Interim reanalysis is produced with a sequential data assimilation scheme, advancing forward in time using 12-hourly analysis cycles [Berrisford et al., 2011]. In each cycle, available observations are combined with prior information from a forecast model to estimate the evolving state of the global atmosphere and its underlying surface. This involves computing a variational analysis of the basic upper-air atmospheric fields (temperature, wind, humidity, ozone, surface pressure), followed by separate analyses of near-surface

[1]Documentation of the IFS can be obtained from the ECMWF website at https://software.ecmwf.int/wiki/display/IFS/Official+IFS+Documentation

parameters ($2m$ temperature and $2m$ humidity), soil moisture and soil temperature, snow, and ocean waves. These analyses are then used to initialise a short-range model forecast, which provides the prior state estimates needed for the next analysis cycle.

ERA-Interim products are freely available on the ECMWF Data Server at 2.5, 1.5, 0.75, and 0.5 degree resolution, which offers flexibility for regional selection and gridding. The ERA-Interim reanalysis used in this study was downloaded from the ECMWF Data Server via the Meteorological Archival and Retrieval System (MARS). The pressure level data used in this case were obtained at six-hourly intervals: 0000, 0600, 1200 and 1800 UTC. The spatial resolution for this data is 0.5° x 0.5° latitude and longitude. In this study, we used ERA-Interim reanalysis for only 32 years (i.e., 1979-2010), because our station observation rainfall data for Northeast Bangladesh spanned only up to 2010, and yet we wanted to compare directly with it. The use of ERA-Interim reanalysis data in this case is to show the large-scale conditions that manifest during the build up to the onset of summer rains. The other fact for using ERA-Interim reanalysis data is that it was readily available in 6-hourly intervals, which makes it somehow precise to explicate the climatological view of diurnal variation in convection, low-level circulation and moisture transport.

2.3 Computation of Vertically Integrated Moisture Flux

2.3.1 Atmospheric water balance

Before analysing the vertically integrated moisture flux, it is important to first understand the atmospheric water balance, which includes both the sources and sinks that account for both inflow and outflow of water vapor flowing over the region, coupled to the rate at which the water is being added or removed from the atmosphere through evaporation and precipitation. Starting from the basic water balance equation as formulated by Peixoto [1973]; Alestalo [1983]; Peixoto and Oort [1992] among others, the atmospheric water vapour budget can be expressed as below:

$$\frac{\partial W}{\partial t} = C + E - P, \tag{2.1}$$

where W, is the total column moisture content (total water storage in the air column), C is the vertically integrated atmospheric moisture flux convergence, E is evaporation from the surface, and P is precipitation. From Eq.2.1, C is further expressed as $C = -\vec{\nabla}\cdot\vec{Q}$ with $\vec{\nabla}$ being the horizontal divergence operator given by

$$\vec{\nabla} = \hat{i}\frac{\partial}{\partial x} + \hat{j}\frac{\partial}{\partial y}$$

in this case, and $\vec{Q}$ being the vertically integrated moisture flux given by;

$$\vec{Q} = \frac{1}{g}\int_{p_{top}}^{p_{surf}} q\vec{V}_h dp \tag{2.2}$$

with g being the gravitational acceleration [9.8 ms^{-2}]; p_{top} and p_{surf} being pressure at the top and surface pressure, respectively; q being the specific humidity in [$kgkg^{-1}$]; dp is the pressure change, *and* $\vec{V_h}$ is the horizontal wind vector in [ms^{-1}] given as;

$$\vec{V_h} = u\hat{i} + v\hat{j} \tag{2.3}$$

where u and v are the zonal (eastward) and meridional (northward) wind components, respectively.

When averaged over area and for sufficiently long time-scales such as a year or even longer, the storage term ($\partial W/\partial t$) on the left hand side of Eq.2.1 becomes negligible compared to the magnitudes of the terms on the right hand side. Hence Eq.2.1 becomes

$$[\bar{P}] \approx [\bar{E}] + [\bar{C}] \tag{2.4}$$

where the over-bar denotes the time average and the square brackets denote the area average. Eq.2.4 gives an overall estimate of the mean water balance for the column of air extending from the surface to the top of the atmosphere over a given region. Areas where evaporation exceeds precipitation (i.e., $E > P$) are moisture sources over which the atmospheric moisture flux diverge, otherwise areas with precipitation exceeding evaporation (i.e., $P > E$) are moisture sinks and hence moisture fluxes converge there.

2.3.2 Vertical integration of moisture fluxes

To compute the vertically integrated moisture flux, we first computed the u- and v-components of pressure-dependent moisture flux ($\vec{q}$) using

$$\vec{q}(p_i) = \frac{(\vec{V_h}q)_{p_i}}{g} \tag{2.5}$$

with $\vec{V_h}$ being the horizontal wind vector and q the specific humidity, which are both defined at the pressure levels p_i with $i = 1,\ldots,18$ in this case and g is gravitational acceleration.

The vertical integration of these fluxes was computed using a method that was previously used by several researchers (e.g., Trenberth [1991]; Simmonds et al. [1999]). This method was preferred because it approximates the continuous integral with finite difference technique based on the trapezoidal rule. Since we wanted to get the vertically integrated moisture flux within the troposphere, we considered all the available data at every pressure level from surface to the top of the troposphere. Fortunately, ERA-Interim data is available at all pressure levels throughout the troposphere. We had data for eighteen pressure levels starting from 1000 hPa to 100 hPa, and also readily available in ERA-Interim data was the surface pressure field. The pressure levels considered in the calculation of the horizontal moisture fluxes were 1000, 975, 950, 925, 900, 850, 825, 800, 750, 700, 650, 600, 550, 500, 400, 300, 200, and 100 hPa level. While several researchers (e.g.,Strong et al. [2002]) have always ignored the levels above 300 hPa saying that the amount of water

vapour there is negligible (or sufficiently small), in our case we never wanted to take such assertions and instead we considered all the levels in the tropospheric column.

Table 2.1: Standard pressure levels (**bolded entries**) and intermediary half levels (not bolded). Units are **hPa**

Pressure level No.	**Pressure level**	Δp
$p_{\frac{1}{2}}$	P_{surf}	
p_1	**1000**	$P_{surf} - 987.5$
$p_{1\frac{1}{2}}$	987.5	
p_2	**975**	**25**
$p_{2\frac{1}{2}}$	962.5	
p_3	**950**	**25**
$p_{3\frac{1}{2}}$	937.5	
p_4	**925**	**25**
$p_{4\frac{1}{2}}$	912.5	
p_5	**900**	**37.5**
$p_{5\frac{1}{2}}$	875	
p_6	**850**	**37.5**
$p_{6\frac{1}{2}}$	837.5	
p_7	**825**	**25**
$p_{7\frac{1}{2}}$	812.5	
p_8	**800**	**37.5**
$p_{8\frac{1}{2}}$	775	
p_9	**750**	**50**
$p_{9\frac{1}{2}}$	725	
p_{10}	**700**	**50**
$p_{10\frac{1}{2}}$	675	
p_{11}	**650**	**50**
$p_{11\frac{1}{2}}$	625	
p_{12}	**600**	**50**
$p_{12\frac{1}{2}}$	575	
p_{13}	**550**	**50**
$p_{13\frac{1}{2}}$	525	
p_{14}	**500**	**75**
$p_{14\frac{1}{2}}$	450	
p_{15}	**400**	**100**
$p_{15\frac{1}{2}}$	350	
p_{16}	**300**	**100**
$p_{16\frac{1}{2}}$	250	
p_{17}	**200**	**100**
$p_{17\frac{1}{2}}$	150	
p_{18}	**100**	**100**
$p_{18\frac{1}{2}}$	50	

Using a redefined method of Trenberth [1991], the standard pressure levels given above are denoted as $p_1, p_2, p_3, \ldots, _{18}$, where $p_1 = 1000, p_2 = 975, p_3 = 950, \ldots, p_{18} = 100$. Then

the intermediate half levels are given by;

$$p_{i+\frac{1}{2}} = \frac{1}{2}(p_i + p_{i+1});\ i = 1, 2, 3, \ldots, 17 \tag{2.6}$$

In order to define the layer thickness (Δp_i), we introduced two more extra pressure levels to demarcate the top and bottom of every layer, as suggested by Trenberth [1991]. Now the first level was set to surface pressure (p_{surf}) as the bottom most and the top most level was set to 50 hPa since we were only interested in moisture flux within the troposphere. This implied that all the other levels were contained in between the surface pressure level and the 50 hPa level [Table.4.1].

While using a pressure coordinate system, the vertical integral of the moisture flux given in Eq.2.2 is redefined using the pressure-dependent moisture flux quantity $\vec{q}(p_i)$, and the equation takes the form;

$$\vec{Q} = \int_{p_{top}}^{p_{surf}} \vec{q}(p_i)dp \tag{2.7}$$

Here one should note that the surface pressure, p_{surf} is not a fixed value but rather varies with topography, and hence this renders the would be upper limit of integration in this case variable. On the other hand, the pressure top (p_{top}) can be fixed at any particular pressure level as one would wish. For our case, we used pressure level top as 50 hPa. Because we only have data available at pressure levels, Eq.2.7 is replaced by finite differences and the vertical integration of moisture flux can now easily be performed using the trapezoidal rule as given below;

$$\vec{Q} = \sum_{i=1}^{18} \vec{q}(p_i)\Delta p_i \tag{2.8}$$

where the summation is over the vertical layers,i, of which there are 18, and Δp_i being the layer thickness defined as;

$$\Delta p_i = p_{i-\frac{1}{2}} - p_{i+\frac{1}{2}};\ i = 1, 2, 3, ..., 18 \tag{2.9}$$

where $p_{i-\frac{1}{2}}$, and $p_{i+\frac{1}{2}}$ are the bottom, and top of the i^{th} layer, respectively. For $p_{\frac{1}{2}}$, we used $p_{\frac{1}{2}} = p_{surf}$, and thus, the thickness (Δp_1) of the lowest layer is p_{surf} - 987.5, which is the intermediary half-level above the 1000 hPa [see Table 4.1].

Since the topography of the study domain was not evenly distributed with some raised terrain and low-lying areas, this brought a technical problem while performing the vertical integrals of the moisture flux at some grid points because the surface pressure there might be greater than 1000 hPa, which is the highest available pressure level in the ERA-Interim data set. In such cases, the surface pressure p_{surf} was used to determine whether the 1000 hPa surface lies above or under the ground. If the pressure of the current level was higher than the surface pressure, then that point laid under the ground and hence, was neglected. Thus, we always need to consider the variability of surface pressure while performing the vertical integrals of moisture fluxes. One way to do this is by use of the time average surface pressure, $\bar{p}_{surf}$ as a limit in vertical integrals (as was the case with Boer and

Sargent [1985]; Boer [1986]). And the other way is to assume $\bar{p}_{surf}$ spatially uniform. But all these can bring substantial errors while evaluating the vertical integrals in areas with significant topographical features. Hence, in all our calculations, we evaluated the vertical integrals using the exact surface pressure at each time and then the time averaging was performed at a later stage.

Based on the above reasons, Eq.2.8 was preferred over Eq.2.7 for calculation of the vertically integrated moisture flux since it approximates the continuous integral with a finite difference that caters for the data which is only available at pressure levels that are not evenly spaced. The layer thickness (Δp_i) was also redefined as below;

$$\Delta p_i = \begin{cases} p_{i-\frac{1}{2}} - p_{i+\frac{1}{2}} \; ; & p_i < p_{surf} \\ 0 \; ; & p_i > p_{surf} \\ p_{surf} - p_{i+\frac{1}{2}} \; ; & p_{i-\frac{1}{2}} \leq p_{surf} < p_{i+\frac{1}{2}} \end{cases} \tag{2.10}$$

where $i = 1, 2, 3, \ldots, 18$, $p_{i-\frac{1}{2}}$ and $p_{i+\frac{1}{2}}$ are the bottom, and top of the i^{th} layer respectively, and $p_{\frac{1}{2}} = p_{surf}$, [see Table.4.1]. The use of this redefined Δp_i was to ensure that only information within the tropospheric column contributes to the summation in Eq.2.8.

2.3.3 Vertical integration of moisture flux divergence

Having already seen how the vertical integrals of the moisture fluxes are handled, the vertical integration of moisture flux divergence is not treated differently, but rather in a similar fashion. For divergence of moisture fluxes ($\mathbf{q}$), the divergence equation in spherical coordinates is given in Eq.2.11 below:

$$\nabla \cdot \mathbf{q}_{(i,j)} = \frac{1}{a \cos\phi} \left(\frac{\partial(qu)}{\partial\lambda} + \frac{\partial(qv \; cos\phi)}{\partial\phi} \right) \tag{2.11}$$

where qu and qv are the zonal and meridional components of moisture flux ($\mathbf{q}$), respectively, a is the radius of the earth [6371000 m], λ and ϕ are longitude and latitude in radians, respectively. But the computed moisture fluxes are still defined at the grid cell centers, yet we need to know the moisture flux inflow and outflow in the cell. This calls for computation of fluxes at the edges of the grid cell while referring to the four cardinal directions *(i-1,j), (i+1,j), (i,j-1)*, and *(i,j+1)*, see Figure 2.1 for illustration.

Since ERA-I data is available on even grids (i.e., $\Delta X = \Delta Y$), the divergence at every grid point (i,j) is evaluated as a finite centered difference approximation of Eq.2.11 as shown below:

$$\nabla_f \cdot \mathbf{q}_{(i,j)} \approx \frac{1}{a \cos\phi_j} \left\{ \frac{q^{\lambda}_{i+1,j} - q^{\lambda}_{i-1,j}}{\lambda_{i+1,j} - \lambda_{i-1,j}} + \frac{cos\phi_{j+1} q^{\phi}_{i,j+1} - cos\phi_{j-1} q^{\phi}_{i,j-1}}{\phi_{i,j+1} - \phi_{i,j-1}} \right\} \tag{2.12}$$

where q^{λ} and q^{ϕ} indicate the components of moisture flux ($\mathbf{q}$) in the longitude and latitude directions, and ∇_f is used to indicate a finite difference approximation to the divergence operator on a longitude-latitude grid.

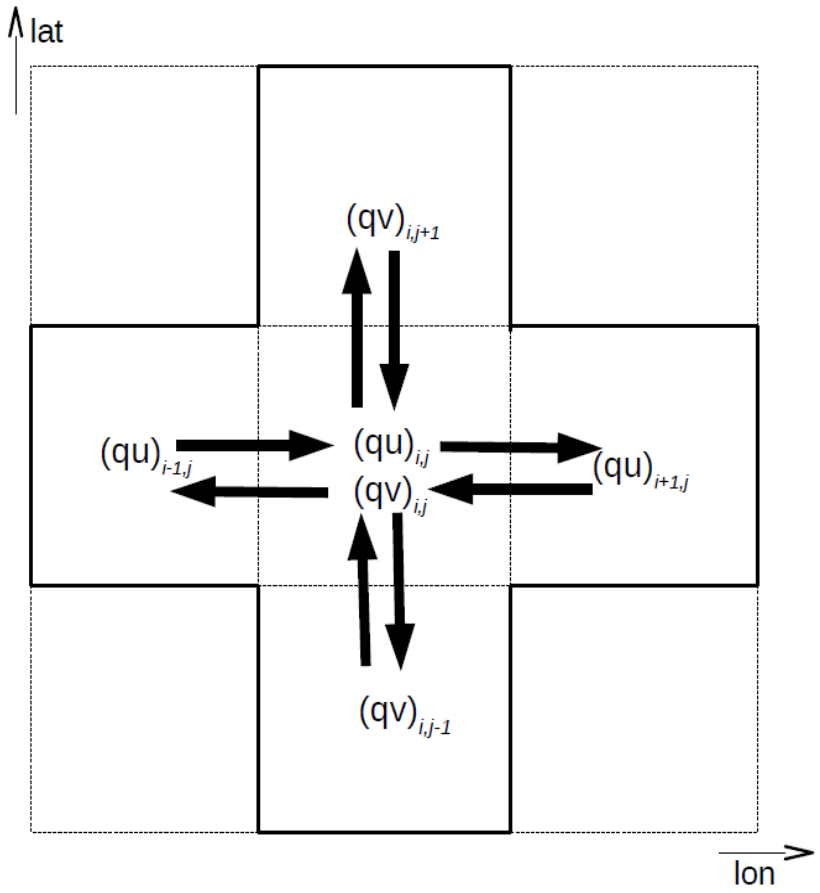

Figure 2.1: Definition of the four components of moisture flux field. qu and qv are the u- and v-components of the horizontal moisture flux, while i and j are grid-cell indices

Finally the vertical integration of moisture flux divergence, $\mathbf{F}_{(i,j)}$ at every grid point (i,j) is given by:

$$\mathbf{F}_{(i,j)} = \sum_{k=1}^{18} (\nabla_f \cdot \mathbf{q}_{(i,j)})_k \Delta p_k \tag{2.13}$$

where $k = 1, 2, 3, \ldots, 18$ corresponds to the pressure levels used in this case, and Δp_k is layer thickness as defined in Eq.2.10. Hence, the data for the vertical integral of moisture flux divergence was computed using Eq.2.13, and the units of the computed divergence are [kg/m^2/s].

Chapter 3

Methods

This chapter presents the different methods applied to the data from the previous chapter 2 to achieve the goals of this thesis. The methods described in this chapter include those used to determine the rainfall onset dates, construction of the composites, and explanation of the technique used to test the statistical significance of the composites.

3.1 Determination of summer rainfall onset

Most previous studies have used winds, outgoing long-wave radiation (OLR), and precipitation with uniform criteria to define the local monsoon/rainfall onset, particularly the Southeast Asian Monsoon (SEAM). This is because all the above mentioned fields have a strong affection with the rainfall onset. To start with, Lau and Yang [1997] used rainfall rate exceeding 6 mm/day to determine the monsoon onset, while Murakami and Matsumoto [1994] used Climatological Pentad Mean (CPM) OLR below 230 Wm^{-2} for the same purpose. Zhang et al. [2002] used rainfall with pentad mean value of 5 mm/day, whereas Zhang et al. [2004] used OLR with threshold pentad value of below 240 Wm^{-2} to determine the monsoon onset. Relative CPM rainfall rate (RR_i), defined by the difference between the pentad mean (R_i) and January mean (R_{JAN}), with $RR_i \geq 5$ mm/day was used by both Wang [2002] and Zhang and Wang [2008] to effectively determine the onset dates in the Asian monsoon region. These uniform criteria are suitable for determination of onset in tropical monsoon regions. But one must take note of the fact that the intensity of the rainy season varies considerably with latitude. With this in mind, a criterion that caters for all these facts, needs to be considered to achieve the desired target.

Recently, Stiller-Reeve et al. [2014] developed an integrated approach (IA) method that aims at reducing the occurrence of false monsoon onset. The IA method incorporates background knowledge into definition got from the local people's perception about monsoon onset up to the test phase that identifies the actual monsoon onset. Since their major aim was to reduce false monsoon onset occurrences, Stiller-Reeve et al. [2014] increased the number of pentads (5-day period) used to define monsoon onset from three or four pentads, which were previously used by Matsumoto [1997]; Wang [2002] to six. They also

constructed the integrated onset matrix (IOM) which contains combinations of six-binary "1"s and "0"s (e.g.,[111010]) with "1" indicating a "hit" when the chosen threshold has been either reached or exceeded, and a "0" indicating that the threshold has not been reached. The IOM was then used for comparison with the combination of 6-moving window pentads to identify whether the onset conditions set are fulfilled. The combination of the 6-binary digits must contain at least four "1"s out the 6-binary digits, with two "1"s fixed at the beginning of the combination and the rest can be interchanged. The IOM has the following 11-possible arrangements;

$$IOM = \begin{bmatrix} 1 & 1 & 0 & 0 & 1 & 1 \\ 1 & 1 & 0 & 1 & 0 & 1 \\ 1 & 1 & 0 & 1 & 1 & 0 \\ 1 & 1 & 0 & 1 & 1 & 1 \\ 1 & 1 & 1 & 0 & 0 & 1 \\ 1 & 1 & 1 & 0 & 1 & 0 \\ 1 & 1 & 1 & 0 & 1 & 1 \\ 1 & 1 & 1 & 1 & 0 & 0 \\ 1 & 1 & 1 & 1 & 0 & 1 \\ 1 & 1 & 1 & 1 & 1 & 0 \\ 1 & 1 & 1 & 1 & 1 & 1 \end{bmatrix}$$

The IA method starts by choosing a meteorological parameter(s) which you want to use to define your onset, then it applies a criterion or threshold to the chosen parameter(s), and finally, it allocates the seasonal transition after satisfying the chosen criterion for the exact onset. The choice of the parameter(s) and the criterion depends on the objective target group and target area. In this you need to know the people you want to communicate to, and in what specific location, because you may find that the onset in that particular region is influenced by local circulation as it may be the case for Northeast Bangladesh.

After scrutinizing the different methods used by different researchers in several publications, Stiller-Reeve et al. [2014]'s IA method was adopted for this research. The meteorological field used to define onset of the summer rains in this study is station observed rainfall data, even though other fields such as OLR, low-level winds, and atmospheric water content also have a direct association with dry to wet transition. The choice of rainfall fields stems from the pilot questionnaire survey carried out in Northeast Bangladesh (Sylhet region) where the majority of the local people in this particular region consider summer rains to be part of the large-scale monsoon. Pentad mean (5-day mean) rainfall was calculated, implying that every year was divided into 73 Julian Pentads (JP). Then a multi-criteria test using several thresholds starting from 5 mm/day to 12 mm/day pentad mean was applied. The reason for doing this was to get the best criterion or threshold that perfectly matches the people's perception about the rainfall onset in Northeast Bangladesh. We used an algorithm similar to that of Stiller-Reeve et al. [2014] to test each pentad mean value separately and then convert each pentad result into a binary vector for each year separately with "1" indicating that the threshold has been reached

and exceeded, and "0" indicating that a threshold has neither been reached nor exceeded. The resulting binary vector of 73 Julian pentads for each year is then stored. For example, considering the year 1990, the resulting binary vector using 11 mm/day is;

[0 0 0 0 0 0 0 0 0 0 0 0 0 0 0 1 1 0 0 1 1 1 1 1 0 0 1 0 1 1 1 1 0 0 1 0 0 1 1 0 0 1 0 1 1 1 0 1 0 1 1 1 1 1 1 0 1 0 0 0 0 0 0 0 0 0 0 0 0 0 0]

Since Stiller-Reeve et al. [2014] used a 6-pentad moving window, we also extended our results in the binary vector to a 6-pentad moving window and test it chronologically against each of the combinations of the binary "1"s and "0"s stored in the IOM. If the 6-pentad binary window matches with the any of the combinations stored in the IOM, then the earliest JP in that window is stored as a first-guess vector. For example, using the above binary vector for the year 1990, if the binary combination from JP16-22 [1],(i.e., 1 1 0 0 1 1) matches one of the combinations in the IOM, then JP16 is stored in the first-guess vector. Hence, the binary vector for the year 1990 gives the following first-guess vector of the JPs matching the IOM combinations:

[16 20 21 22 29 30 44 45 50 51 52 53].

This method also allows for the analysis of the time between all the JPs in the first-guess vector (e.g., the one above) before the onset date is declared. It goes further to discard an entry in the first-guess vector as a false onset if the time difference between two adjacent entries is more than nine pentads (45 days). The 9-pentad separation criterion is chosen since it accounts for the chance of immediate break periods that occur shortly after the onset [Adamson and Nash, 2013].

After testing the different thresholds starting from 5 mm/day to 12 mm/day pentad mean value using Stiller-Reeve et al. [2014]'s method, the 11 mm/day threshold was considered to define the onset of the summer rainfall in Northeast Bangladesh. Although this value looks quite bigger compared to other thresholds that have been used in other regions to determine the rainfall onset, it gives the mean onset pentad value (JP26) that corresponds to the local people's perception about rainfall onset in Northeast Bangladesh [Stiller-Reeve et al., 2015]. This is because Northeast Bangladesh receives huge amounts of precipitation during the summer months, hence this threshold best defines the summer rainfall onset in this region. Using this threshold, the earliest onset is found in 1990, 1994, and 2005 (JP16) and latest onset is found in 1986 (JP36), as shown in Figure 3.1. The normal onset (mean onset pentad) is JP26 shown with a red-dashed line in Figure 3.1.

[1]There are 73 Julian pentads (5-day periods) in a 365 day year. JP16 refers to the 16th Julian pentad after the start of the year.

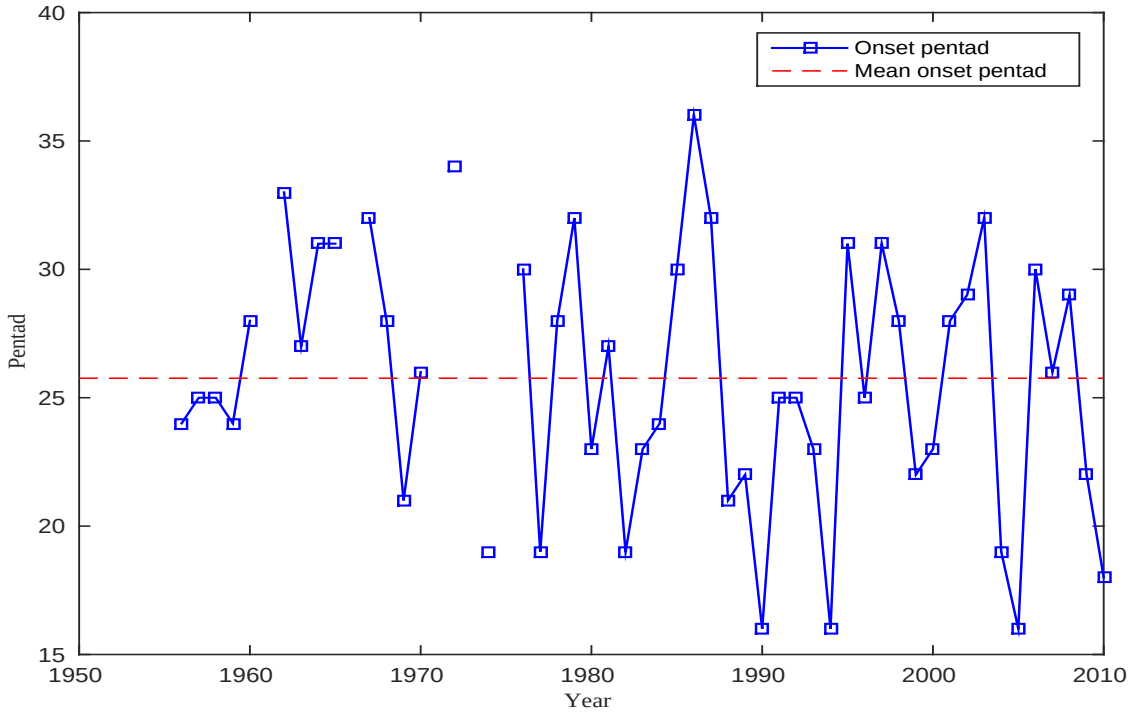

Figure 3.1: Time series of rainfall onset dates for Sylhet region (in pentad) obtained using Stiller-Reeve et al. [2014]'s method with 11 mm/day threshold for the period from 1956 to 2010. March starts from pentad 13, April from pentad 19, and May from pentad 25 up to the end of pentad 30. The gaps indicate years with missing data

3.2 Composite Analysis

Given that each rainfall season has its unique temporal and spatial patterns, complexity sets in especially if research is intended to span over a long period of time. Sometimes the individual events occur in a unique way and don't give a consistent signal that may be relied upon for applications. This means that in order to get any reliable information that can be used to draw a conclusion, something must be done to this data to reveal a consistent signal from the individual events. In this current study, this complexity is overcome by using the composite technique to investigate the large scale synoptic conditions that occur during the individual rainfall events.

The composite method involves the selection of case studies for a given variable based on a given relationship with a fundamental condition and thereafter performing averaging, Okoola [1999]. It also involves taking the averaged pattern of the given parameter based on a given classification. As our study focuses on summer rains in Northeast Bangladesh, composites were constructed basing on the onset of the summer rainfall in this region. The onset pentads that were obtained using the method in section 3.1, were selected from the ERA-Interim reanalysis data for different parameters e.g., precipitation, specific humidity, evaporation, vertically integrated moisture flux and flux divergence, temperature, geopotential height and thickness, and wind at different isobaric levels for the period spanning from 1979 to 2010, and thereafter compositing them.

The power of this technique is to highlight the dominant features that can be derived from the uniquely averaged events [Ogwang et al., 2012; Laken and Čalogović, 2013]. Therefore, the composite tends to mask the extreme unique events and maintains the consistent features over the averaging period and space. This makes the composites easy to interpret and hence, they can be relied upon to make hypotheses on the factors that influence the patterns observed in individual cases. This technique has been applied for other studies over several parts of the world (e.g Reeve and Kolstad [2011]; Ogwang et al. [2012]; Laken and Čalogović [2013]; Fujinami et al. [2014]).

3.2.1 Lead-lag composite method

In order to assess the nature and time evolution of the systems that may lead to summer rains in Northeast Bangladesh, the lead-lag composite method was used. With this method, we looked at several days prior to the onset that was determined by our method and several days after the onset. Since we were using pentads to elucidate our onset, we also used pentads to construct the lead-lag composite maps. This helped us to monitor some of the mechanisms that are at play during the onset of the summer rains. For our lead-lag case, we constructed composite maps of the four pentads before the onset and four pentads after the onset. That is, we assessed twenty days before the onset and twenty days after the onset (from pentad(-4) to pentad(+4)). This was presumably the best way which we could base on to explicate the different mechanisms that may be at play during the build up to these summer rains.

3.3 Statistical Significance

After constructing the composites for the different parameters, the next step was to assess their statistical significance with regards to their connection with summer rainfall. Testing for significance is very important especially if someone wants to show the relevance or impact of some change that may occur as a result of a new step, a trend or transition as it was in our case. It also helps in drawing conclusions by showing how confident you are with the obtained results. To test whether something is statistically significant, it means that the calculated p-value (probability of rejecting the null hypothesis that is true) is less than the chosen significance level. There are many ways that can be employed to test the statistical significance of variations over composites of a field variable. These include among them; the bootstrapping method, Monte Carlo method, Mann-Kendall method, Student's t-test, Analysis of Variance, and others. In our case, we chose a Monte Carlo method.

3.3.1 Monte Carlo Method

The Monte Carlo (MC) method is a very powerful and useful technique that is often applied in cases where it is difficult or even impossible to measure all individuals in a population. But such a task can easily be done by this MC method. The MC method uses random sampling of the datasets themselves, and makes no assumptions regarding the properties of the data. But while using the MC method, one should keep in mind that for better results from the MC-analysis, both the number of unique samples and the number of simulations should be relatively large. Therefore, the total number of unique simulations which can be generated is calculated as;

$$MC_{sims} = \frac{m!}{n!(m\ -\ n)!} \tag{3.1}$$

where MC_{sims} is the number of unique simulations, n is the subsample size (i.e., size of the composites), and m is the parent population size.

In this study, the parent population size used was 32 since we had a 32-year period, and the sample size used was 20 since this was relatively large compared to our parent population and gave better MC convergence. We binned the data at each grid point and then used the binned data to create 1000 artificial composites at each grid point for a period of $pentad \pm 4$ using MC simulations. The resulting probability density functions (PDFs) of the 1000 MC simulations at each grid point for every pentad were normalised, and then compared with each adjacent pentad for $pentad \pm 4$ to get the overlap coefficient.

3.3.2 Overlap coefficient

The overlap coefficient (OVC) is the percentage of overlapping regions of two normal distributions. In other words, it is the area of intersection below the two density curves as illustrated in Figure 3.2. In this study, we compared two consecutive pentads to obtain the overlap at every grid point from one pentad to the next for $pentad \pm 4$. Then the OVC was obtained by dividing the overlap at every grid point by the number of MC simulations (1000 in this case). An example illustrating the OVC is given in Figures 3.3 and 3.4 for precipitation.

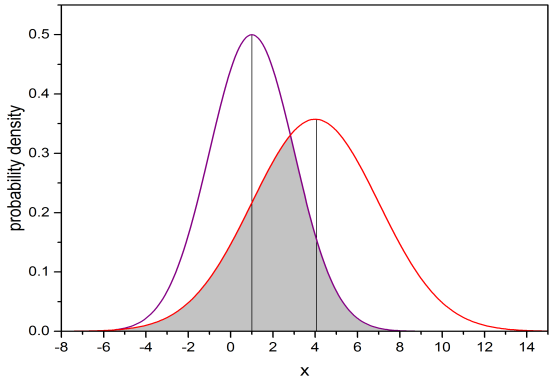

Figure 3.2: An illustration showing the overlap region (shaded gray) obtained after comparing two PDFs at the same grid point in the consecutive pentads

Figure 3.3 gives the time series of overlap coefficient from pentad to pentad for an average over Northeast Bangladesh, while Figure 3.4 shows statistical differences between the the two consecutive pentads during the onset of the summer rains. The percentage of overlap (overlap coefficient) between the pentads is shown on y-axis in Figure 3.3, while in Figure 3.4, it is shown by the colours. The high overlap coefficient values indicate that little change occurred, while the low overlap coefficient values mean a large change in the regime. The strong regime transition from pentad (0) to pentad (+1) is distinctly visible over Northeast Bangladesh when the percentage takes a huge drop from higher values to values $\leq$25% (0.25) [at pentad difference 5 in Figure 3.3, and at ptd(0)-ptd(+1) in Figure 3.4].

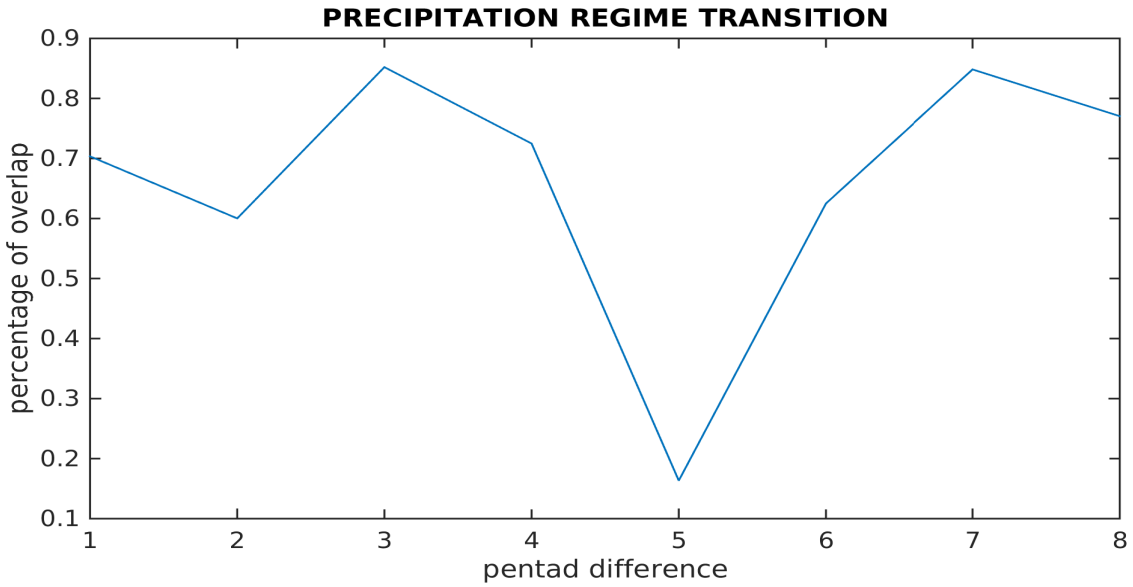

Figure 3.3: Time series of pentad difference showing a huge drop in the OVC for precipitation averaged over Northeast Bangladesh

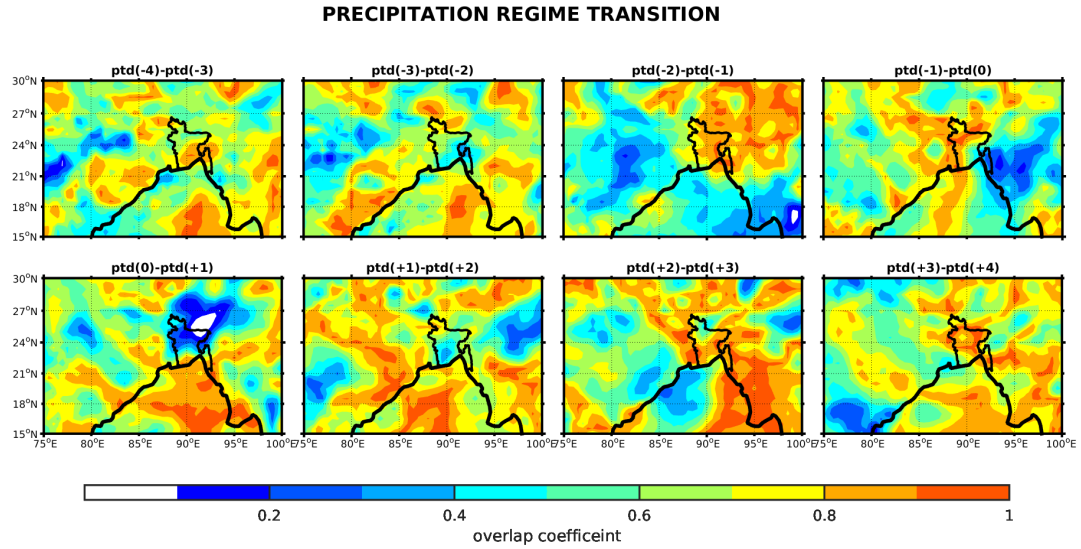

Figure 3.4: An example showing the statistical differences at each grid point between two consecutive pentads for precipitation field before and after the onset (pentad 0) of summer rains. The colours show the percentage overlap at each grid point between the pentads.

Chapter 4

Results and Discussion

This chapter presents the results obtained using the data and methods from the previous chapters 2 and 3, respectively and their discussion. The results are discussed in relation to the objectives of this study and where necessary, a comparison with results of previous research by other researchers is made.

4.1 Climatological results for precipitation over Northeast Bangladesh

4.1.1 Rainfall trend

Figure 4.1 shows the mean annual rainfall amount at Sylhet station in Northeast Bangladesh, for the period 1956 - 2010. The figure reveals a seasonal variation in rainfall amount received among the different years in this region. Although our main focus is on summer rains that occur in March - May (MAM), it is also important to recognise the season before and after the MAM season . Results from Figure 4.1 show that there is almost no rainfall received in the December-February (DJF) season, some significant amount received in MAM, and then huge rainfall amount received in the JJAS (monsoon) season. It is also revealed in the same figure that in 1980, the amount of rainfall received during the MAM season was higher than the rainfall amount received in the JJAS season. Further analysis reveals that on average, 40.8, 987.9, 2641.6, and 238.2 mm of rainfall is received in DJF, MAM, JJAS, and October-November (ON) season, respectively in Northeast Bangladesh [Table 4.1]. This implies that 1.0%, 25.3%, 67.6%, and 6.1% of the total annual rainfall received in Northeast Bangladesh occurs in DJF, MAM, JJAS, and ON season, respectively [Table 4.1]. Daily average rainfall [Figure 4.2, calculated for the period 1956 - 2010] reveals that on average, the highest daily rainfall amount in Northeast Bangladesh is recorded in May, followed by April, August, September, June, July, and least in March over the period 1956 - 2010. The results from Figure 4.2 are in agreement with the findings of Islam and Uyeda [2005] on the character of summer rains and monsoon rains, very intensive rains in MAM (summer), and less intensive rains in JJAS (monsoon season). The

heavy rainfall in April and May helps to balance the least rainfall in March, and hence contributes greatly to the high MAM season rainfall amount that is seen in Figure 4.1. Hence, it is evident from Figures 4.1 and 4.2 that the heavy rains in Northeast Bangladesh start earlier in the MAM season which is the Bangladesh summer, before the large-scale monsoon season (JJAS) sets in. Thus, this signifies the early monsoon onset that was alluded by Matsumoto [1997] and Ashfaq et al. [2009].

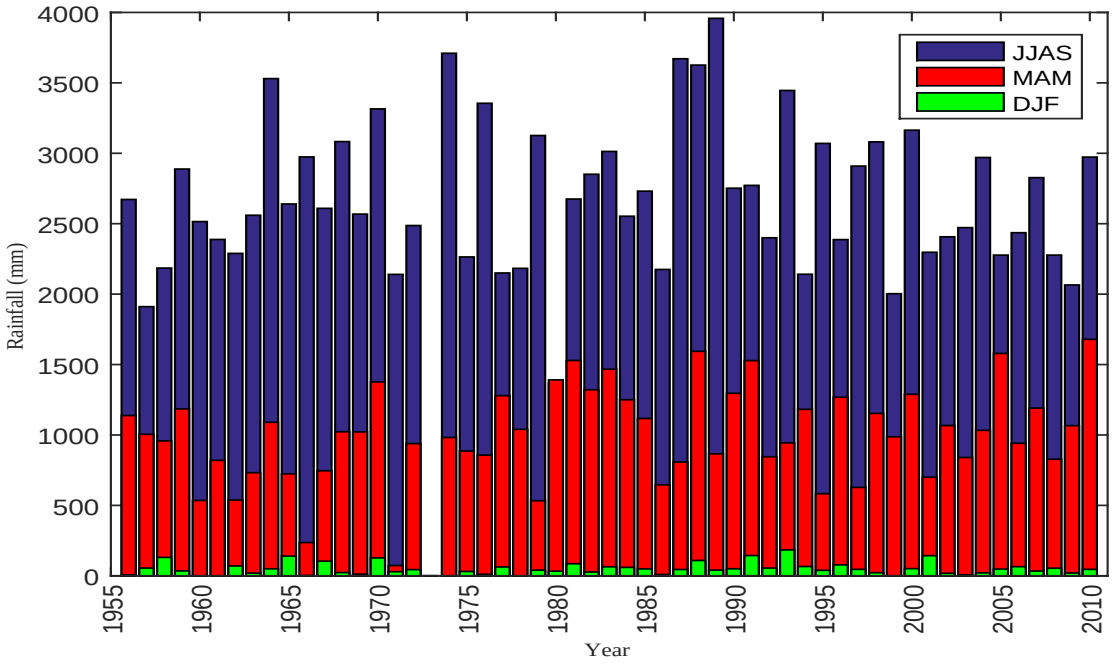

Figure 4.1: Seasonal rainfall amount received in Northeast Bangladesh for the period 1956 - 2010.

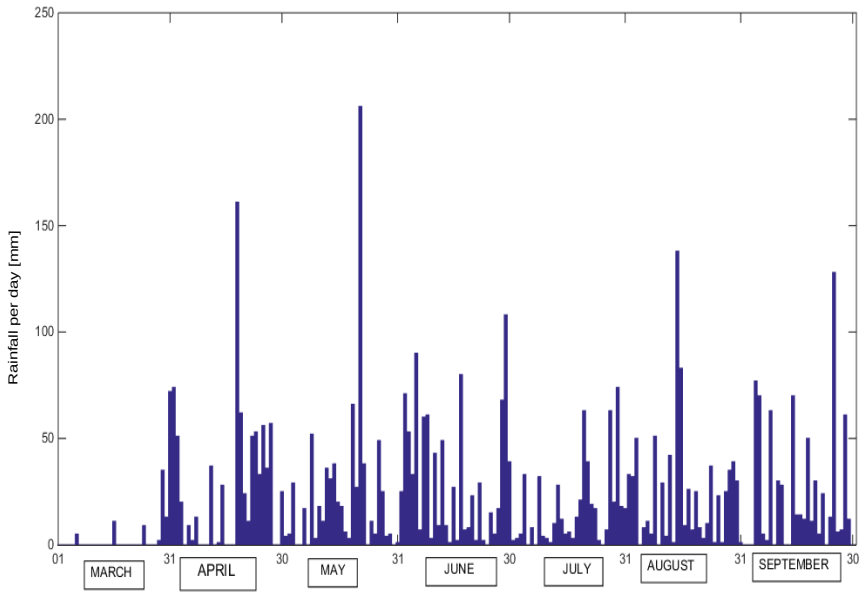

Figure 4.2: Time series of daily mean rainfall amount for the months of March - September received in Northeast Bangladesh for the period 1956 - 2010.

Table 4.1: Distribution of rainfall among season in Northeast Bangladesh. Analysis based on Sylhet station rainfall observed data for the period 1956-2010

Season	Average Rainfall (mm)	Season Total (mm)	Season contribution (%)
DJF	40.8	2244	1.0
MAM	987.9	54334	25.3
JJAS	2641.6	145288	67.6
ON	238.2	13100	6.1

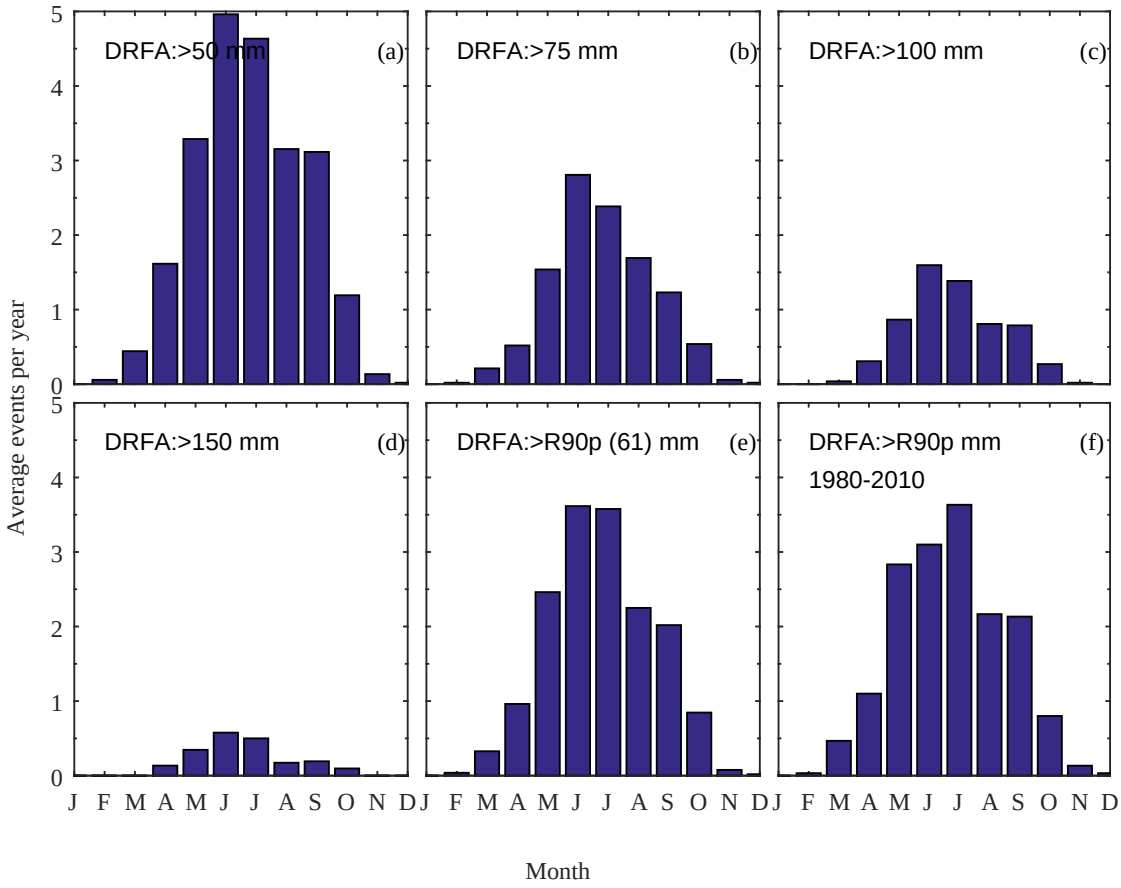

Figure 4.3: Heavy rainfall events received in Northeast Bangladesh for the period 1956 - 2010. DRFA stands for daily rainfall amount.

To assess the intensity of rainfall received over Northeast Bangladesh on the monthly basis, the average number of heavy rainfall events every year were considered for each month spanning over the study period. Figure 4.3 shows the average heavy rainfall events received per month in Northeast Bangladesh during the study period. The different thresholds used to determine the heavy rainfall events in Northeast Bangladesh were: 50, 61, 75, 100, and 150 mm [Figure 4.3 (a)-(f)]. These thresholds were each applied to daily rainfall amount that was received in Northeast Bangladesh to get the heavy rainfall events during the study period. The 61 mm threshold was used because it is the 90^{th} percentile value calculated for the observational rainfall data on the rain days for the period between 1956-2010. The 90^{th} was used in this case because it is widely used as a measure for extreme rainfall events. From Figure 4.3, it can be seen that many of the heavy rainfall events occur during May to September period, with June and July having the highest number of heavy rainfall

events for all the thresholds. It is also important to note that the heavy rainfall events in May are often higher than or equal to those in August and September (two monsoon months) for all the thresholds used in this study, [Figure 4.3]. Interestingly when the period from 1980 - 2010 is considered, the heavy rainfall trends in May seem to catch up with June (almost equal) as shown in Figure 4.3(f), and hence seasonal evolution from May to June. This means that the rainfall pattern in May during the previous decades has become closer to that in June, and hence confirming that the rainy season starts earlier in Northeast Bangladesh. Not only the early onset of the rainy season is visible from this plot, the figure also reveals an increase in the number of heavy precipitation days from March to June and then a decrease in the heavy precipitation events from July to January [Figures 4.3(a) - (e)]. It is also worthy to note that the heavy precipitation events over the period from 1980 - 2010 increased continuously from March to July, thereafter decreasing to almost same number in August and September before a further drop from October to December [Figure 4.3].

4.1.2 Wettest and driest years

Sylhet station observation rainfall data was used to estimate the time series of the summer rainfall in Northeast Bangladesh. Figure 4.4 shows the time series of the Northeast Bangladesh summer rainfall anomalies. The year of 1973 is not considered in our analysis since there was no data recorded during that year due to political turmoil in Bangladesh. For the period 1956 - 2010 (1979 - 2010), the analysis reveals that the mean summer rainfall for the 55 (32) years over Northeast Bangladesh was 23.9 (24.8 mm/day), and 329.3 (366.1 mm/month), respectively. The six wettest and driest summers together with their attributes are shown in Table.4.2. When we consider the period over which the ERA-Interim data overlap with the precipitation records of Sylhet station, we see that all the wettest summers still remain the same as those for the entire station precipitation records. However, for the case of driest summers, only two out of the six driest summers prevail in the period over which the ERA-Interim data overlaps with the station precipitation records [Table.4.2, bolded entries]. This implies that there has been a significant change in summer rainfall in the study region since all the wettest summers are found in the climatological period of 1981 - 2010, with only one driest summer appearing during the period 1981 - 2010. The wettest and driest summers are used here as indicators of wettest and driest years, respectively. This is because when you receive much rainfall in the period that precedes the actual rainy season, then chances are higher that the year will turn into a wet year as this rainfall contributes greatly to the annual rainfall amount received in that particular year, and the reverse is true in case of little rainfall during the summer period.

During the study period (1956 - 2010), the year of 2010 was found to be the wettest year with 1679 mm of rainfall during the MAM season, while 1971 was the driest year with 73 mm of rainfall received during the MAM period.

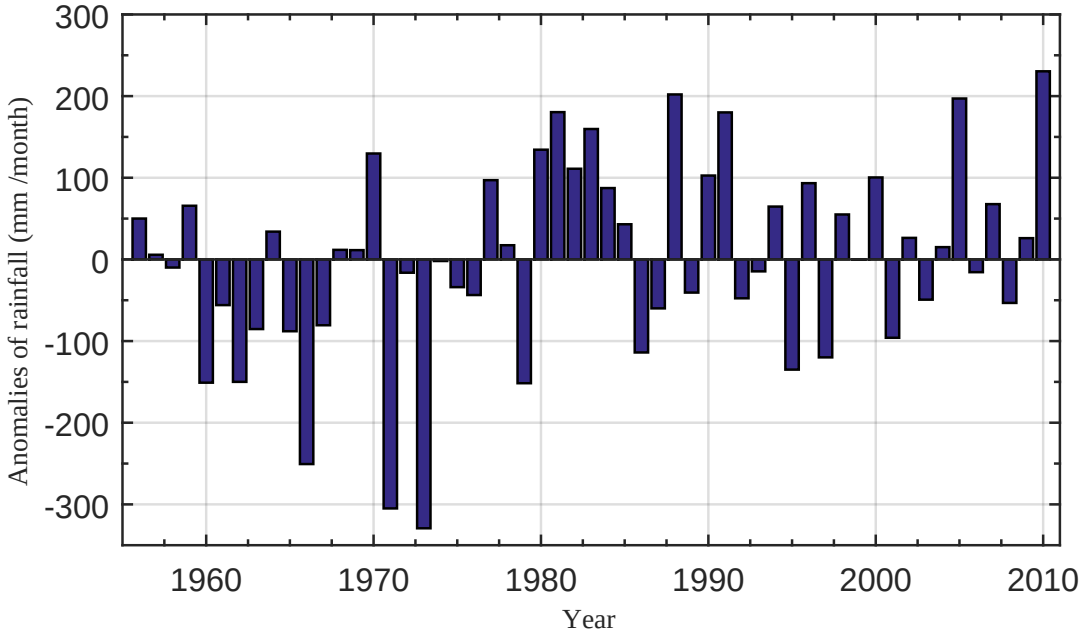

Figure 4.4: Time series of summer rainfall anomalies over Northeastern Bangladesh (in mm month^{-1}). **Note:** 1973 had missing data.

Table 4.2: Classification of wet and dry summers for Northeast Bangladesh based on time-average rainfall (mm month^{-1})

Type	Year	Rainfall	Anomaly
Wet	1981	1529	180.3797
	1983	1467	159.7030
	1988	1594	202.0364
	1991	1528	180.0364
	2005	1579	197.0364
	2010	1679	230.3697
Dry	1960	535	-150.9636
	1962	538	-149.9636
	1966	236	-250.6303
	1971	73	-304.9636
	1979	**533**	**-151.6303**
	1995	**583**	**-134.9636**

4.2 Precipitation and Moisture in the atmosphere based on ERA-Interim

Having seen in the previous section that the heavy precipitation in Northeast Bangladesh starts earlier in summer months of March - May, we now turn our focus to understanding the moisture sources and the seasonal evolution of the summer rains. In order to understand the moisture sources better, the analysis was carried out on the moisture fields in the atmosphere before and after the onset of the summer rains in Northeast Bangladesh. The moisture fields considered here are; precipitation, evaporation, vertically integrated

moisture flux and flux divergence in the troposphere, total column water, and specific humidity.

4.2.1 Precipitation

The onset pentads of the summer rainfall in Northeast Bangladesh obtained from the daily observation rainfall data from Sylhet station were also extended to the precipitation field in the ERA-interim reanalysis data to obtain the a wider view of the precipitation pattern prior to and after the onset in Northeast Bangladesh. The lead-lag composites of precipitation presented in Figure 4.5 reveal that precipitation in the Northeast Bangladesh begins earlier in the year than in any other part of Bangladesh. Four pentads prior to the onset (i.e., pentad (-4)) at least receive 3 - 6 mm/day in Northeast Bangladesh than elsewhere in Bangladesh [Figure 4.5]. The intensity of precipitation gradually increases from pentad (-4) onwards around Northeast Bangladesh in the build up to onset. On the large scale, the precipitation pattern moves eastward across the domain during the onset of the summer rains in Northeast Bangladesh.

Figure 4.5 also shows a moderate area of precipitation with about 12 - 18 mm/day confined in the extreme north end of Brahmaputra Valley far away from Northeast Bangladesh right from pentad (-4) and only shows a gradual increase as other areas of precipitation also manifest in the surrounding elevated topography and the southern part of Brahmaputra Valley towards the onset in Northeast Bangladesh. From pentad (0) onwards, a clear transition in precipitation pattern is observed, with PDF overlaps of 0 - 25% across Northeast Bangladesh, the Meghalaya Plateau, some parts of the Brahmaputra valley and the Himalayas. The increase in the intensity of precipitation is drastic, from 12 - 15 mm/day at pentad (0) to 21 - 27 mm/day at pentad (+1) and thereafter showing a steady increase within the season. The heavy precipitation over Northeast Bangladesh is seen to spread from the southern slope of the Meghalaya Plateau, the Brahmaputra Valley, the Himalayas, and the other elevated topography east of Northeast Bangladesh. One suggestion for this heavy precipitation over these areas is probably due to lifting of moist air by these high topographic features, which leads to strong moisture convergence [see subsection 4.2.3]. According to Fujinami et al. [2014], these topographic features influence the localised heavy rainfall in the windward regions, hence, Northeast Bangladesh being situated on the windward side of the Meghalaya Plateau and the other high elevated topographic features to its east benefits from this relationship.

4.2.2 Evaporation

In Figure 4.6, the lead-lag composites of evaporation reveal an general increase in evaporation in most parts of Bangladesh, except in Northeast Bangladesh which shows a decrease in evaporation rate from 4 mm/day at pentad (-4) to 2.5 mm/day at pentad (+1). This significant decrease in evaporation marks the clear transition in the evaporation regime from pentad (0) to pentad (+1) with an overlap between 0 - 25% in the PDFs over North-

east Bangladesh. Also other parts Bangladesh, the Meghalaya Plateau, Brahmaputra Valley in India, and some parts of the Bay of Bengal, experience a moderate change (25 - 50% PDF overlap) in evaporation rate during this transition from pentad(0) to pentad (+1). Still in the same figure, a lot of evaporation takes place in the Bay of Bengal (3.5 - 5.0 mm/day), most parts of Bangladesh (3.5 - 4.0 mm/day), while areas in Myanmar, some parts of India, and the Himalayas have low evaporation rates of 0.5 - 3 mm/day.

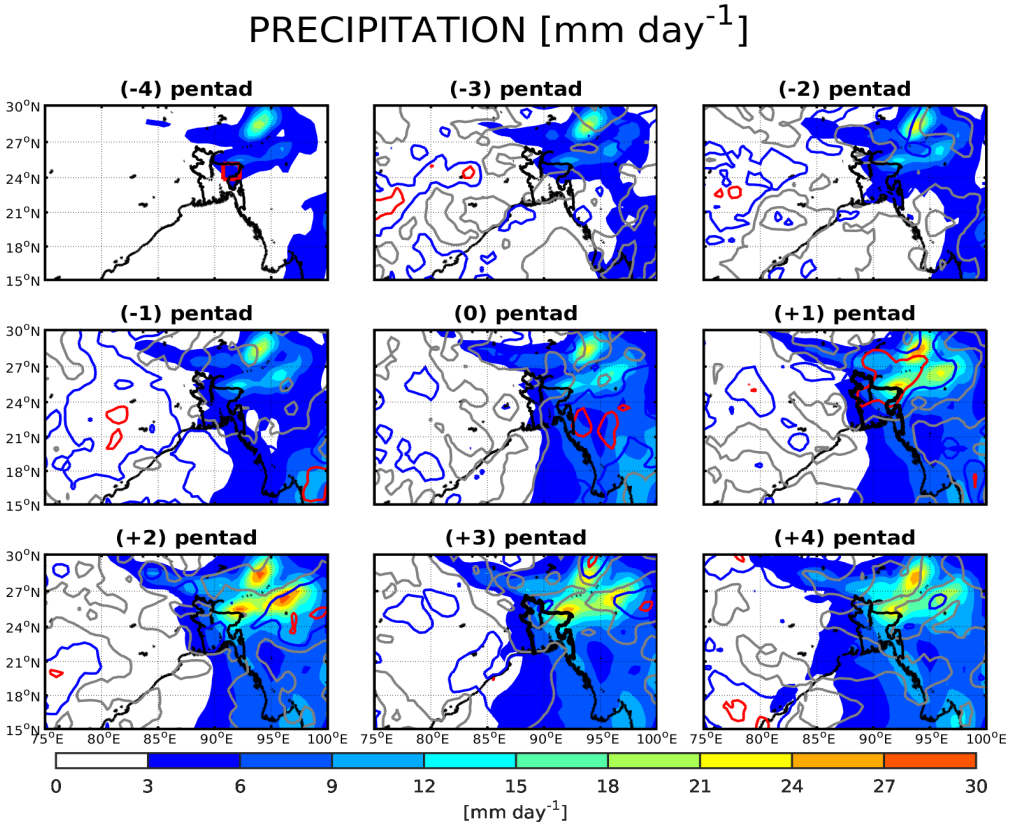

Figure 4.5: Lead-lag composite for precipitation. The contour lines in red, blue, and grey colour represent the 0-25%, 25-50%, and 50-75% PDF overlaps, respectively. The red square box in pentad (-4) indicates Northeast Bangladesh.

In summary, the areas around Northeast Bangladesh which have much increased heavy precipitation [Figure 4.5], have low evaporation rates [Figure 4.6]. This is because precipitation locally cools the atmosphere through latent heat release. We have also seen that over Northeast Bangladesh, evaporation decreases further as precipitation increases within the season. This is because when you have a lot of precipitation in an area, the temperature reduces and hence, less evaporation takes place. The same reason is valid for the drastic decrease in evaporation rates over Northeast Bangladesh at pentad (+1) immediately after the onset of the summer rainfall in this region.

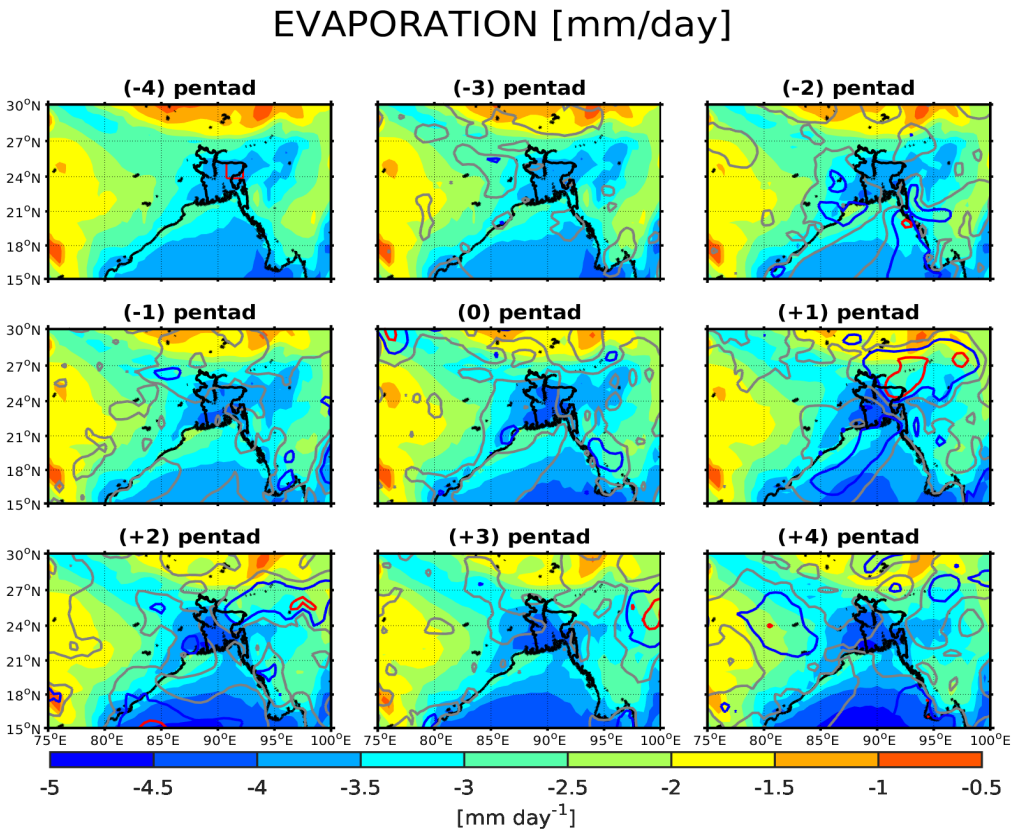

Figure 4.6: As in Figure 4.5, but for evaporation.

4.2.3 Vertically integrated moisture flux and flux divergence

Figures 4.7 and 4.8 show the composites of the vertically integrated moisture flux in the whole tropospheric column prior to and after the onset of the summer rains in Northeast Bangladesh with the zonal and meridional flux PDF overlap, respectively. Generally, we see from these two figures that strong tropical and mid-latitude moisture flux transport influence during the onset of the summer rainfall in Northeast Bangladesh. An increase in the moisture flux in the vertical tropospheric column from 200 - 250 kg m^{-1} s^{-1} before onset pentad (0) to 300 kg m^{-1} s^{-1} and above after onset is observed. The moisture transport pattern also changes from moderate westerly/northwesterly before the onset to strong southwesterly after onset, bringing much moisture from the Bay of Bengal towards northeastern Bangladesh. Figure 4.7 shows a moderate regime transition in the zonal moisture flux at pentad (+1) with 25 - 50% overlap in the PDFs at almost every grid point across entire Bangladesh and the surrounding parts of India. A more drastic regime transition in moisture fluxes is observed at pentad (+1) with the meridional flux showing a significant lower percentage overlap of 0 - 25% (red line) just along the western coast of the Bay of Bengal and western border of Bangladesh, enclosed by a moderate overlap of 25 - 50% that covers entire Bangladesh, as well as some parts of the Bay of Bengal and India [Figure 4.8]. This suggests that the meridional component of moisture flux changes from moderate northwesterly to strong southwesterly flow at the western coast of the Bay of Bengal and western border of Bangladesh. Also a 25 - 50% overlap shows up in the onset

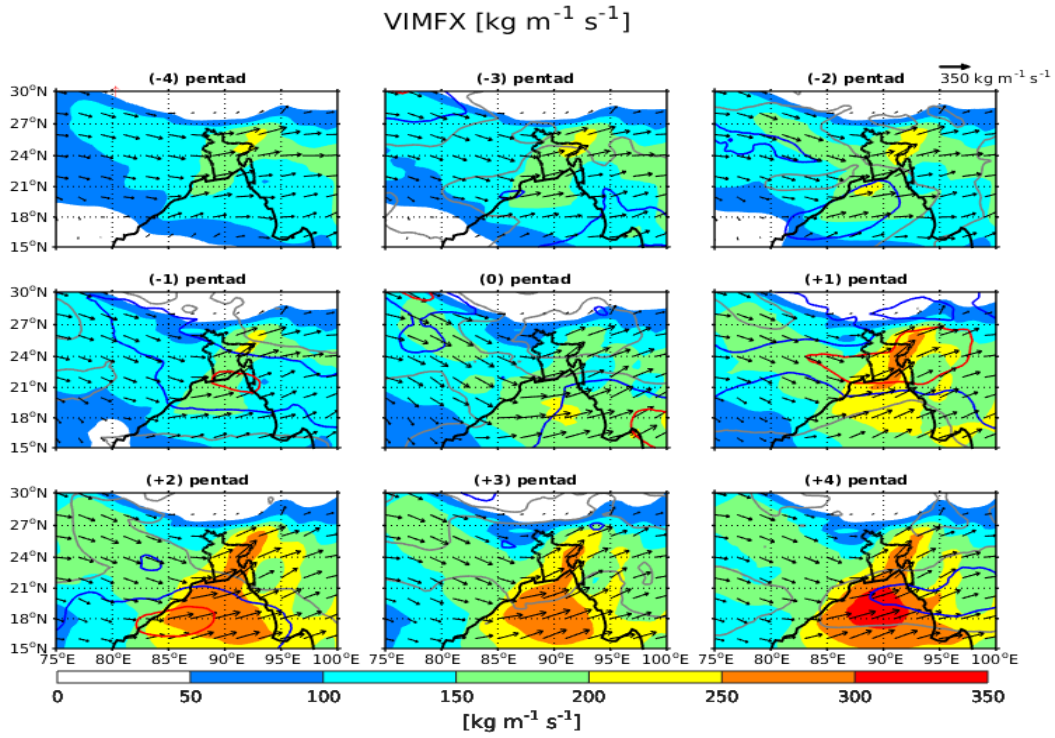

Figure 4.7: Lead-lag composites of vertically integrated moisture flux (VIMFX) in the whole tropospheric column with the zonal moisture flux PDF overlap. The contour lines in red, blue, and grey colour represent the 0-25%, 25-50%, and 50-75% PDF overlaps, respectively.

pentad (0) in India where we have a high meridional moisture flux coming from northwest [Figure 4.8]. This implies that a moderate change in moisture transport is exhibited by the meridional moisture flux component in India during the onset of the summer rains in Northeast Bangladesh. It further signifies that the meridional component of moisture flux has a strong influence on the moisture flow pattern on the build up to the onset of the summer rainfall in Northeast Bangladesh.

The vertically integrated moisture flux is further divided into two parts; the lower part (surface up to 600 hPa level, Figure 4.9), and the upper part (600 to 100 hPa level, Figure 4.10). This illustrates the vertical structure of moisture flux. In the lower troposphere, the moisture transport is strongly influenced by the low-level strong southwesterly flow from pentad (+1) onwards, while in the upper troposphere, moisture transport is strongly influenced by the westerly flow. Figure 4.9 reveals that much of the moisture in the tropospheric column is contained in the lower levels over Northeast Bangladesh with about 150 - 210 kg m^{-1} s^{-1} before the onset, followed by a drastic increase to about 30 - 60 kg m^{-1} s^{-1} at pentad (+1) immediately after the onset. From pentad (+1) onwards, a gradual increase in the moisture flux exists in the lower troposphere within the season. Figure 4.10 reveals that the upper-level moisture flux blows eastward across Bangladesh, with upper-level westerlies providing the main transport mechanism. Moisture transport in the upper troposphere is very small across Bangladesh, with flux vectors and magnitudes of 20 - 30 kg m^{-1} s^{-1} before the onset, and a slight increase of about 10 kg m^{-1} s^{-1} in Northeast Bangladesh after the onset. Over Northeast Bangladesh, the moisture flux

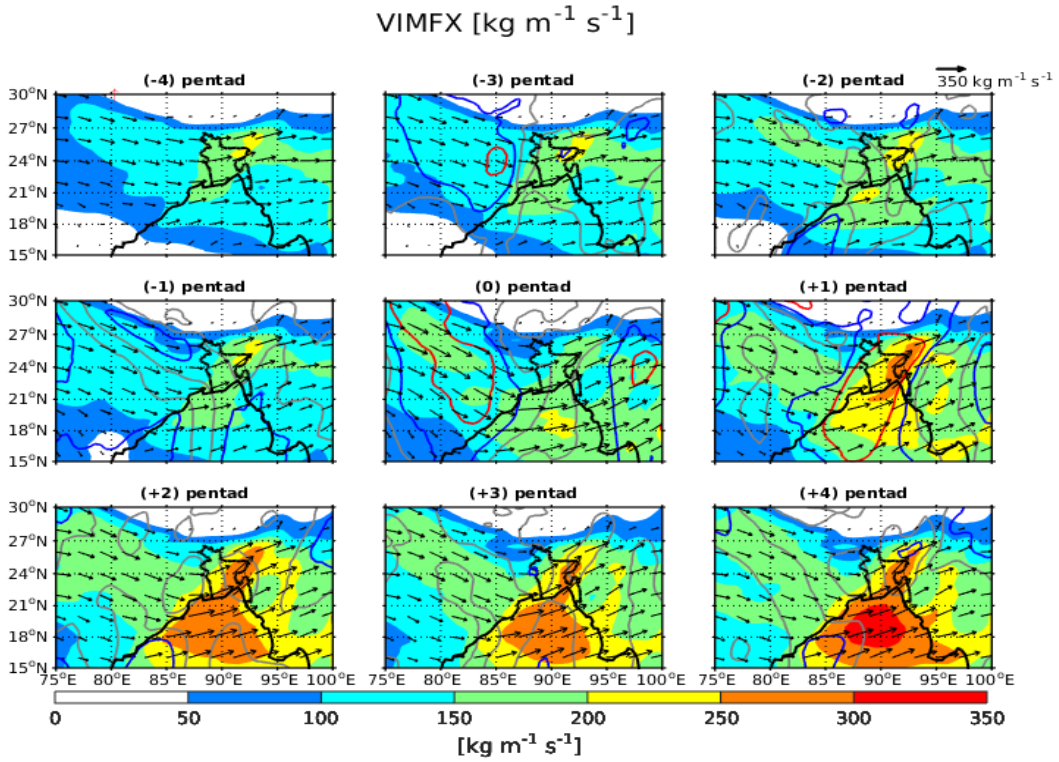

Figure 4.8: As in Figure 4.7, but with the meridional moisture flux PDF overlap.

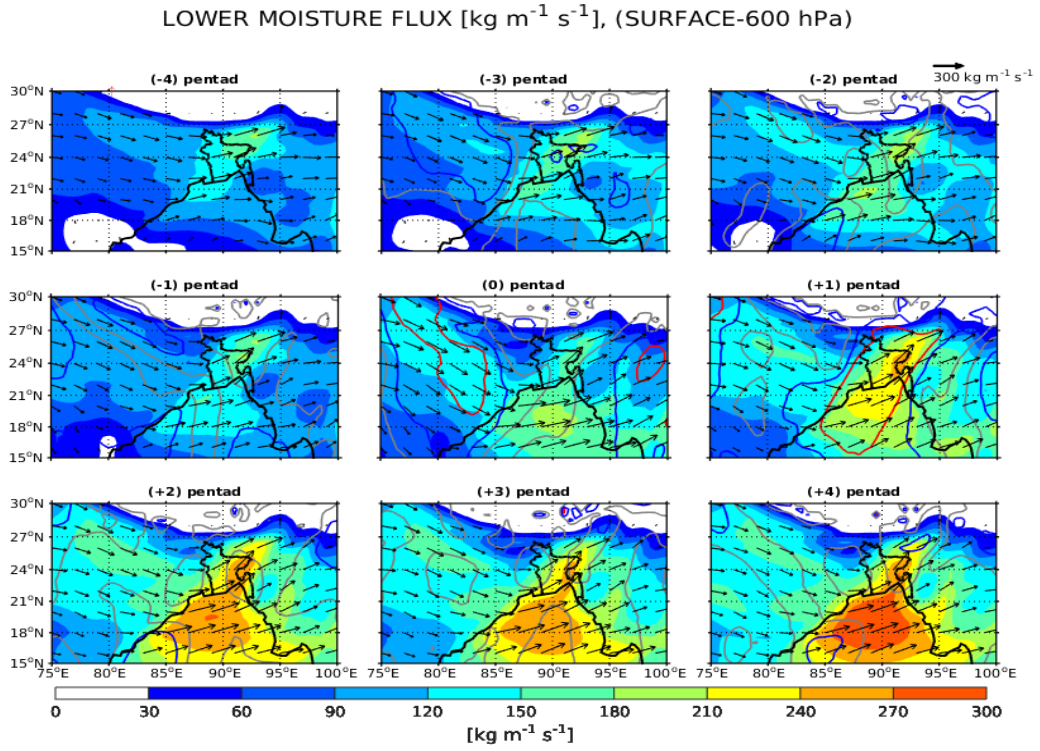

Figure 4.9: As in Figure 4.7, but for lower-level troposphere (surface - 600 hPa) in kg m^{-1} s^{-1}.

in the upper layer can reach 30 - 40 kg m^{-1} s^{-1} after the onset, accounting for 12% - 13% of the total tropospheric column moisture flux (250 - 300 kg m^{-1} s^{-1}). This shows that the contribution of the upper-level moisture flux to the vertical integral of moisture

flux over Northeast Bangladesh is so small compared to the contribution of the lower level moisture transport. Although the context is different, Simmonds et al. [1999] found similar characteristics of the vertical moisture flux distribution over China during the summer.

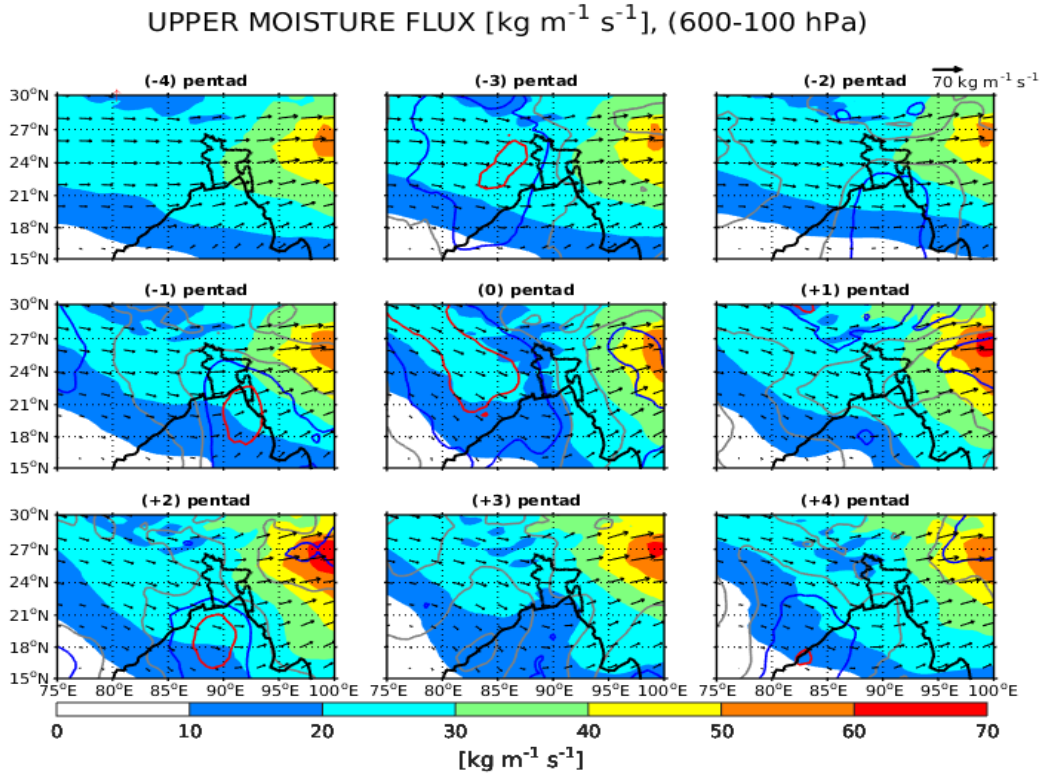

Figure 4.10: As in Figure 4.7, but for upper-level troposphere (600-100 hPa) in kg m^{-1} s^{-1}.

The lead-lag composites of the vertically integrated moisture flux divergence, here considered as total water convergence (TWC) [Figure 4.11] reveal that a lot of moisture converges around the Meghalaya Plateau, the Himalayas, and other elevated topography around Northeast Bangladesh. There is also a moderate to strong area of moisture convergence with about 15 - 20 mm/day, present in the extreme north end of the Brahmaputra Valley from pentad (-4) through pentad (+4) that is seen to increase gradually as the onset builds up and only increases its intensity to 30 mm/day after the onset [Figure 4.11]. This area of moderate to strong moisture convergence corresponds with the moderate to strong area of precipitation [Figure 4.5], and the area with the lowest evaporation rate [Figure 4.6]. Thus, this points to a strong link between moisture convergence, precipitation, and evaporation over this region. At pentad (+1), a clear regime transition in the vertical moisture flux convergence manifests over the areas covering the Meghalaya Plateau, the Brahmaputra valley, the whole northern, as well as some parts of central and eastern Bangladesh [red contour in Figure 4.11]. The moisture convergence in Northeast Bangladesh increases from 5 mm/day to 20 mm/day, and thereafter spreads along the northern and eastern borders of Bangladesh. But prior to the onset, the areas near the lower eastern coast of Bay of Bengal experience a strong regime transition in the moisture convergence [red contour at pentad (-1) in Figure 4.11]. This implies that the moisture first converges over the lower eastern coast of the Bay of Bengal before advecting north-

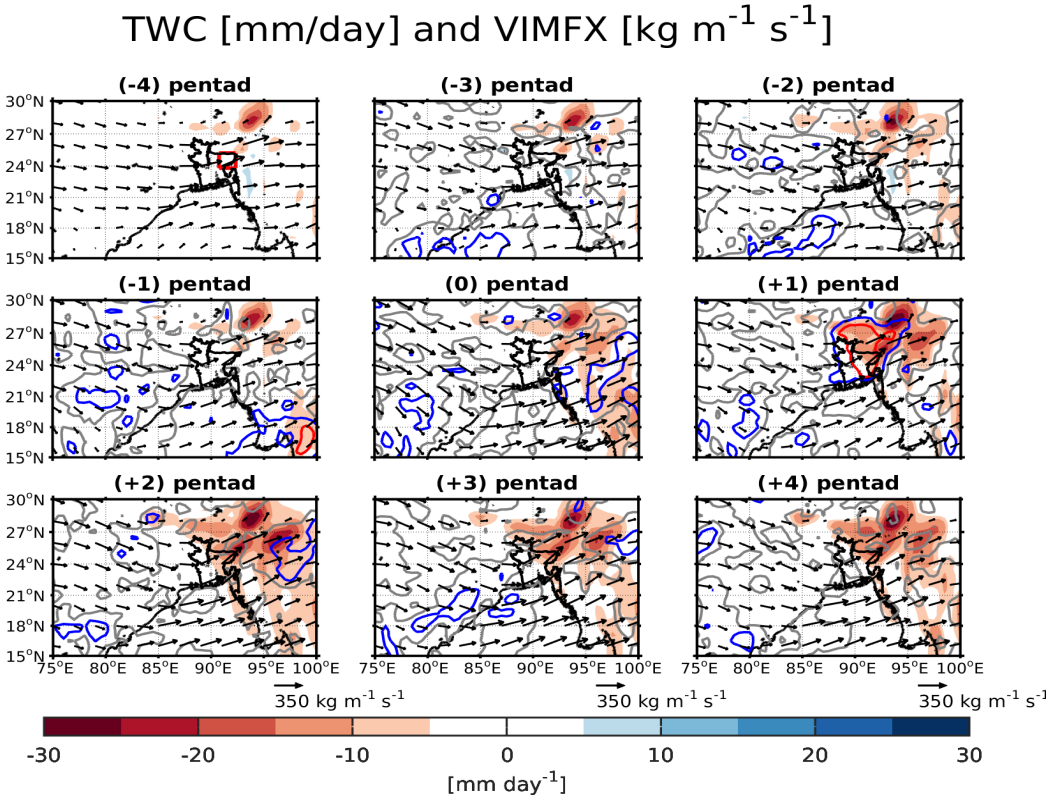

Figure 4.11: As in Figure 4.7, but for total water convergence (TWC) in mm/day, with vertically integrated moisture flux in kg m^{-1} s^{-1}.

westward towards Northeast Bangladesh. We can not leave this unnoticed that most parts of our domain show less moisture convergence or divergence of between -5 to 5 mm/day, and there is also a weak signal of moisture divergence around the lower eastern border of Bangladesh with less than 10 mm/day from pentad (-4) to pentad (-2).

Overall, this analysis reveals that much of the moisture flowing into Bangladesh comes from the Bay of Bengal, transported by the low-level southwesterlies towards Northeast Bangladesh, and that much of it is contained in the lower to mid-troposphere. This southwesterly moisture flux inflow enhances moisture convergence over Northeast Bangladesh and the surrounding mountainous areas after onset and hence, high chances of increased rainfall. It is also observed that the areas with strong moisture convergence receive heavy precipitation, and have low evaporation rate too. This attests the strong link between moisture convergence, precipitation, and evaporation. The analysis has also shown that the Meghalaya Plateau and the other mountains to the east of Northeast Bangladesh play a significant role in overturning the low-level warm moist air coming from the Bay of Bengal, and hence strong moisture convergence over Northeast Bangladesh. Further more, the analysis has shown that the meridional component of the low-level southwesterly moisture transport towards Northeast Bangladesh plays an important role in the formation and increasing rainfall over Northeast Bangladesh. It can be argued that the abundant supply of moisture by the low-level southwesterlies from the Bay of Bengal, coupled with its blocking by the Meghalaya Plateau and the other high-elevated topography east of Northeast Bangladesh leads to the development of the precipitation systems during the

months of March-May as suggested by Rafiuddin et al. [2010, 2013].

By taking a close look at the three moisture variables (precipitation, evaporation and vertically integrated moisture flux divergence/convergence), the balance in the atmospheric water vapour is closely established over Northeast Bangladesh and the surrounding mountainous areas. This is because mountains north and east of Northeast Bangladesh tend to block much of the moisture that comes from the Bay of Bengal, turning the area into a moisture convergence zone (moisture sinks). And when the moist winds are forced to rise over these mountains, a lot of condensation occurs higher up, which results into precipitation.

4.2.4 Total Column Water

The lead-lag composites of total column water in the atmosphere reveal a gradual increase in the total column water from pentad (-4) to pentad (+4), with a clear build up to the onset (pentad (0)) and a great deal of water in the atmospheric column from the onset onwards [Figure 4.12]. The amount of water in the atmospheric column increases from 34 - 42 kg m^{-2} before onset (pentad (0)) to 42 kg m^{-2} and above from onset onwards.

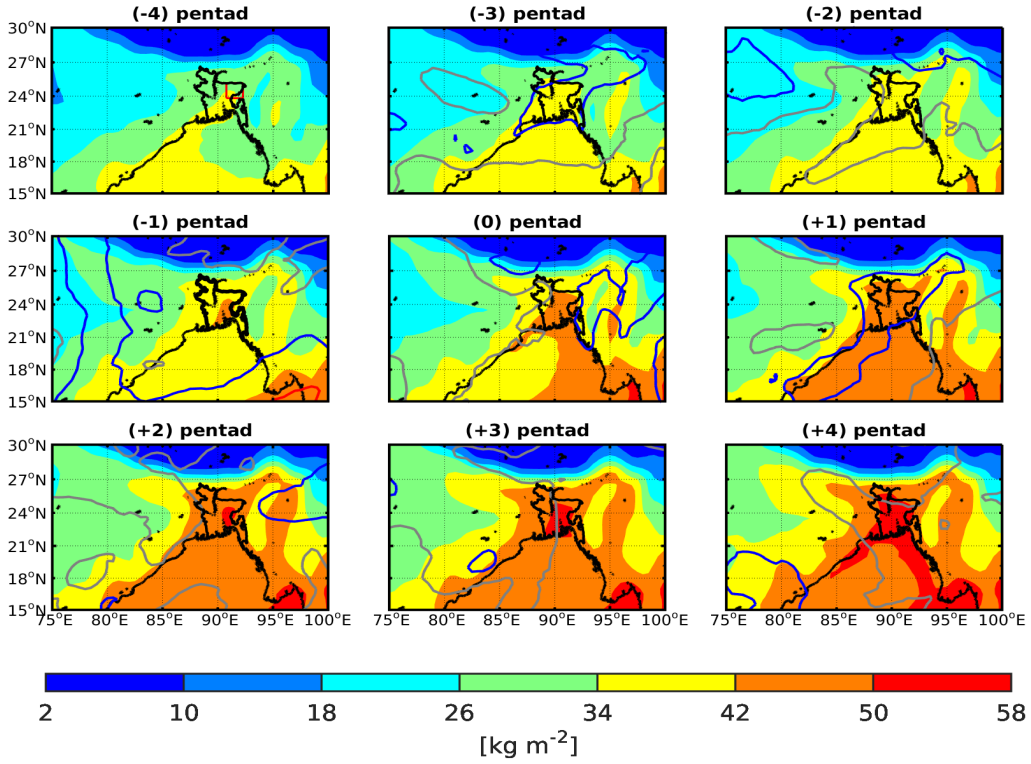

Figure 4.12: Lead-lag composites for total column water in the atmosphere. The red contour, blue contours and the grey contours show 0-25%, 25-50%, and 50-75% overlap of the PDFs with the neighbouring pentads at the same grid points, respectively. The red square box in pentad (-4) shows Northeast Bangladesh.

This continuous increase of the total column water as the onset nears indicates an increase in the precipitable water content towards the onset of summer rains. A drastic increase in the total column water is seen at pentad (-1) at the lower end of the eastern coast of

Bay of Bengal, where a 0 - 25% PDF overlap manifests over those grid points [Figure 4.12]. This drastic increase in total water in the atmospheric column we see around this region can be attached to the drastic increase in moisture convergence over this region during this period [see pentad (-1), Figure 4.11]. From Figure 4.12 still, we see that the bulky of the moisture in the atmospheric water column comes from Bay of Bengal and spreads northward over Bangladesh. A continuous decrease of total column water as you move northward away from the tropics is clearly seen in Figure 4.12, which attests to the fact that tropics hold more moisture than high latitudes due to the Clausius-Clapeyron relation [1]. Since the atmospheric water vapour is very important for both convection and precipitation to occur, the much water in the atmospheric column over Northeast Bangladesh during this period favours the onset the summer rains.

4.2.5 Specific Humidity

Figures 4.13 to 4.15 show the lead-lag composites for specific humidity at 925, 850, and 600 hPa level. Figure 4.13 shows generally a gradual increase in specific humidity at 925 hPa from pentad (-4) to pentad (+4) across Northeast Bangladesh , but with remarkable increase of 2 g/kg from onset (pentad (0)) to pentad (+1). This remarkable increase is also indicated in the enclosure of the blue contours in pentad (+1), [Figure 4.13]. The same figure also reveals that there is much moisture near the surface in Northeast Bangladesh prior to the onset of the summer rainfall in this region, which later spreads across the country as the rain season sets in. There is also a discontinuity between hot and dry cooler air over India near western Bangladesh and the warm moist air over Bangladesh, starting from pentad (-2) onwards, and becomes more clear after the onset (pentad(0) to pentad (+4), [Figure 4.13]. This discontinuity is a manifest of a dry-line, separating the warm moist air over Bangladesh and the hot and dry cooler air mass over India at this level. The warm moist low-level air over Bangladesh comes from the Bay of Bengal being transported by the southerly/southwesterly winds that prevail during this period [Figure 4.9]. When these two air masses interact, they create unstable conditions that are favourable for the development of convection along this dry-line as suggested by Weston [1972]. This interaction can also help in the development of ATSs, which are also described as squalline type of precipitation systems by Rafiuddin et al. [2010].

At 850 hPa [Figure 4.14], the dry-line still shows up though it is not well defined as it was at 925 hPa level. The moisture at 850 hPa also shows a gradual increase as a build up to the onset, with a more defined increase of 2 g/kg in specific humidity from 10 - 12 g/kg to 12 - 14 g/kg over Northeast Bangladesh occurring from onset pentad (0) to pentad (+1) and later across the whole country and the neighbouring parts of eastern India and Myanmar. This characteristic increase or change in moisture content at 850 hPa over Northeast Bangladesh after the onset is clearly shown by the red contour at pentad (+1).

[1] see Appendix C

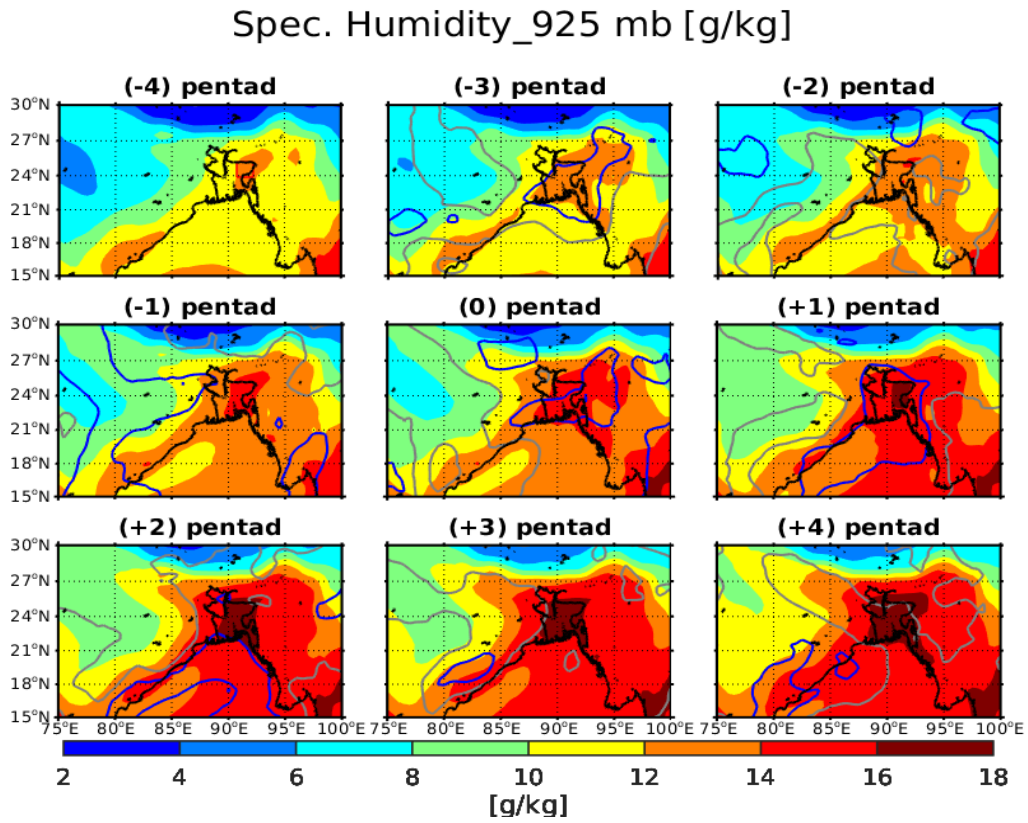

Figure 4.13: Lead-lag composites of specific humidity at 925 hPa level. The red- square box in pentad (-4) indicates Northeast Bangladesh. The blue, and gray contours show 25 - 50%, and 50 - 75% overlap of the PDFs with neighbouring pentads at the same grid point.

At 600 hPa [Figure 4.15], the moisture becomes less over Northeast Bangladesh and the whole country with 2 g/kg before the onset, and a slight increase of 1 - 2 g/kg after the onset. This slight increase in moisture after the onset is also captured by the transitional overlap of the PDFs at 25 - 50% [blue contours in Figure 4.15]. A more significant change in the moisture content at 600 hPa is observed in pentad (-1) on the lower eastern coast of Bay of Bengal, with a 0 - 25% overlap. Also a trace of the Indian-Myanmar Trough (IMT) is clearly discernible at this level.

In summary, Figures 4.13 - 4.15 show a drastic decrease of moisture with height across Northeast Bangladesh, (i.e., from 10 - 18 g/kg at 925 hPa to 2 - 5 g/kg at 600 hPa). This drastic decrease in specific humidity shows that the moist layer is quite shallow across Northeast Bangladesh, with much moisture only confined to the lower levels. The huge amount of moisture at these lower levels can be attributed to the strong low-level southerly/southwesterly flow of moist winds from the Bay of Bengal across Bangladesh towards Northeast Bangladesh.

Further more, Figures 4.13 to 4.14 revealed that the dry-line near western Bangladesh is quite shallow since it is only confined to lower-levels. Even though this dry-line is quite shallow, it can cause convective instabilities even at higher levels that may result in the development of convective systems along it. These convective systems may eventually move eastward towards Northeast Bangladesh as a result of moderate strong westerlies in

the mid-troposphere. This argument is in line with the findings of Rafiuddin et al. [2013] who suggested that the convective instabilities that result in development of convective systems are a result of the southerly moist air inflow at lower levels, and that they are later intensified by moderate to strong westerlies in the mid troposphere.

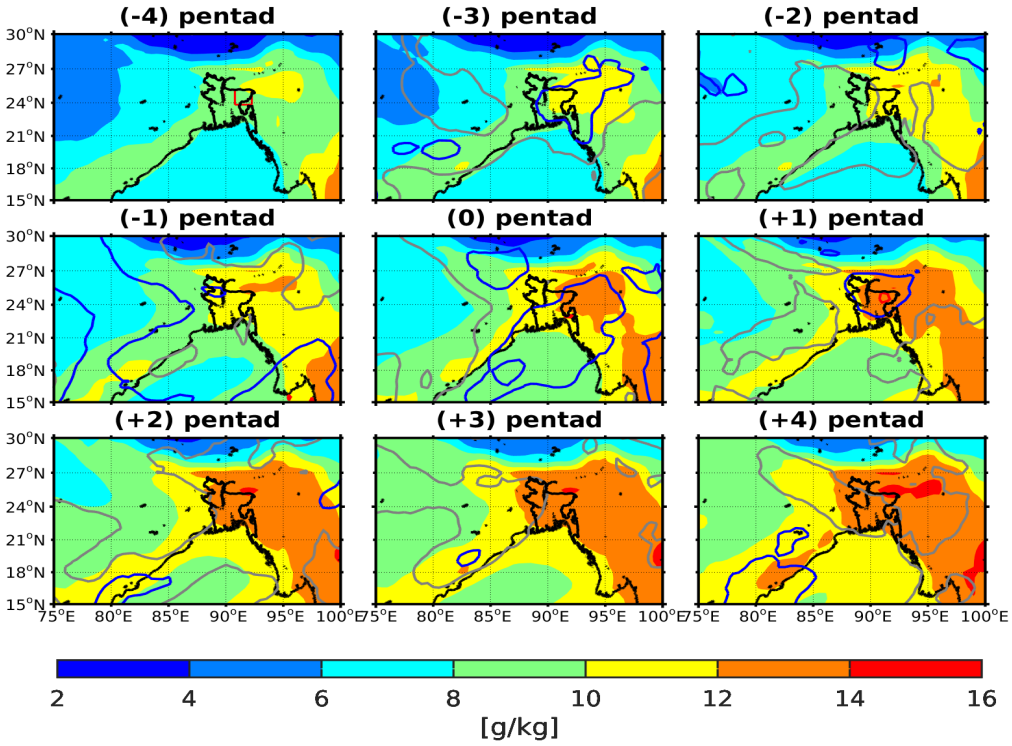

Figure 4.14: As in Figure 4.13 but for 850 hPa level, and the red contour in pentad (+1) shows 0-25% overlap of the PDFs with the neighbouring pentads at the same grid point

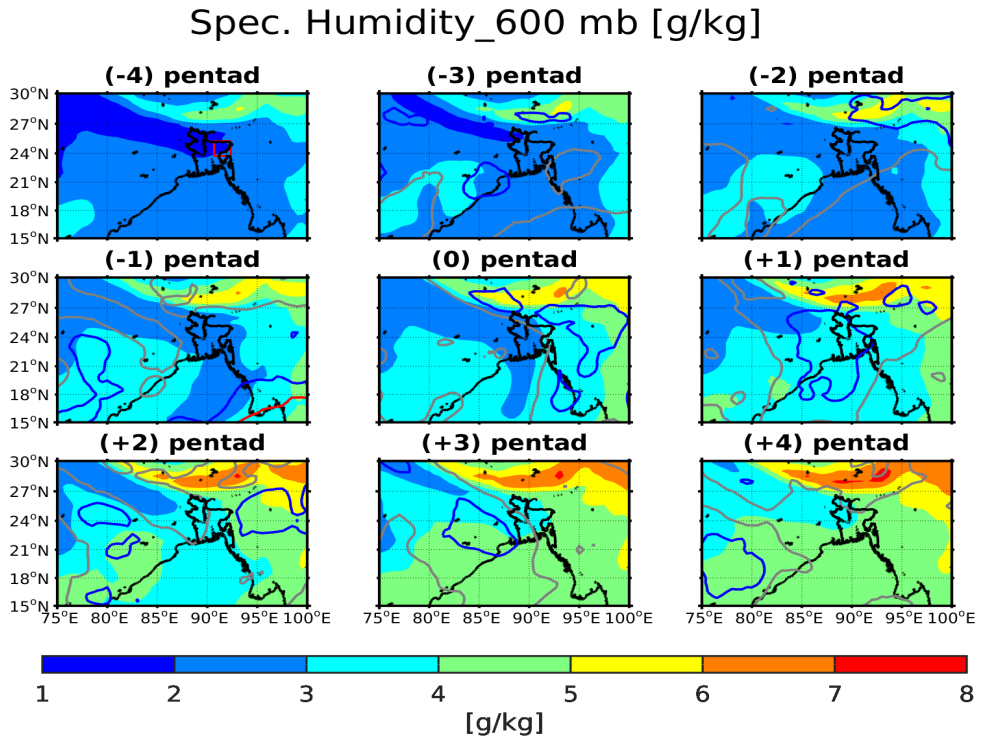

Figure 4.15: As in Figure 4.13 but for 600 hPa level, and the red contour in pentad (-1) shows 0-25% overlap of the PDFs with the neighbouring pentads at the same grid point

It is also seen from Figures 4.13 - 4.15, that there is no clear-cut transition in the specific humidity field near the surface (at 925 hPa level) and at upper-levels but rather a gradual increase of moisture from pentad (-4) to pentad (+4). This means that it may not need a drastic increase or change in the moisture pattern for convection to occur, but rather a manifestation of a drastic increase or change in any other variables may act in combination with moisture to influence convection in Northeast Bangladesh.

4.3 Synoptic Conditions before and after onset

In the previous section, we looked at moisture sources and the seasonal evolution of the summer rains. We learnt that much of the moisture first converges around the Meghalaya Plateau and other elevated topography in the vicinity of Northeast Bangladesh before it converges over Northeast Bangladesh at the onset of the summer rains, and also the heavy precipitation over Northeast Bangladesh spreads from these elevated topographic feature. So now we look at the synoptic conditions prior to, and after the onset of summer rains in Northeast Bangladesh. The results are split according to the different parameters used in this study and are as presented below:

4.3.1 Mean Sea level pressure

The mean sea level lead-lag composites [Figure 4.16] reveal the development of a shallow low pressure system in India, with its trough extending towards Bangladesh. The low pressure system starts to manifest from pentad (-3) with its center between 1004 and 1006 hPa, extending towards western Bangladesh. This low pressure system deepens, and its trough extends further into Bangladesh and past Bangladesh during the build up to the onset of summer rains. A more shallow deepened low pressure system with its centre at 1000 hPa is seen at pentad (+1) confined to India, with its trough now stronger and covering the whole of Bangladesh [Figure 4.16]. From pentad (+1), the low pressure centre extends further northwestward in India and southeastward towards western Bangladesh. The surface pressure lowers as a result of warm rising air, which later cools aloft to become more dense and form clouds. This in the end results in cold air rushing to fill the low pressure area, forcing more warm air to be displaced upwards, and hence the low pressure system deepens. The deeper the low pressure system becomes, the faster the cyclonic vorticity and circulation. This hypothesis suggests that when the low pressure system becomes further deeper from onset, the winds also become stronger, which in the end results in advection of more moisture towards Northeast Bangladesh, and hence, convectivity is enhanced around Northeast Bangladesh. To support this, Ohsawa et al. [2000] suggested that the rainfall increases when the trough is situated at the foot of the Himalayas as a result of the synoptic-scale convective activity being much more vigorous to the south of the trough axis.

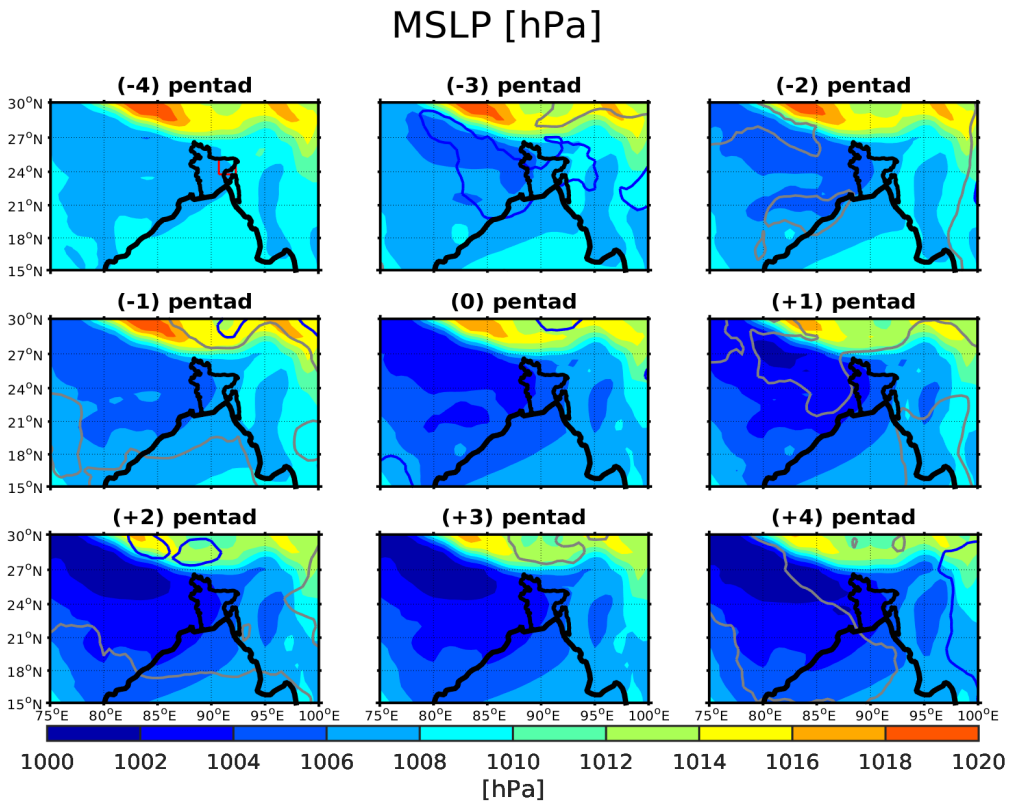

Figure 4.16: Lead-lag composites for Mean sea level pressure. The blue contours show 25 - 50% overlap of the PDFs with neighbouring pentads at the same grid point, while the gray contours represent the 50 - 75% overlap of the PDFs.

4.3.2 Geopotential height

Figures 4.17 to 4.19 show the lead-lag composites for geopotential height at 700, 600, and 500 hPa, respectively. Lower values of geopotential height at 700, 600, and 500 hPa indicate the troughs in the middle troposphere, while higher values indicate the presence of ridges. At both 700 and 600 hPa in Figures 4.17 and 4.18, respectively, the trough is visible from pentad (-4) prior to the onset, and becomes well developed over Bangladesh starting from the onset (pentad (0)) when it extends further south to about 19°N. This trough is what is termed the India-Myanmar trough (IMT) in this work, which was previously called the India-Burma trough (IBT) [Wang et al., 2011]. Wang et al. [2011] described the IMT to be located between 87.5°E and 100°E, with its mean position being 90°E-92.5°E, while extending from the southern edge of the Tibetan Plateau to about 15°N. Indeed our results in Figures 4.17 to 4.19 affirm to Wang et al. [2011]'s description about the location of the IMT. The IMT deepens over Bangladesh as geopotential height decreases at around 90°E.

Figures 4.17 and 4.18 further reveal that from the onset onwards, the mid-tropospheric anticyclone is clearly confined to India, to the west of this trough. At 500 hPa level, the IMT is not so well defined as it looks to be fading out at this level due to the raising of the 500 hPa geopotential height [Figure 4.19]. The IMT only starts to manifest at pentad

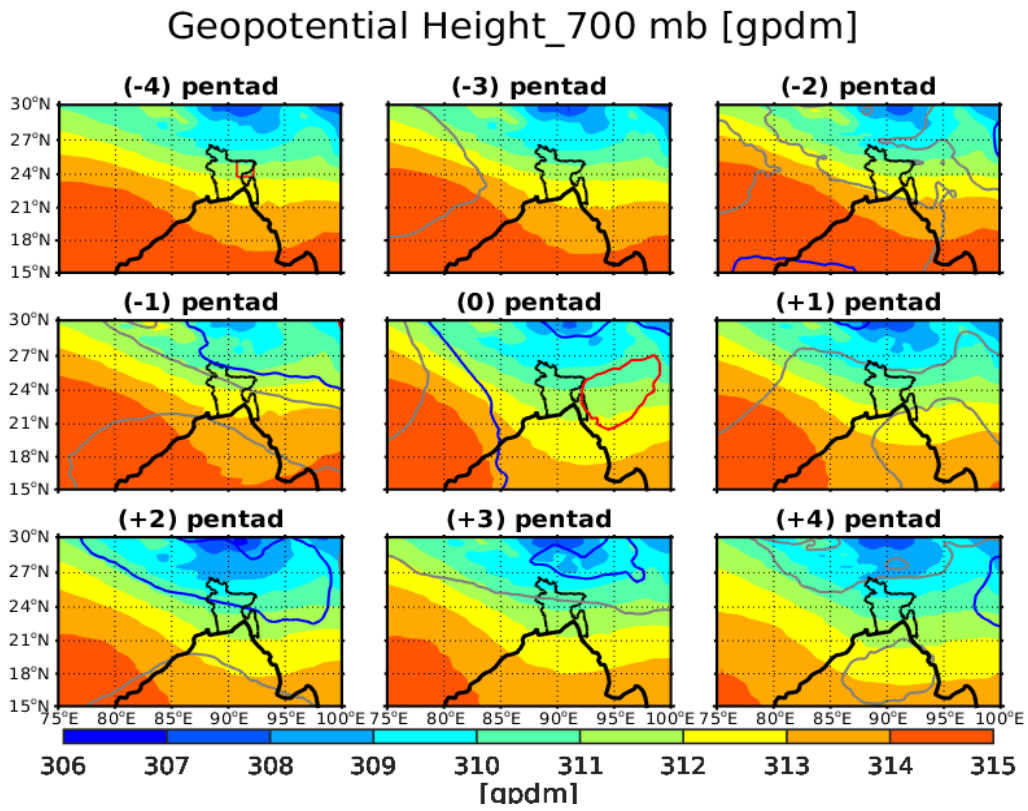

Figure 4.17: Lead-lag composites for geopotential height [gpdm] at 700 hPa. The red contour, blue contours and the grey contours show 0-25%, 25-50%, and 50-75% overlap of the PDFs with the neighbouring pentads at the same grid points, respectively.

(-1) prior to the onset, and becomes more established from onset (pentad (0)) onwards [Figure 4.19]. Incidently, the IMT revealed in Figures 4.17 to 4.19 coincides with the low-pressure trough we saw in Figure 4.16. According to Wang et al. [2011], the IMT is strongly connected to this trough, and influences the southwesterly flow which is present at the low-levels during this period [see Figures 4.21 and 4.25 later]. The southwesterly airflow has a strong link to the onset of the summer rains in Northeast Bangladesh which fall before the beginning of the large-scale monsoon in this region. Matsumoto et al. [2007] linked the IMT to the onset of the summer monsoon season over the South China Sea. Despite the differences in season and region, our results reveal a strong link between the IMT and the onset of the summer rains in Northeast Bangladesh being clearly evident, with precipitation [Figure 4.5] increasing over Northeast Bangladesh as the IMT deepens. After the onset, precipitation over Northeast Bangladesh (east of the trough) show a remarkable increase in its intensity as the IMT further deepens and stretches further eastward, while the regions immediately to the west of the trough-line (such as India) also begin to receive little precipitation. This attests to the strong correlation of the IMT and the summer rainfall in Northeast Bangladesh. Although the seasons may differ, Wang et al. [2011] also confirmed the strong linkage between the winter IMT and precipitation over southern and eastern Asia. During their study, it was found that when the IMT deepens and shifts eastward, regions to its east receive enhanced precipitation while regions to the west of the trough-line (much of India) receive decreased precipitation.

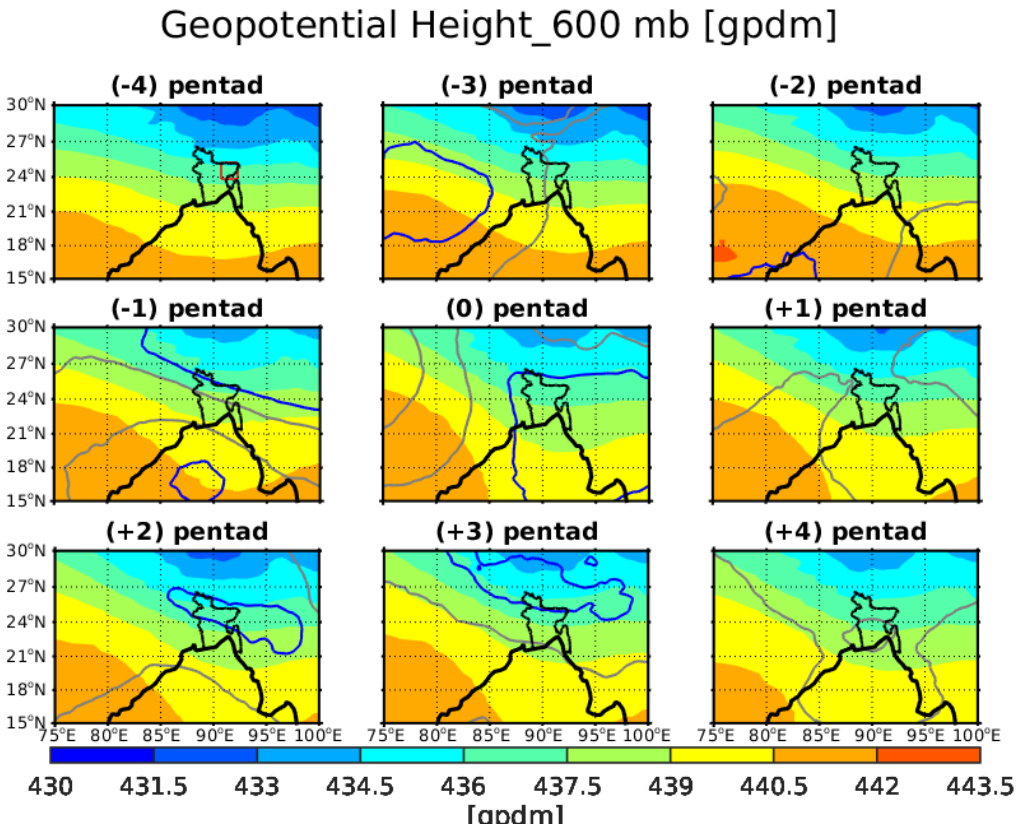

Figure 4.18: As in Figure 4.19, but for 600 hPa level

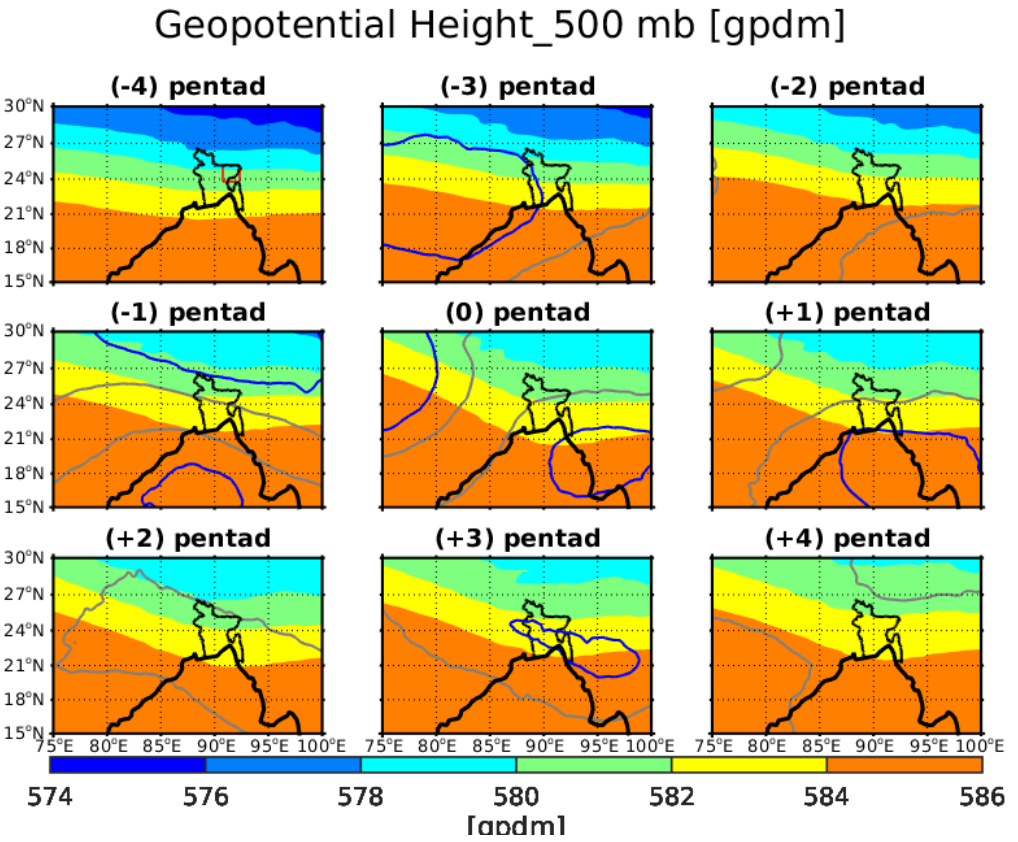

Figure 4.19: As in Figure 4.19, but for 500 hPa level

4.3.3 Wind and Temperature at different isobaric levels

In this section, we consider wind and temperature at 925, 850, 600, and 200 hPa levels to assess the conditions prior to the onset and after the onset of summer rains. The lead-lag composites of both wind and temperature at these pressure levels are obtained from the ERA-I reanalysis data using onset dates [see section 3.1].

4.3.3.1 Wind and Temperature at 925 hPa

Figure 4.20 presents the lead-lag composites of temperature at 925 hPa level. From this figure, we see a thermal (heat) low with temperatures of about 301 - 303 K developing from pentad (-4) over India. The heat low starts to intensify to temperatures of about 303 - 306 K from pentad (-2) and extends closer to the western parts of Bangladesh as a build up to the onset of the summer rains in Northeast Bangladesh. From onset onwards, the heat low becomes well developed and more intense, extending even closer to Bangladesh. This in turn makes Bangladesh to be located at the eastern edge of the thermal low. The heat low is caused by the intense rapid insolation and surface heating of the Indian land surface during the months of March - May. A quick notice is that the heat low and the low pressure system [Figure 4.16] are collocated. This is not surprising because the strong solar heating during this period makes the air in the lower troposphere warmer, less dense, and eventually rise up, hence creating a void that is instantly filled up by the surrounding cooler air. This in turn lowers the surface pressure, and thus a low pressure area is created where the heat low is situated. In a similar argument, Allcock and Ackerley [2015] described the heat low as a low pressure area created after warm air rises during the daytime strong solar heating. When the heat low intensifies, the low pressure system further deepens [see Figure 4.16]. Saeed et al. [2011] found a strong link between the intensification of the heat low and the significant decrease in pressure over the Arabian Sea.

Figure 4.20 also reveals that the temperature over Northeast Bangladesh and the surrounding areas to its west and south is about 296 - 298 K before the onset (pentad (0)), and remain the same during the onset period up to pentad (+4) in the areas to the west and south of Northeast Bangladesh, whereas the temperature over Northeast Bangladesh suddenly drops down by about 3 - 5 K immediately after the onset from pentad (+1) onwards. The sudden drop in temperature over Northeast Bangladesh shows a clear transition of the temperature regime after the onset of the summer rains in the region. This clear transition (0 -25% PDF overlap) in temperature regime from onset to pentad (+1) is also visible in areas north of Northeast Bangladesh and around the eastern coast of the Bay of Bengal, while the whole of eastern Bangladesh, Myanmar, areas around the eastern coast of the Bay of Bengal, and the Meghalaya plateau exhibit a moderate change (25 - 50% PDF overlap) in temperature regime during the onset [Figure 4.20]. The drop in temperature over Northeast Bangladesh from pentad (+1) onwards, makes Northeast Bangladesh cooler than all the other surrounding areas to its west and south [Figure 4.20].

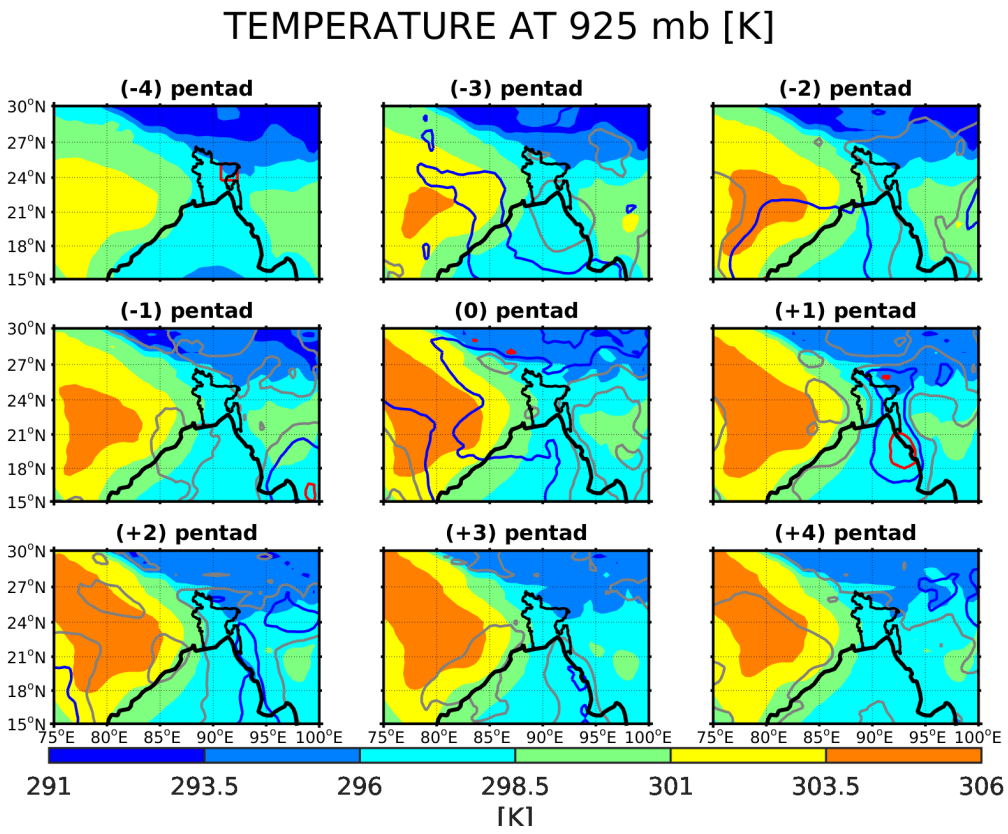

Figure 4.20: Lead-lag composite of temperature at 925 hPa.The red- square box in pentad (-4) indicates Northeast Bangladesh. The red,blue, and grey contours show 0-25%, 25-50%, and 50-75% overlap of the PDFs with neighbouring pentads at the same grid point, respectively.

The cooling could be a result of the evaporative cooling from the intensive rain we see from pentad (0) onwards [Figure 4.5]. This cool air could be trapped in the region due to the surrounding topography such as the Meghalaya Plateau to its north, and other mountains to the east of Northeast Bangladesh. Kataoka and Satomura [2005] observed a similar scenario of the cooling over Northeast Bangladesh relative to surrounding areas during their simulations of the diurnal cycle of precipitation in June 1995. They referred this cooling over Northeast Bangladesh to the existence of a cold pool of air, which they later found to trigger precipitation over the region through lifting of the low-level moist southwesterly flow to LFC below the height of the Meghalaya Plateau. Although the seasons may differ, our results support the conclusions of Kataoka and Satomura [2005].

Figures 4.21 to 4.23 reveal a strong low-level warm moist southwesterly winds flowing from the western coast of the Bay of Bengal across Bangladesh, directed towards Northeast Bangladesh. From pentad (-4), we see a moderate northwesterly flow of about 4 - 6 m/s from India, and later turns into moderate southwesterlies at the western coast of the Bay of Bengal as the onset nears. There are places around the eastern coast of the Bay of Bengal that experience a significant change in wind speeds at pentad (-1) and onset pentad (0). However, a clear transition from moderate to strong moist southwesterly flow of about 8 - 10 m/s directed towards Bangladesh manifests along the western coast of the Bay of Bengal, the whole of southern, central, eastern and western parts of Bangladesh [Figure

4.21]. This clear transition in the wind regime at 925 hPa from onset (pentad (0)) to pentad (+1) is shown with a 0 - 25% overlap in PDFs at every grid point (red contour in pentad(+1), Figure 4.21).

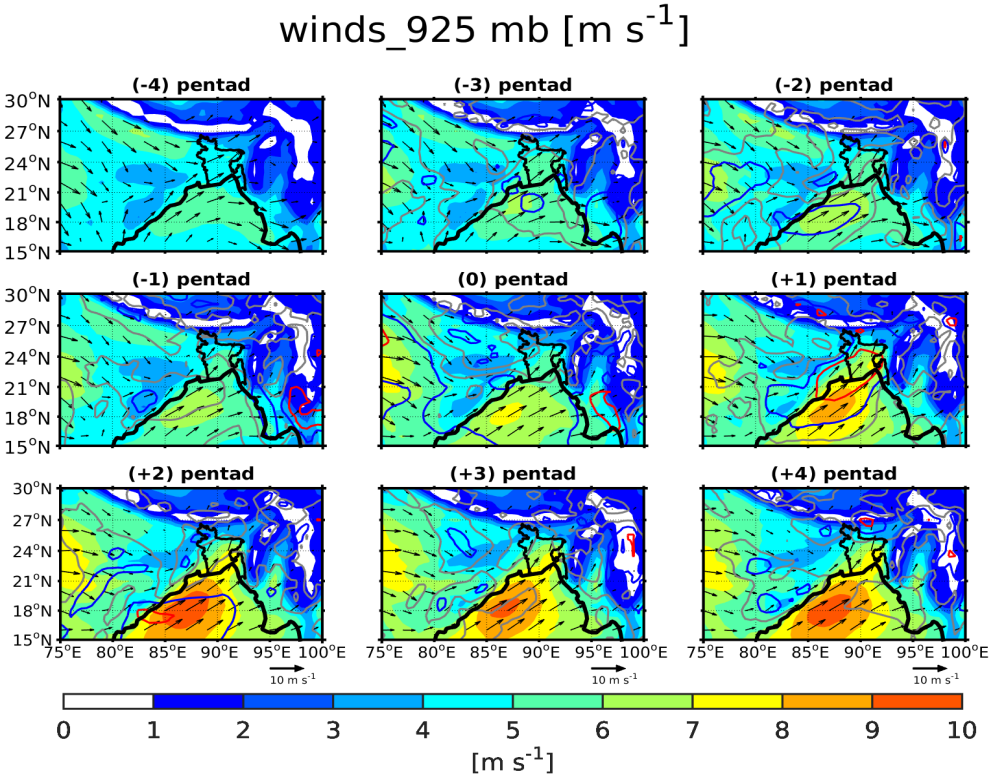

Figure 4.21: Lead-lag composites for winds at 925 *hPa* level with wind speed PDF overlap. The red, blue, and grey contours show 0-25%, 25-50%, and 50-75% PDF overlaps, respectively.

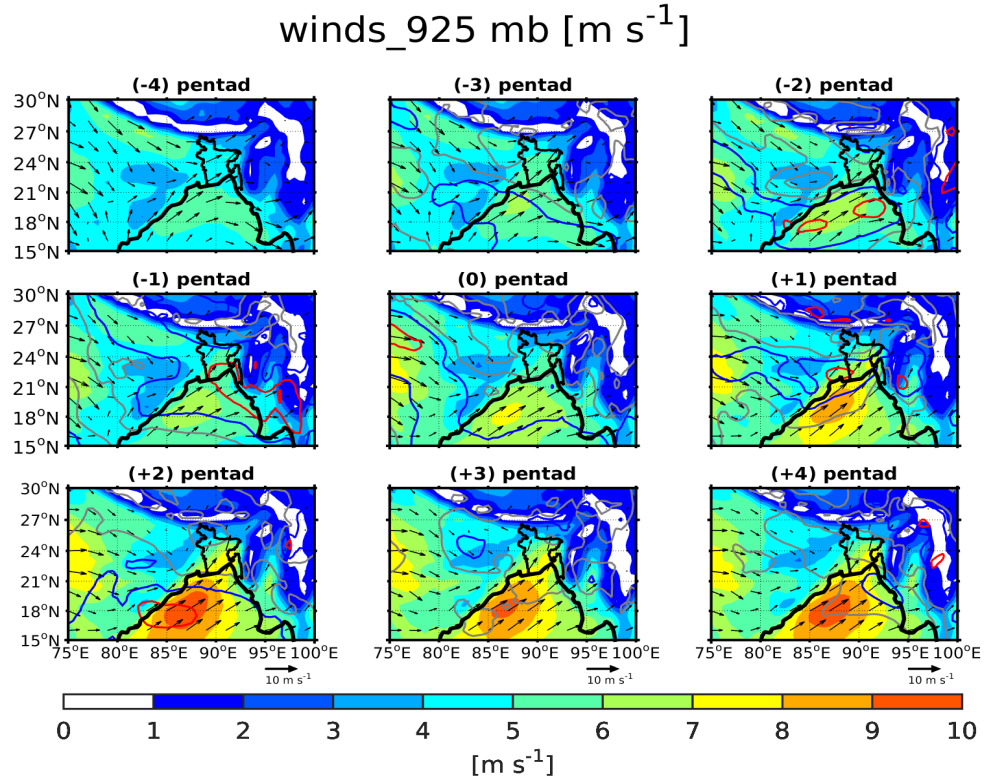

Figure 4.22: As in Figure 4.21, but with zonal wind PDF overlap.

Thereafter, the southwesterlies gradually continue to become stronger within the season. The zonal component of the southwesterly winds at 925 hPa show a significant change starting two pentad prior to the onset [i.e., pentad(-2) and pentad(-1), in Figure 4.22], where the 0 - 25% overlap of the PDFs occur in Bay of Bengal, the lower southern end of Bangladesh, eastern coast of the Bay of Bengal, and parts of Myanmar. At pentad (+1) immediately after the onset, a clear transition in the zonal wind component is seen at the boundary between the upper western coast of the Bay of Bengal, India, and southwestern Bangladesh. Figure 4.23 shows a clear transition in the meridional wind component covering the whole of Bangladesh, parts of India, and Bay of Bengal at pentad (+1) with 0 - 25% PDF overlap. Figure 4.23 also reveals that the transition in the wind pattern at onset is strongly influenced by the meridional component of wind compared to what the zonal component contributes to this transition.

Conclusively, Figures 4.21 - 4.23 show that the southwesterly flow of wind regime at 925 hPa during the onset of the summer rains in Northeast Bangladesh agrees with the conditions of the low-level atmospheric circulation during onset of the large-scale monsoon season over Bangladesh suggested by Zhang and Wang [2008]. The presence of the stronger winds over the Bay of Bengal at pentad (+1) onwards, suggests a possibility of having sea breeze circulations during this period. We say this because when we combine the prevailing southwesterly winds with the surface temperature gradient [Figure 4.20], we can see conditions that are favourable for the development of the daytime sea breeze circulation. As the sea breeze propagates inland during the nighttime, it could trigger convection. In another location in the sub-tropics, Simpson et al. [2007] showed that 70 - 80% of the rainfall over Chennai during the southwest monsoon is due to the sea

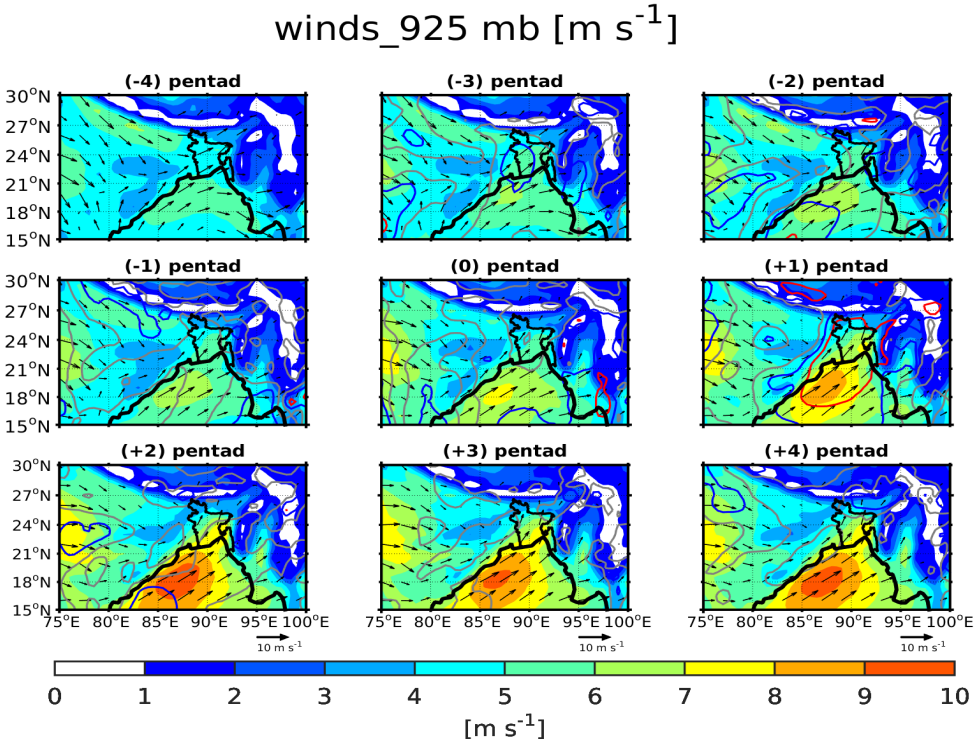

Figure 4.23: As in Figure 4.21, but with meridional wind PDF overlap.

breeze induced convection. Partially, we also speculate that the sea breeze circulations can be among the mesoscale mechanisms responsible for either initiation or increase of the rainfall we see over Northeast Bangladesh [Figure 4.5] during the summer months of March to May.

4.3.3.2 Wind and Temperature at 850 hPa

Figure 4.24 also shows the development of the heat low at 850 hPa from pentad (-4), and intensifying with the build up to the onset (pentad (0)). The temperatures of this well distinguished feature now range between 294 K at pentad (-4) to about 300 K from pentad (-3) onwards. But as the heat low intensifies and becomes well established, it extends closer to western Bangladesh. On the other hand, the temperatures in Northeastern Bangladesh are between 290 - 292 K at pentads (-4), (-3), and (-2), but they increase by 2.5 K to 294.5 K at pentad (-1) to become uniform like in all other parts of Bangladesh [Figure 4.24]. From pentad (-1), the temperatures remain constant at 294.5 K throughout the whole country at the onset and the rest of the pentads thereafter. This implies that temperatures at this level do not vary much before and after the onset of the summer rains in Northeast Bangladesh. But two notable features are; 1) the temperatures are greater than 273 K, which implies that warm cloud process can occur, and 2) the heat low over India is still well developed and intensifies from the onset onwards. This heat low has a significant impact on the circulation pattern at this level and the other lower levels below 850 hPa that is seen over Bangladesh during this period.

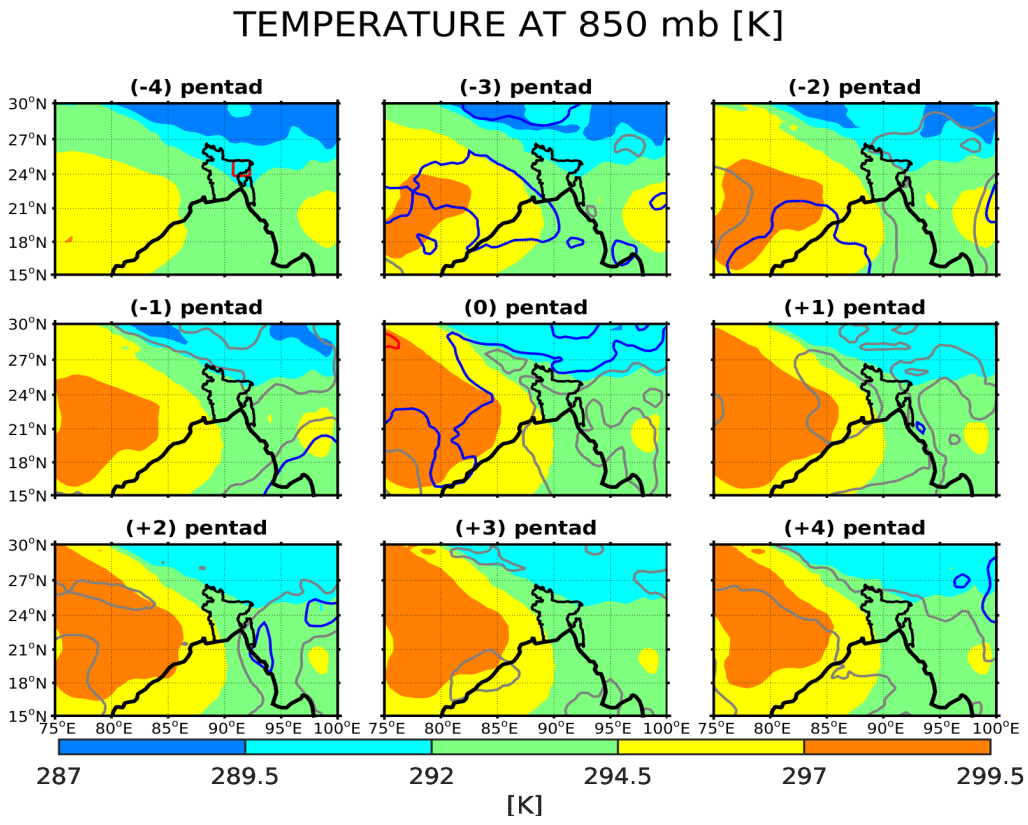

Figure 4.24: As in Figure 4.20, but for temperature at 850 hPa.

Figures 4.25 to 4.27 show the behaviour of the winds at 850 hPa level before and after the onset of the summer rains. The flow pattern still changes from moderate northwesterly flow (3 - 6 m/s) before the onset to strong southwesterly flow after the onset. A clear transition in the overlap PDFs of 0 - 25% in wind speed is seen at pentad (+1) covering almost entire Bangladesh, and areas around the eastern coast of the Bay of Bengal and Myanmar at the onset pentad [Figure 4.25]. In Figure 4.26, the clear transition in the zonal wind with 0 - 25% PDF overlap observed at the lower southwestern part of Bangladesh and the Bay of Bengal at pentad (+1), while areas around Northeast Bangladesh exhibit a 25 - 50 % overlap in the PDFs at pentad (+1). A more clearly defined transition with 0 - 25% PDF overlap in the zonal wind component covering the southern sector of Bangladesh, upper eastern and western coast of the Bay of Bengal and parts of Myanmar occur at pentad (-1) before the onset. The meridional wind component shows a clear transition of the wind pattern with PDF overlap of 0 - 25% at pentad (+1), stretching from the Bay of Bengal across entire Bangladesh and areas around north and northeastern Bangladesh, [Figure 4.27]. The change in the wind speed and direction at 850 hPa during the onset is also greatly influenced by the meridional wind component rather than the zonal component. Figures 4.25 - 4.27 also show that the typical characteristics of large-scale monsoon low-level atmospheric circulation suggested by Zhang and Wang [2008] are fulfilled across Bangladesh since the winds change their direction and strength from moderate northwesterlies/westerlies to strong southwesterly flow prior to the onset at pentad (0). This shows that the rainy season has already started in this area basing on the characteristics of lower level winds at both 925 and 850 hPa.

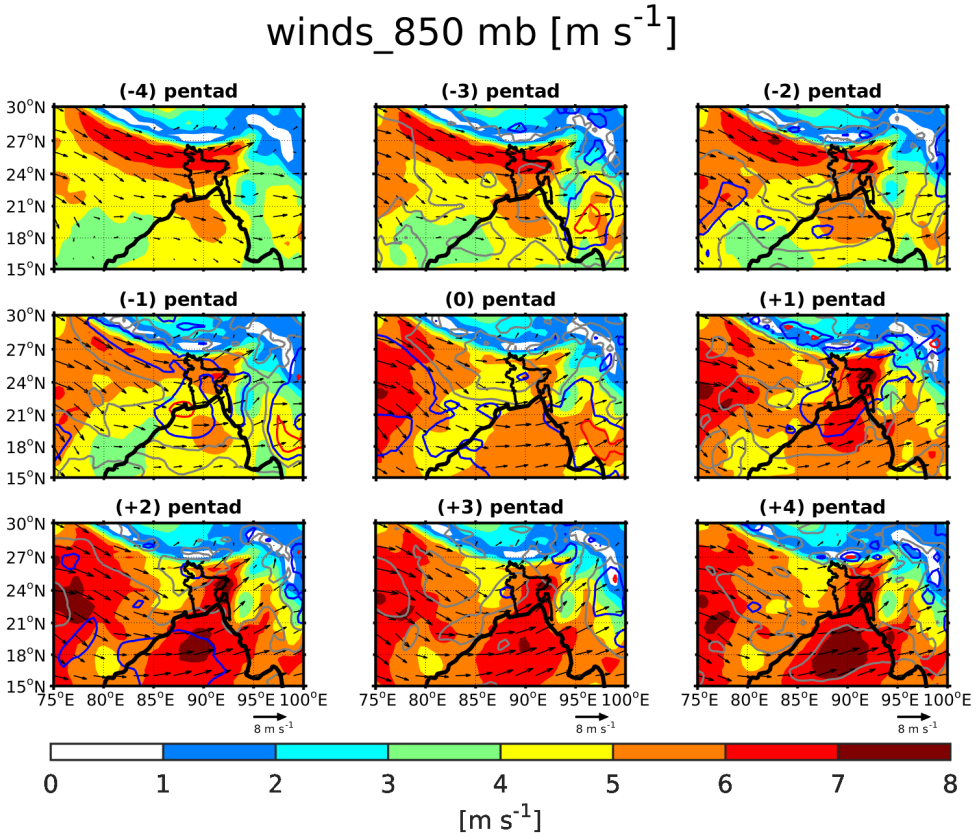

Figure 4.25: Lead-lag composites for winds at 850 *hPa* level with wind speed PDF overlap. The red, blue, and grey contours show 0-25%, 25-50%, and 50-75% PDF overlaps, respectively.

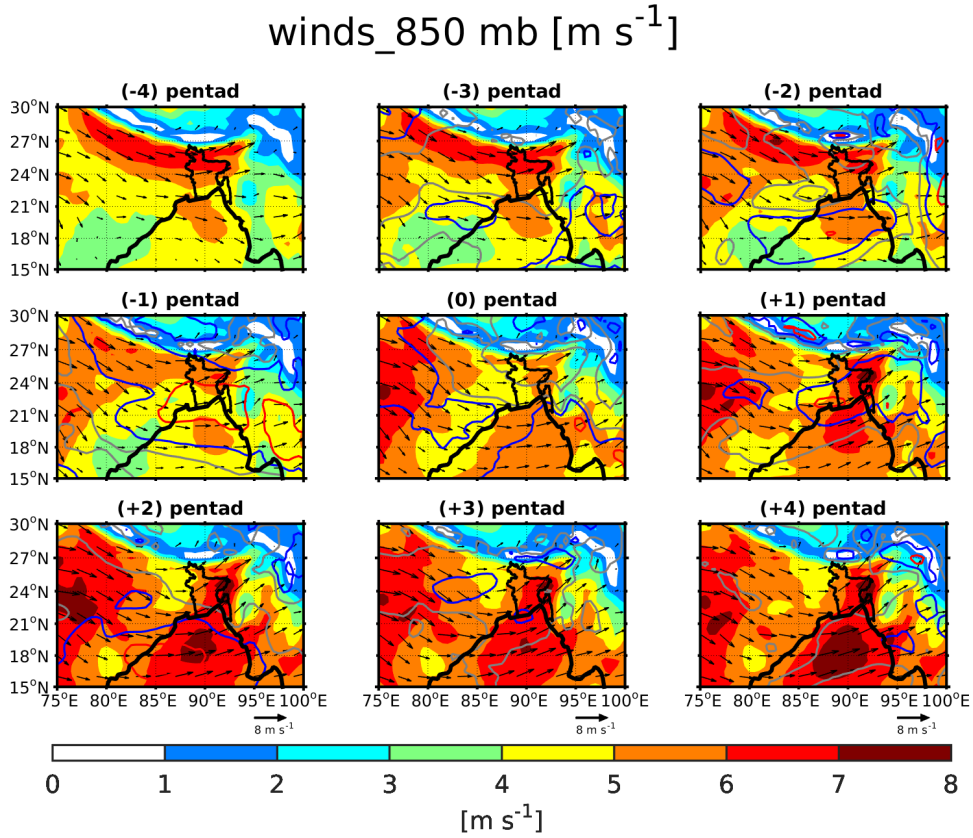

Figure 4.26: As in Figure 4.25, but with zonal wind PDF overlap.

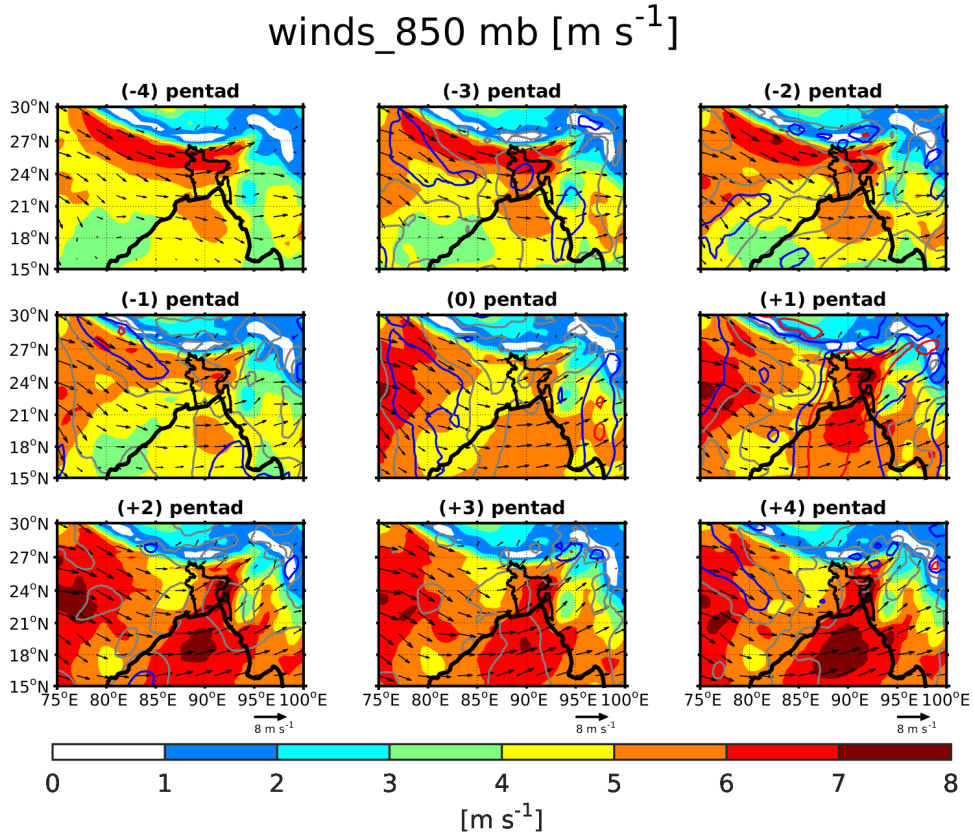

Figure 4.27: As in Figure 4.25, but with meridional wind PDF overlap.

4.3.3.3 Wind and Temperature at 600 hPa

The temperatures at 600 hPa [Figure 4.28] over almost entire Bangladesh is between 273 - 274.5 K at pentad (-4). At both pentad (-3) and pentad (-2), the temperatures are 273 - 274.5 K and 274.5 K - 276 K over the northern and southern sector of Bangladesh, respectively. Then from pentad (-1) to pentad (+3), entire Bangladesh has temperatures between 274.5 - 276 K, and 276 - 277.5 K at pentad (+4). There is no significant change in temperature regime at 600 hPa in Northeast Bangladesh as the temperatures remain almost constant between 274.5 - 276 K throughout the country from pentad (-1) up to pentad (+3). The temperatures at this level show a similar trend to that of 850 hPa [Figure 4.24], with temperatures only increasing by 3 K over northern Bangladesh at pentad (-1) and thereafter remaining constant at 276 K, with exception at pentad (+4) when they further increases to 277.5 K. Also at 600 hPa level [Figure. 4.28], the heat low disappears, confirming that it is a low-level phenomenon. To this support, Rácz and Smith [1999] defined heat lows as shallow disturbances usually confined below 700 hPa. Studies of heat lows in different parts of the world reveal that heat lows usually form in arid to semi-arid land areas in low latitudes, especially during the summer months when solar insolation is very strong [Rácz and Smith, 1999; Spengler et al., 2005; Spengler and Smith, 2008]. For example, heat lows occur over the Iberian Peninsula [Alonso et al., 1994], Australia [Spengler and Smith, 2008], western Pakistan and northern India [Ramage, 1971], northern and southwestern Africa [Ramage, 1971], Saudi Arabia, China, and others.

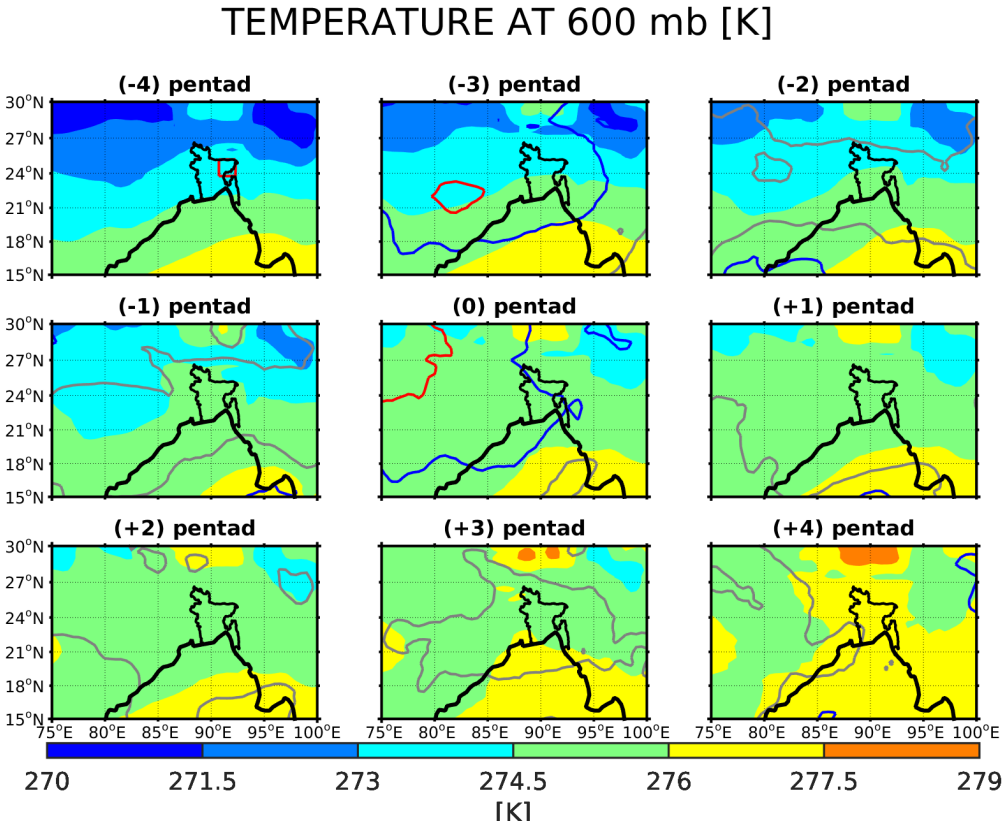

Figure 4.28: As in Figure 4.20, but for temperature at 600 hPa .

Spengler and Smith [2008] and Allcock and Ackerley [2015] described the heat low as a prominent low-level atmospheric circulation feature common during the summer months. Hence, the heat low in our results seems to act with the same characteristics. This heat low has strong impact on the low-level circulation pattern, whereby the low-level winds change from moderate northwesterlies to strong southwesterlies just on the eastern edge of the thermal low [Figures 4.21 and 4.25]. Also the flow pattern of the moisture flux vectors tend to change from westerly/northwesterly to southwesterly just on the eastern edge of the heat low [Figure 4.7 and 4.8]. This can also be an impact caused by the heat low that intensifies and extends into western Bangladesh prior to, and after the onset of the summer rains in Northeast Bangladesh. Allcock and Ackerley [2015] confirmed the strong influence of the heat low on the low-level atmospheric circulation pattern.

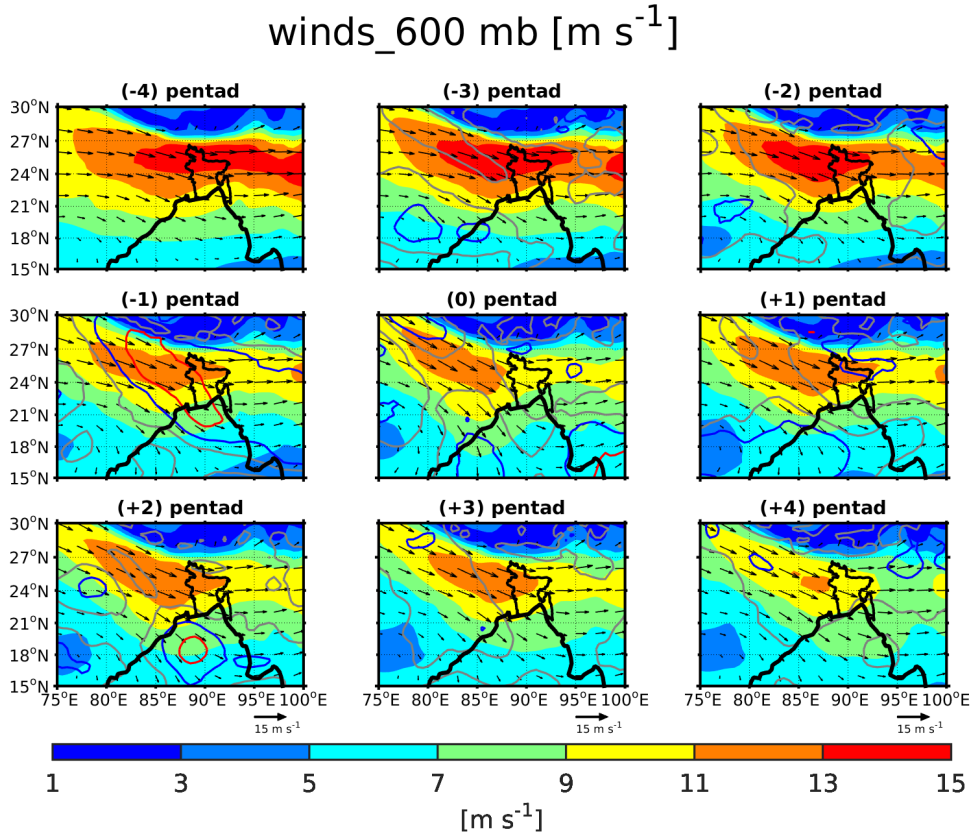

Figure 4.29: Lead-lag composites for winds at 600 hPa level with wind speed PDF overlap. The red, blue, and grey contours show 0-25%, 25-50%, and 50-75% overlaps, respectively. The strong/clear regime transition in wind speed occurs at pentad (-1)[red contour] across India, western and southern Bangladesh, and at the upper coast of the Bay of Bengal, and in areas around the lower eastern coast of the Bay of Bengal at onset (pentad (0)).

The winds at 600 hPa [Figure 4.29 - 4.31] show a very strong northwesterly flow coming from the western part of India and higher latitudes towards Bangladesh decelerating into the Bay of Bengal and at the same time, turning into a strong to moderate westerly flow across Bangladesh. From pentad (-4) to pentad (+4), there is a weak to moderate anticyclonic circulation over India near the western coast of the Bay of Bengal. The anticyclonic circulation becomes well developed from the onset at pentad (0) onwards, with its centre confined further in India. The wind speeds around this anticyclonic circulation

is between 3 - 9 m/s, with its centre having winds of 3 - 5 m/s from pentad (-2) onwards. The anticyclonic circulation at this level is collocated with heat low at lower troposphere [Figures 4.20 and 4.24]. This means that the heat low at the lower levels is well aligned with the upper-level anticyclone that can be seen starting from this level. The total wind, together with its zonal and meridional wind components at 600 hPa, all show a clear regime transition at pentad (-1) and onset (pentad (0)) across India, Bangladesh, the Bay of Bengal and the western parts of Myanmar [Figures 4.29 - 4.31]. The wind speeds of the westerly/northwesterly flow is 13 - 15 m/s across the whole of northern Bangladesh from pentad (-4) to pentad (-2), and then drops down to about 9 - 11 m/s during the onset at pentad(0). The westerly winds increase their speed by 2 m/s at pentad (+1) immediately after the onset, and then drops down again to 9 - 11 m/s from pentad (+3) onwards. The westerly winds at this level show that the large-scale monsoon in Northeast Bangladesh is yet to start, confirming that it is rather the local circulations influencing the summer rains in this region.

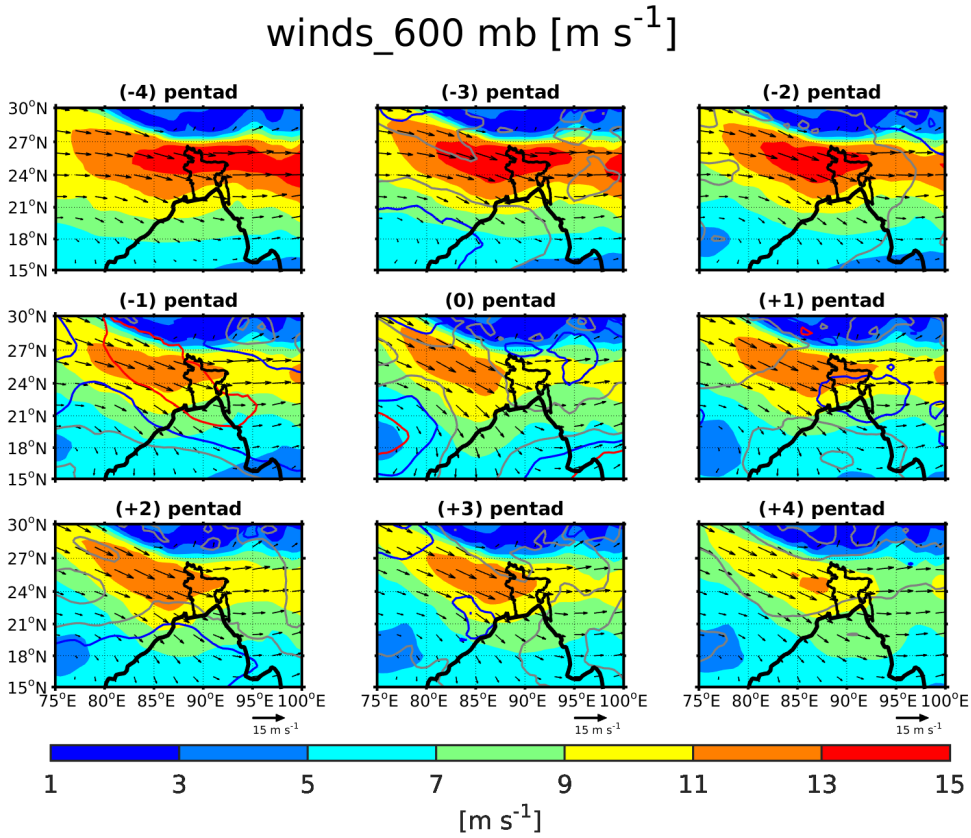

Figure 4.30: As in Figure 4.29, but with zonal wind PDF overlap. The clear regime transition in zonal winds occurs at pentad (-1)[red contour] across India, most parts of Bangladesh, upper coast of the Bay of Bengal, and Myanmar, while areas around the lower eastern coast of the Bay of Bengal and some parts of India show a clear transition at onset (pentad (0)).

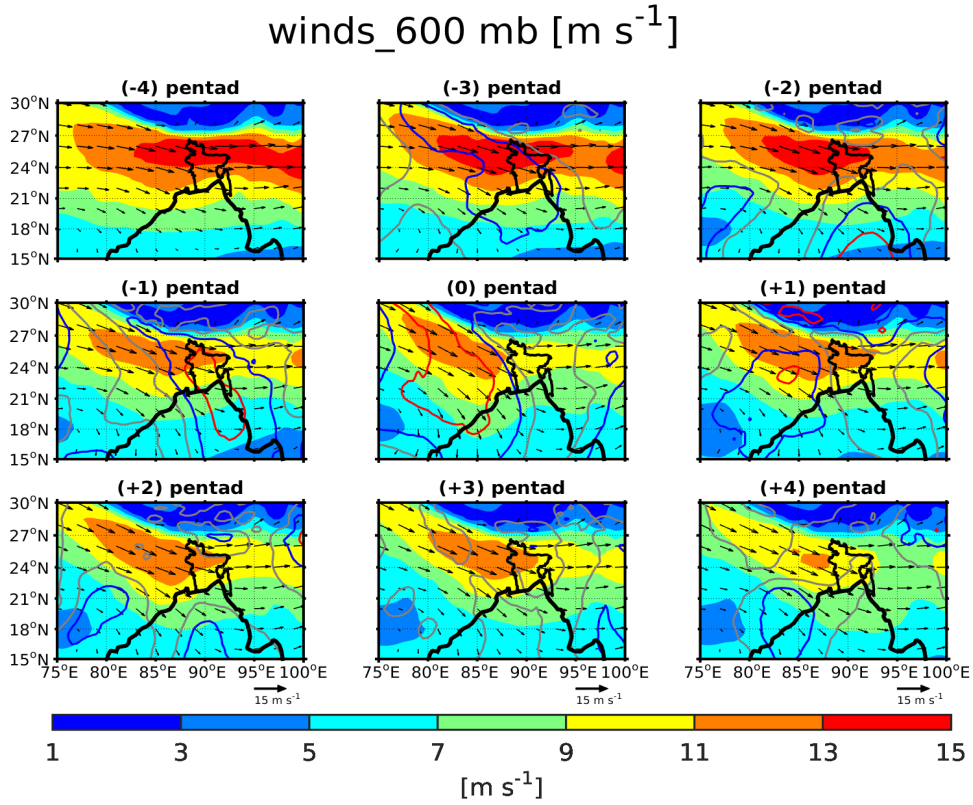

Figure 4.31: As in Figure 4.29 , but with meridional wind PDF overlap. The strongest regime transition is at pentad (-1) over Bangladesh, at onset (pentad (0)) over India and western coast of the Bay of Bengal and at pentad (+1) in some parts of India.

4.3.3.4 Wind and Temperature at 200 hPa

As expected, the temperatures at 200 hPa level [Figure 4.32] are much lower than the temperatures at the previous lower and mid-tropospheric levels. Figure 4.32 also shows that the whole Bangladesh has its temperatures between 221 - 222 K from pentad (-4) to pentad (-2), and 222 - 223 K from pentad (-1) to pentad (+1). Then the temperatures change to 224 K from pentad (+2) to pentad (+4) in the whole of Bangladesh, with exception at pentad (+3) where the temperatures drop down by 1 K from 224 K at pentad (+2) to 223 K almost everywhere apart from Northwest Bangladesh. At this level, the temperature difference is much larger compared to temperatures at 600 hPa level, which further shows that an upper-level anticyclone is already forming over this region. This upper-level anticyclone can be tracked starting from pentad (-3) onwards and intensifies at pentad (+2) onwards. Nothing can be said about its weakening in pentad (+3), despite the change being hardly significant with 50 - 75% overlap in the PDFs at those grid points.

The winds at 200 hPa and the PV2000 surface [see Figure A.1 in appendix A, and Figure B.1 in appendix B, respectively] show typical characteristics of pre-monsoon winds at upper levels across our entire domain. These upper-level winds show a strong westerly jet across entire Bangladesh which contrasts the definition that the winds at upper-levels must have an easterly jet component during the monsoon onset as suggested by [Zhang and Wang, 2008]. This further attests that the large-scale monsoon has not yet started

but rather the summer rains are due to local circulation.

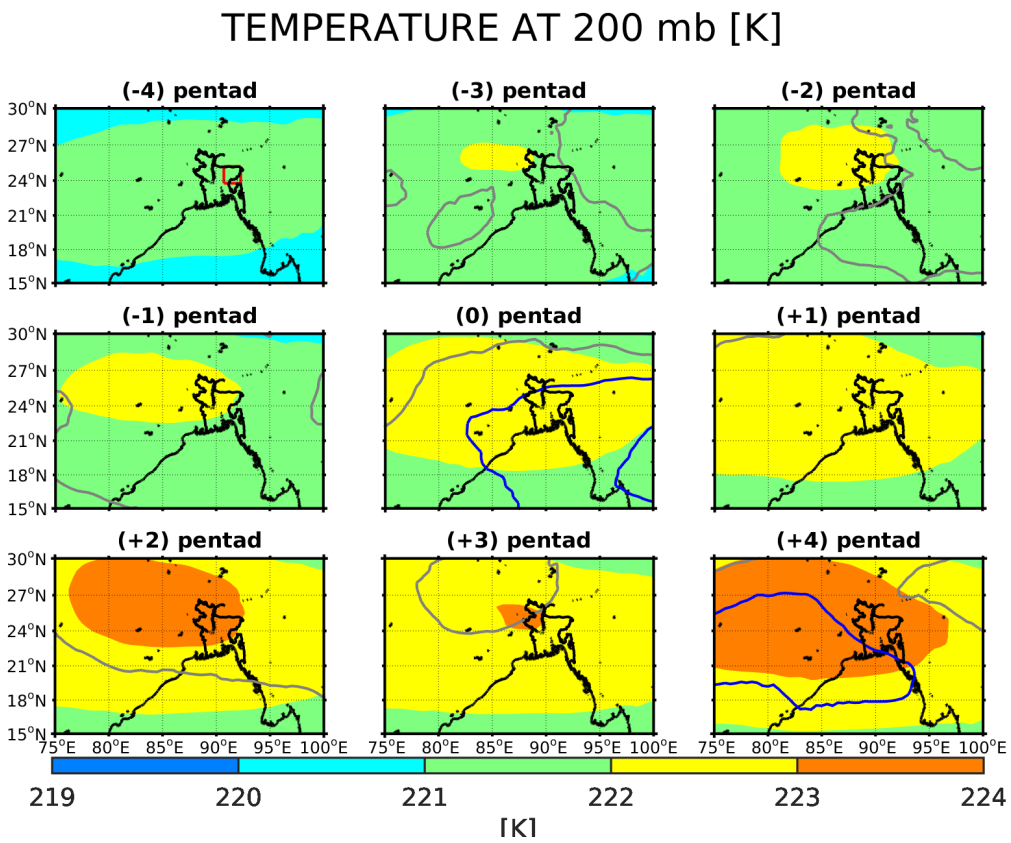

Figure 4.32: As in Figure 4.20, but for temperature at 200 hPa .

4.3.3.5 Vertical cross-section of Temperature

Figure 4.33 shows the lead-lag vertical temperature taken along 24.5°N latitude. This figure also reveals the existence of a heat low at lower levels up to aroud 850 hPa, with its temperature in the range of 308 - 310 K. It also shows that the heat low extends up to around 91°E in Bangladesh. The steep temperature gradient from the onset indicates the intensification of the heat low as it extends further into western Bangladesh. From the onset, the temperatures over Northeast Bangladesh (93°E) drop by 2 K below 900 hPa from 309 K . This implies that a cold pool of air exists over Northeast Bangladesh as the temperatures are slightly lower than in the surrounding areas. The temperatures over Northeast Bangladesh again rise to 309 K from pentad (+3). The vertical temperature profile also shows the decrease of temperature with height, as higher temperatures have been found in the lower troposphere, and lower temperatures in the upper troposphere.

In summary, we have seen the existence of the heat low as a low-level phenomenon that strongly influences that circulation at both lower-and middle tropospheric-levels. This heat low exhibit typical characteristics of all the other heat lows around the world in terms of its latitude location and time of occurrence. The low-level winds at both 925 and 850 hPa show a southerly/southwesterly flow across entire Bangladesh during the onset of the summer rains in Northeast Bangladesh, which is a typical characteristic of the low-

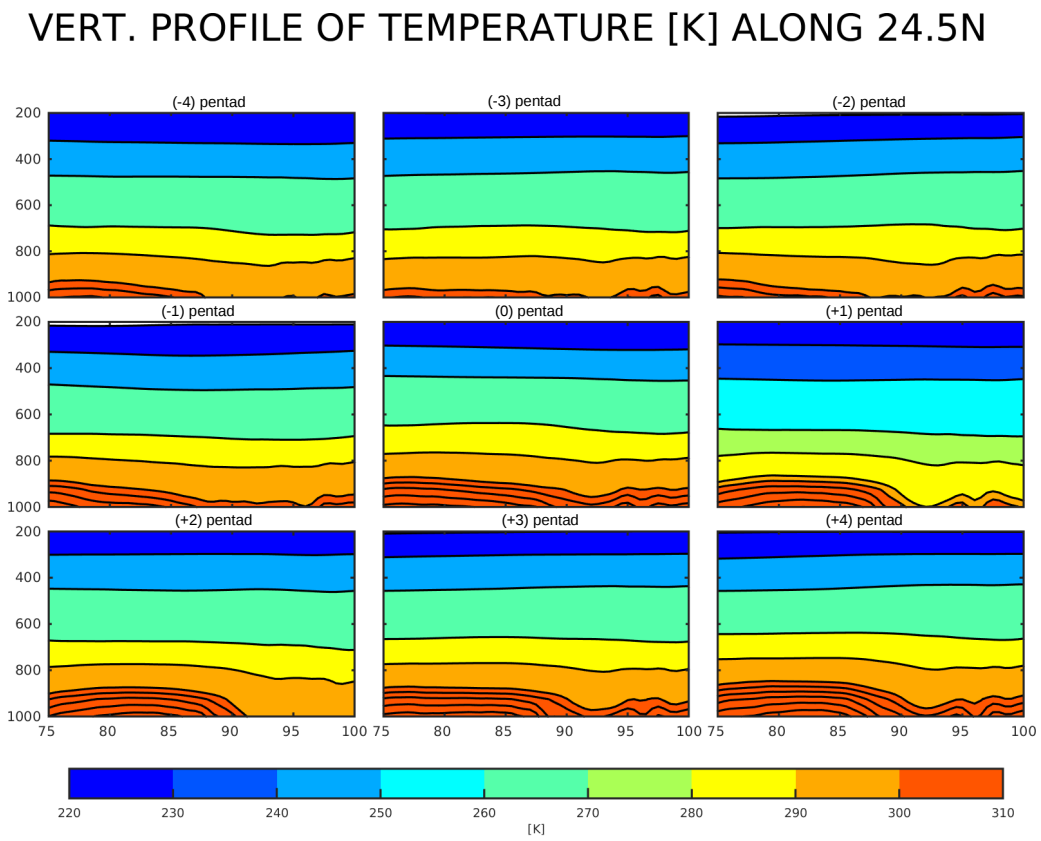

Figure 4.33: Lead-lag vertical profile of temperature along 24.5N. The lower troposphere has additional contours in the interval of 2 K from 300 - 310 K.

level atmospheric circulation during the onset of the large-scale monsoon over Bangladesh. However, the winds at upper-levels (600 hPa, 200 hPa, and the PV2000 surface) show a strongly westerly jet over Bangladesh during the onset of the summer rains in Northeast Bangladesh. This is a typical character of pre-monsoon winds at upper levels which contrasts the characteristics of upper-levels winds (i.e., an easterly jet component) during the monsoon onset as suggested by [Zhang and Wang, 2008]. Thus, this attests that the actual large-scale monsoon has not yet started but rather the summer rains are due to local circulation. It also confirms that the summer rains are not part of the large-scale monsoon. On the other hand, the cooling at 925 hPa level over Northeast Bangladesh immediately after the onset of summer rains points to the existence of the cold pool of air. This cold pool of air is trapped in the region by the surrounding elevated topography, that is the Meghalaya Plateau and the other mountains east of Northeast Bangladesh. From this, we can speculate that when the warm moist southwesterly air mass from Bay of Bengal converges with this cold pool of air, it is forced to rise over the low-level cold pool before reaching the Meghalaya Plateau, and hence precipitation being triggered over Northeast Bangladesh as suggested by Kataoka and Satomura [2005]; Murata et al. [2011].

Similarly, we also speculate that when the strong southerly/southwesterly warm moist flow from the Bay of Bengal reaches the Meghalaya Plateau and the other mountains to the east of Northeast Bangladesh, it is blocked and eventually forced to rise over the

elevated topography. As it rises, it cools and forms convective clouds on the windward side of these mountains, which later condense. This in turn induces orographic rainfall on the windward sides of these high elevated mountains. And since Northeast Bangladesh is located on the windward side of the Meghalaya Plateau and the other mountains to its east, hence heavy precipitation received during the summer months of March - May can be a result of orographic uplifting of the warm moist southerly/southwesterly flow by the Meghalaya Plateau and the other surrounding mountains to its east. Notwithstanding, Rafiuddin et al. [2010] suggested that the strong southwesterly winds intensify the local convective activity when they are blocked and forced to rise by high-elevated topography to the north and east of Bangladesh. In the same context, Sato [2013] suggested that these strong low-level southerly/southwesterlies play a vital role in the formation of convection and the heavy precipitation received around Meghalaya Plateau because they are capable of overcoming the vertical stratification barrier provided by the Meghalaya Plateau and when they are forced to rise, they can even reach the lifting condensation level (LCL).

4.3.4 Thickness

Figure 4.34 presents the thickness lead - lag plots for the lower half of the troposphere (1000 - 500 hPa). The lead - lag atmospheric thickness between 1000 and 500 hPa is used as a measure of the mean temperature in the lower part of the troposphere prior to the onset

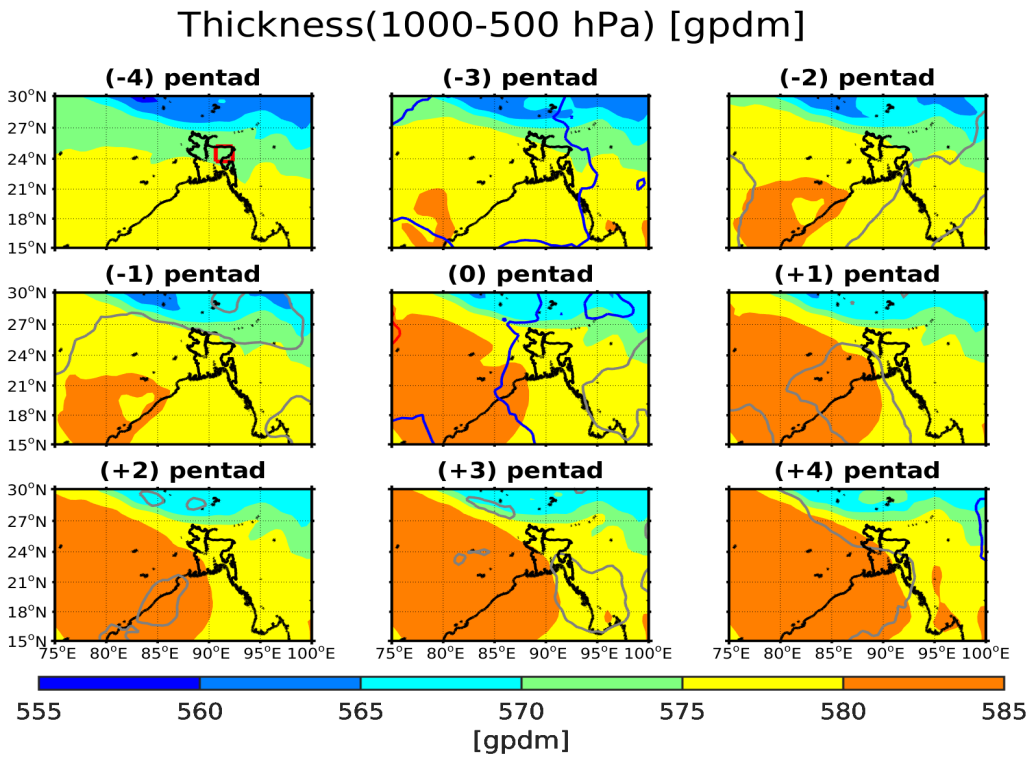

Figure 4.34: Lead-lag composite of thickness between the 1000-500 hPa level. The red- square box in pentad (-4) indicates Northeast Bangladesh. The red,blue, and grey contours show 0-25%, 25-50%, and 50-75% overlap of the PDFs with neighbouring pentads at the same grid point, respectively.

and afterwards. It shows how warm (higher values) or cold (lower values) the atmosphere is before and after the onset of summer rains in Northeast Bangladesh. This figure reveals a more clear build up of the heat low in India near the western part of Bangladesh as the onset builds up, starting from pentad (-3) along the lower western coast of the Bay of Bengal, while it starts to penetrate into western Bangladesh at pentad (+1). The heat low in this case is indicated by the higher values of thickness above 580 gpdm, and it shows that warm air is being advected from India and the Bay of Bengal into Bangladesh. This heat low as we have already discussed in section 4.3.3, has a strong impact on the low-level circulation in this region. Lower values of thickness between 555 - 565 gpdm are found in the Himalayas, and increase slowly southward towards Bangladesh. This means that the cold air is being advected from the Himalayas towards north Bangladesh.

4.3.5 Vertical Stratification

Figures 4.35 and 4.36 show the vertical stratification of the atmosphere, here defined as the vertical difference of both potential temperature (θ), and equivalent potential temperature (θ_e) between 925 hPa and 600 hPa, respectively. Figure 4.35 reveals that the vertical difference in θ over Northeast Bangladesh is 14 - 16 K prior to the onset (i.e., from pentad (-4) to pentad (0)), and 16 - 18 K from pentad (+1) onwards. This shows that the mean stratification of θ after the onset is 2 K higher than that before the onset of the summer rains in Northeast Bangladesh. The mean stratification of θ over India is between 4 - 10

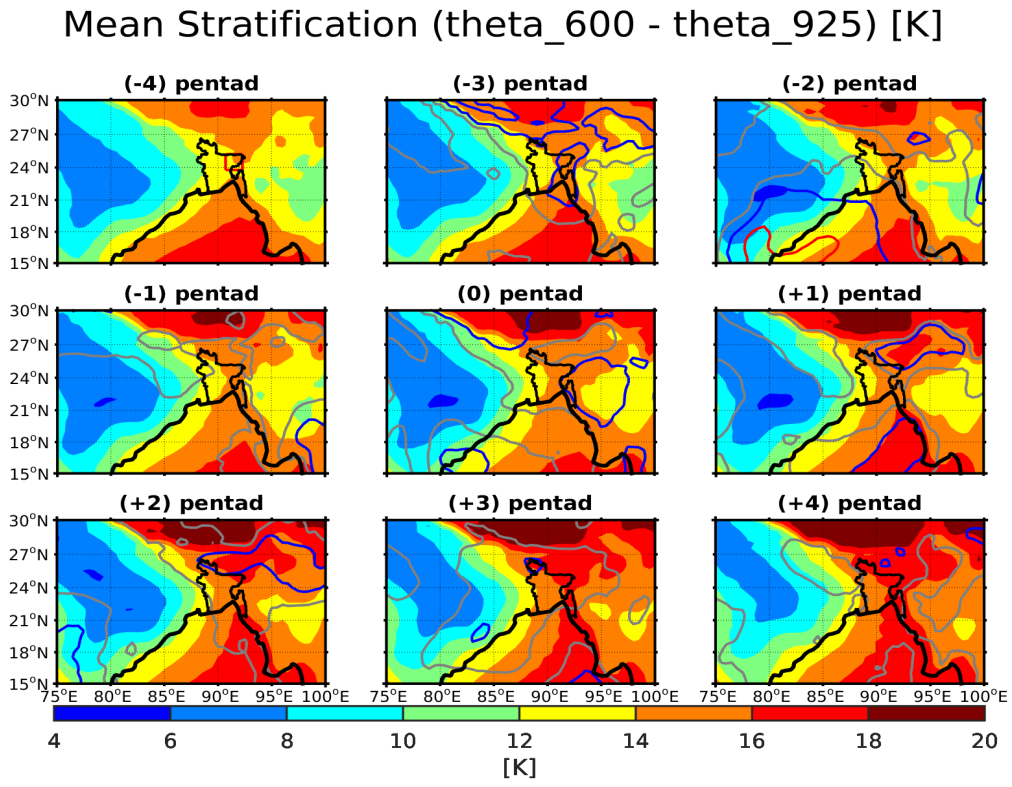

Figure 4.35: Lead-lag composite for mean stratification of potential temperature between 925 hPa and 600 hPa levels. The red,blue, and grey contours show 0-25%, 25-50%, and 50-75% overlap of the PDFs with neighbouring pentads at the same grid point, respectively.

K, which is almost similar before and after the onset. This difference is much less than the difference across Bangladesh, and this is due to the presence of the heat low in India that is confined to lower levels of the troposphere [see Figures 4.20, 4.24, and 4.34]. By considering θ alone, the lower half of the troposphere seems to be stable as the mean stratification of θ is positive across our domain. However, when equivalent potential temperature (θ_e) is considered, the lower half of the troposphere is unstably stratified [Figure 4.36]. That is, θ_e decreases with altitude between 925 hPa to 600 hPa over Bangladesh. This is shown by the negative values in the mean stratification of θ_e from pentad (-4) onwards. And this is not surprising because θ is with reference to dry air and yet θ_e is a function of moisture and temperature which both decrease with height in the troposphere. As we have already seen that both temperature [Figures 4.20, 4.24, 4.28, and 4.32] and moisture [Figures 4.13 - 4.15] decrease with height, and that the lower troposphere cointains much moisture than the upper troposphere [Figures 4.9 - 4.10], hence the decrease of θ_e with height in the lower half of the troposphere [Figure 4.36]. The decrease in θ_e with height increases from pentad (-4) onwards and becomes much more pronounced after the onset [Figure 4.36]. This really shows that the lower-level convective instabilities build up around the time of onset, and the fact that θ_e decreases with height signifies that convection can easily be triggered during this period since the atmosphere is unstable to vertical motions. Furthermore, Figure 4.36 reveals that the progression in the intensification of the lower-level convective instabilities slightly reverses after pentad (+2), and then revamp at pentad (+4). Less instabilities are found in India most especially where the heat low is located [Figures 4.20, 4.24, and 4.34], while neutral to stable conditions can be seen over the Himalayas.

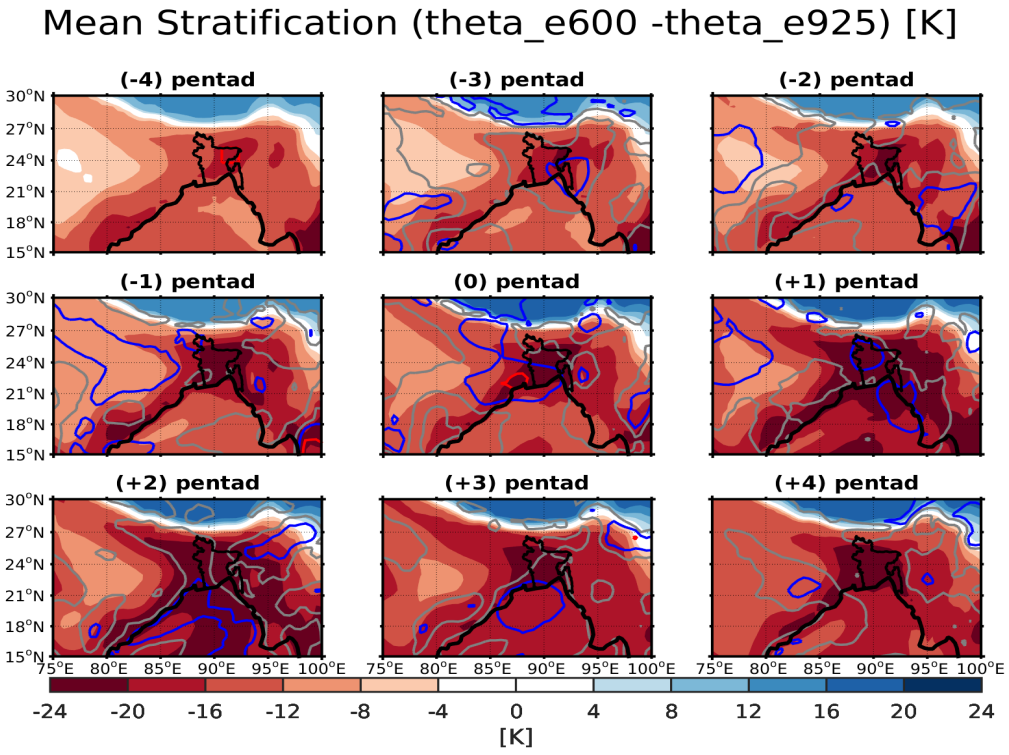

Figure 4.36: As in Figure 4.35, but for Equivalent potential temperature. The red, blue, and gray contours refer to 0-25%, 25-50%, and 50-75% overlap of PDFs, which show a strong, moderate, and weak regime transition in mean stratification of θ_e, respectively.

To further examine the stability of the atmosphere over Northeast Bangladesh during the onset of the summer rains, vertical cross sections of potential temperature (θ), and equivalent potential temperature (θ_e) were used. Figure 4.37 presents the vertical profiles of both θ and θ_e taken over Northeast Bangladesh before and after the onset. From this figure, the vertical profile of θ_e [Figure 4.37(a)] shows clearly that Northeast Bangladesh is very moist, and the environment is unstable at lower levels up to 600 hPa both before and after the onset, and hence confirming the results in Figure 4.36. The strong convective instability in the lower to mid-troposphere could be associated with the abundance of much moisture in the lower atmosphere [Figures 4.9, and 4.13 - 4.15] supplied by the southwesterly winds [Figures 4.21 - 4.23, and 4.25 - 4.27]. This large atmospheric instability favours the development of convective systems over this region during this period, most especially when it combines with low-level moist southwesterly flow from the Bay of Bengal. Rafiuddin et al. [2010] mentioned that the large instability during the pre-monsoon months of March - May can also lead to the organisation of deep convection over the region. From mid to upper atmosphere, the environment becomes stable but less moist before and after the onset since a smaller fraction of moisture is contained in the mid-to-upper levels, [see Figure 4.10]. Two pentads after the onset [i.e., at pentad (+2), red line in Figure 4.37], the troposphere is nearly neutral at mid-levels between 600 - 500 hPa, and then becomes stable from 500 hPa higher up. This means that the mid-troposphere is almost well-mixed at pentad (+2).

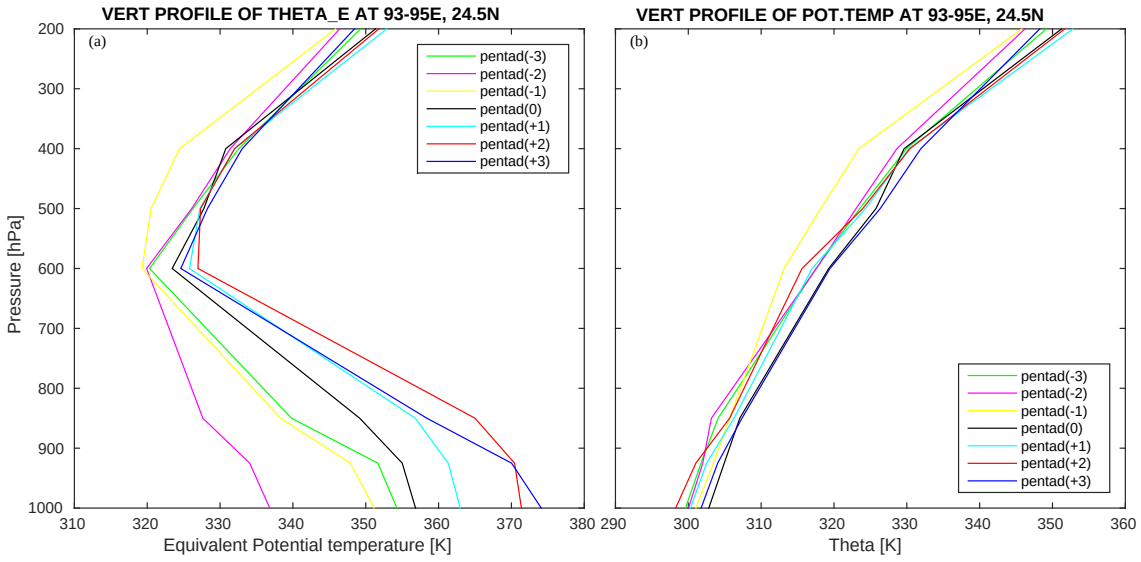

Figure 4.37: Vertical profiles of (a) equivalent potential temperature, and (b) potential temperature taken over Northeast Bangladesh at 24.5°N, 93 – 95°E.

The vertical profile of θ reveals that θ increases with height before and after the onset of the summer rains in this region, [Figure 4.37(b)]. From pentad (-3) to onset (pentad (0)), θ increases and then decreases immediately after onset at the lower-most levels (surface - 850 hPa). Figure 4.37(b) also shows a drastic increase in θ from pentad (-1) to onset (pentad(0)), followed by a drastic drop in θ by about 4 K at pentad (+1) immediately after the onset of the summer rains. The potential temperature continues to drop further at pentad (+2) by about 2 K, before it increases again drastically at pentad (+3). The drastic

increase of θ prior to the onset (i.e., from pentad (-1) to pentad (0)), can be attributed to the drastic increase in temperature prior to the onset, [see Figures 4.20, 4.24, 4.28, and 4.32], while the drastic drop in θ immediately after the onset (i.e., from pentad (+1) onwards) can be attributed to the intensive rainfall from the onset onwards [Figure 4.5], which reduces the temperature by evaporatively cooling the atmosphere. Figure 4.37 also reveals that the vertical profiles of both θ_e and θ are almost similar from 400 hPa to 200 hPa, due to little moisture contained in upper levels of the atmosphere. The same figure further reveals that both θ_e and θ are almost equal from 300 hPa to 200 hPa, which attests that the moisture at upper-levels above 300 hPa is almost negligible.

4.4 Diurnal variation of precipitation, low-level wind, evaporation, moisture flux and water convergence

Now that we have seen the rainfall climatology in Northeast Bangladesh, moisture sources, seasonal evolution of summer rains, together with the synoptic conditions prior to and after the onset of the summer rains in the previous sections, we now look at the diurnal variation of the moisture fields and low-level winds over Northeast Bangladesh. This section focuses on the diurnal variation of precipitation, evaporation, low-level wind, vertically integrated moisture flux and water convergence in the Northeast Bangladesh and its major aim is to see whether the late night-early morning rainfall maximum is robust in ERA-interim. It also aims at finding the likely causes of this late night-early morning maximum in Northeast Bangladesh. Again, the lead-lag composite analysis at each time step is used. The time used in ERA-Interim is Universal Coordinated Time (UTC), but the Bangladesh Standard Time (BST) is 6 hours ahead of the UTC, that is BST = UTC + 6 hours. This means that 1800 - 0000UTC is 0000 - 0600 BST, which marks midnight-early morning in Bangladesh. From here onwards, we utilise BST as our time of reference to describe the diurnal variation of the above parameters since we are looking at Northeast Bangladesh which uses BST as its time.

4.4.1 Precipitation, evaporation, wind, moisture flux and water convergence at 1800 BST

Figure 4.38 shows less convective activity at 1800 BST in Northeast Bangladesh before and after the onset of the summer rains in this area. The rain starts from the Meghalaya Plateau (pentad (-4)) before it spreads over Northeast Bangladesh from pentad (-3) onwards. The accumulated rainfall amount received in Northeast Bangladesh during this time over the past 6 hours is less than 2 mm before the onset (pentad (0)), and about 4 - 6 mm after the onset. The rainfall amount suddenly increase by about 3 mm at pentad (+1) after the onset, which clearly shows the strong transition in precipitation regime around Northeast Bangladesh. After pentad (+1), precipitation shows a gradual increase of 1 mm in the rainfall amount received over Northeast Bangladesh at pentad (+2), and thereafter, followed by a reduction in rainfall amount received over the region. Also from pentad (+1)

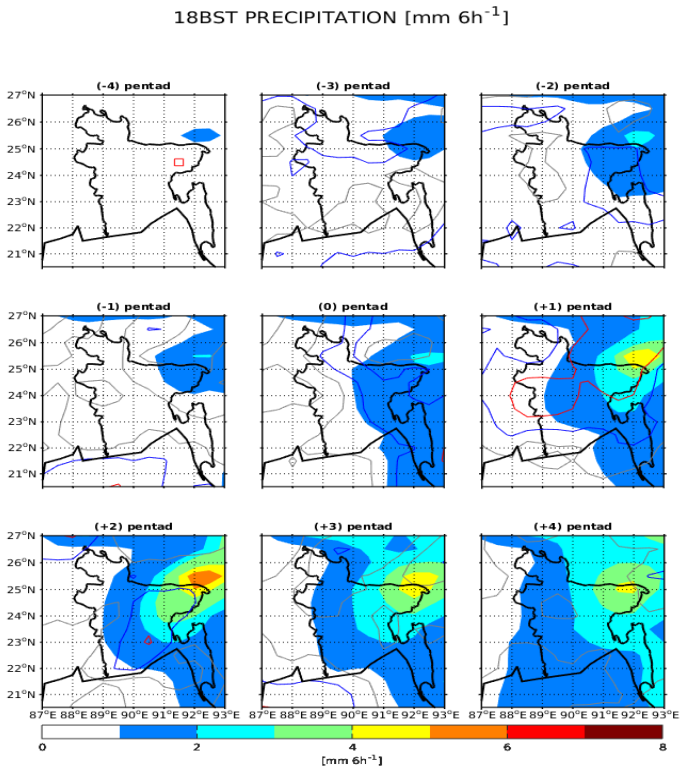

Figure 4.38: Lead-lag composite for precipitation [mm/6h] at 1800 BST. The red, blue, and gray contours represent the 0-25%, 25-50%, and 50-75% PDF overlaps, respectively. The areas around Northeast Bangladesh show a clear regime at pentad (+1) [red contour] with an increase in rainfall amount.

onwards, precipitation spreads southward and westward to other places in Bangladesh. At 1800 BST, the evaporation rate is quite high with values between 0.4 - 0.8 mm over the past 6 hours across Bangladesh before the onset, and only shows a further reduction in Northeast Bangladesh at pentad (+2) after onset [Figure 4.39]. The high evaporation rate observed at this time before the onset could be due to strong solar heating of the summer sun in the afternoon hours, while the reduction in the evaporation rate after onset in Northeast Bangladesh could be due to the increase in precipitation over the previous 6 hours. The low-level winds at 950 hPa over Northeast Bangladesh are very weak with speeds of 2 - 4 m/s before the onset, and only show a slight increase in their speeds to about 5 - 6 m/s after the onset [Figure 4.40]. The moisture flux over Northeast Bangladesh increases from pentad (-4) to pentad (-2), and then drops down by 50 kg/m/s at pentad (-3) up to onset (pentad (0)), [Figure 4.41]. After the onset, the moisture flux increases drastically from 250 kg/m/s to about 350 kg/m/s at pentad (+1), thereafter showing no remarkable change but only extending southward to other places. Figure 4.42 reveals water (moisture) first converges over the Meghalaya Plateau from pentad (-4) to pentad (-3) before it converges over Northeast Bangladesh from pentad (-2) onwards. Moisture convergence suddenly increases at pentad (+1) to about 5 - 7 mm over the past 6 hours, thereafter showing a gradual increase over region. The increase in moisture convergence at 1800 BST over Northeast Bangladesh after the onset can be attributed to both the increase in southwesterly moist flow from the Bay of Bengal towards the region and the

increase in precipitation which reduces the evaporation rate over the region.

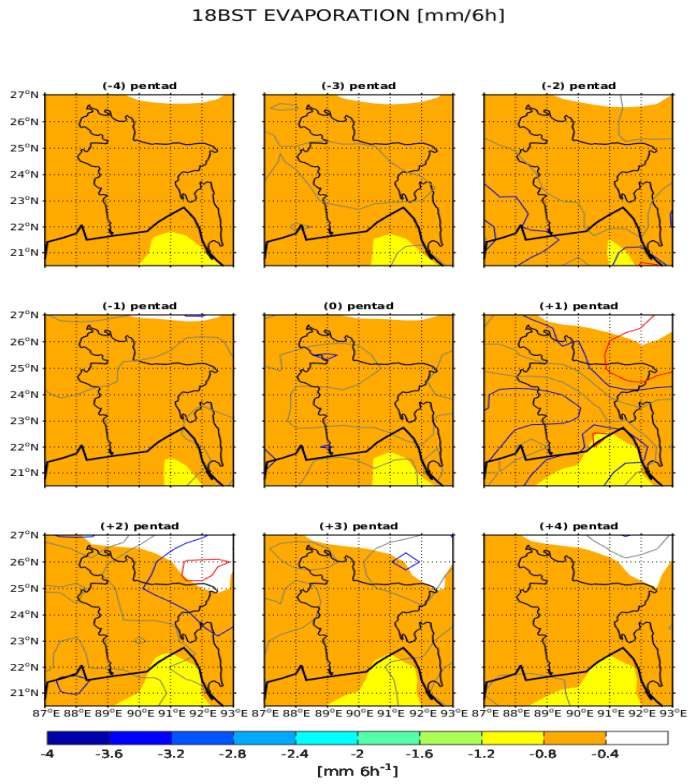

Figure 4.39: As in Figure 4.38, but for Evaporation [mm/6h] at 1800 BST.

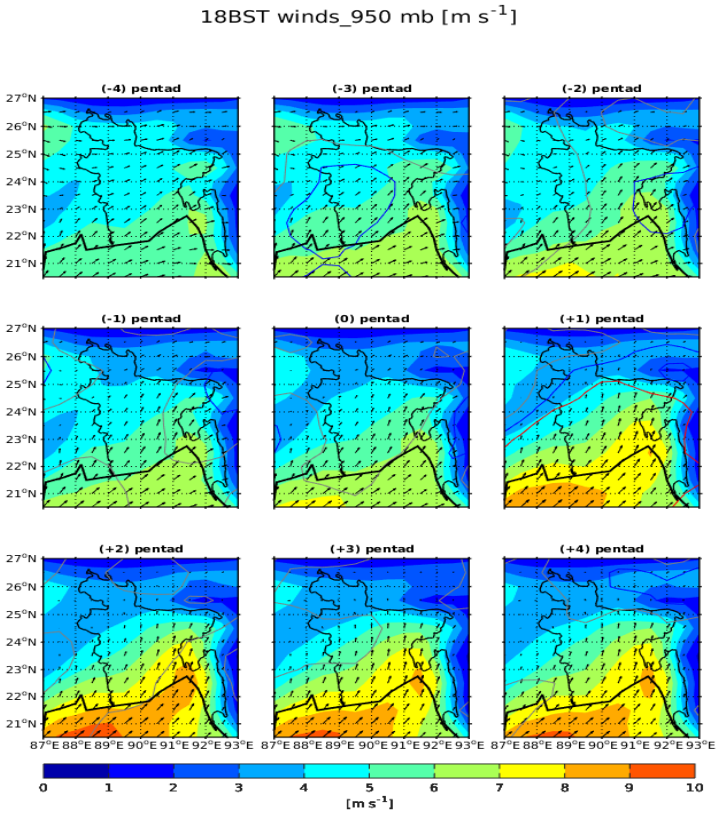

Figure 4.40: As in Figure 4.38, but for winds at 950 hPa [m/s] at 1800 BST.

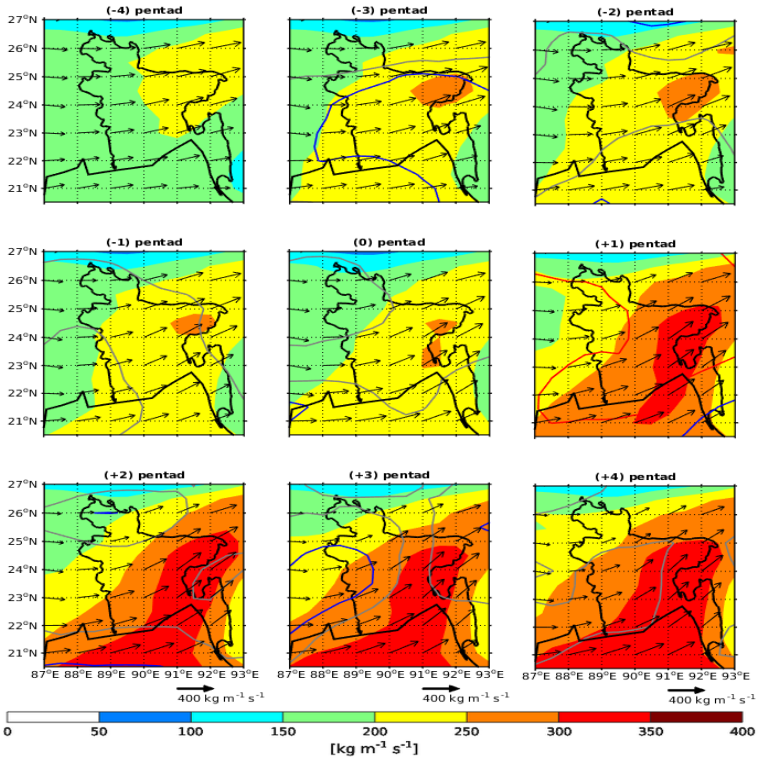

Figure 4.41: As in Figure 4.38, but for Vertically integrated moisture flux [kg/m/s] at 1800 BST. A clear regime transition is visible at pentad (+1) [red contour] almost across entire Bangladesh.

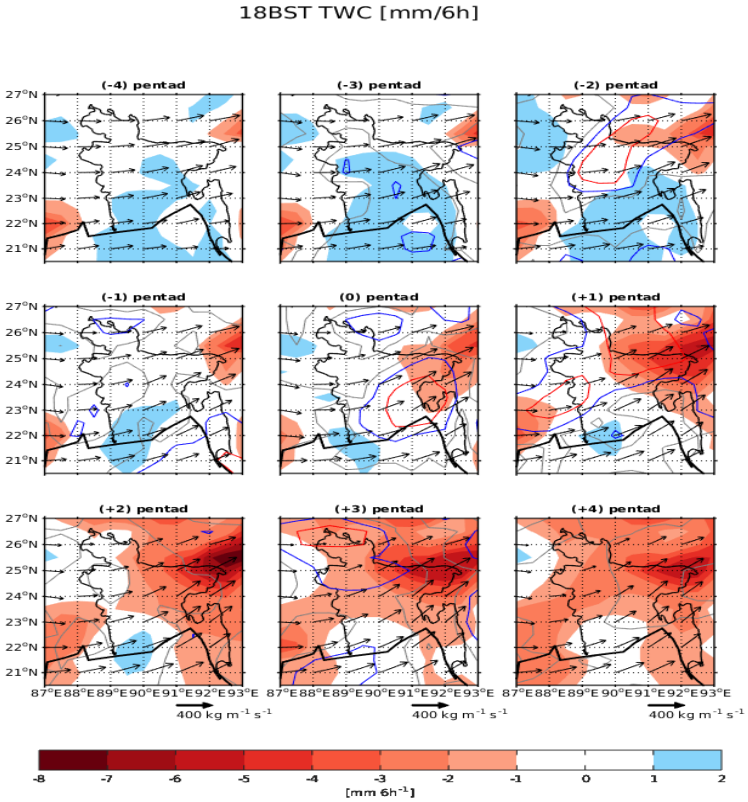

Figure 4.42: As in Figure 4.38, but for total water convergence [mm/6h] at 1800 BST. The clear regime transition is shown by red contours, while the blue contours show moderate transition.

4.4.2 Precipitation, evaporation, wind, moisture flux and water convergence at 0000 BST

At 0000 BST, the precipitation activity increases in the areas around Northeast Bangladesh [Figure 4.43]. The rain increases over the Meghalaya Plateau from pentad (-4) onwards, likewise in Northeast Bangladesh. The accumulated rainfall amount received over the past 6 hours at this time in Northeast Bangladesh is between 2 - 4 mm before the onset (pentad (0)), and about 4 - 7 mm after the onset. A drastic increase of about 4 mm of rainfall is observed at pentad (+1) immediately after the onset, and afterwards rainfall shows a gradual increase in the amount as the season progresses.

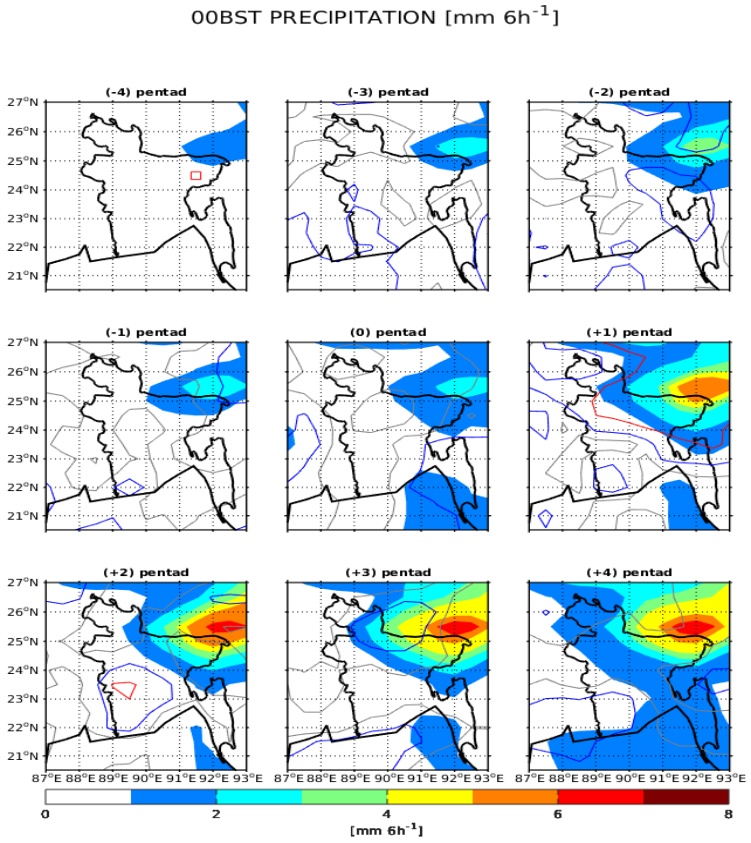

Figure 4.43: Lead-lag composite for precipitation [mm/6h] at 0000 BST. The red, blue, and gray contours represent the 0 - 25%, 25 - 50%, and 50 - 75% PDF overlaps, respectively. The areas around Northeast Bangladesh show a clear regime at pentad (+1) [red contour] with an increase in rainfall amount, while the blue contours show a moderate transition over that area.

The evaporation rate at 0000 BST is 0 - 0.4 mm across the whole country from pentad (-4) to pentad (+4), with a further decrease captured over Northeast Bangladesh at 0 - 25% overlap PDFs at pentad (+1) [Figure 4.44]. Figure 4.45 shows an increase in wind speed acceleration from pentad (-4) to pentad (+4) across Northeast Bangladesh and entire Bangladesh by 0000 BST. The increase in wind speed from 2 - 4 m/s before the onset to 5 - 7 m/s after the onset of the summer rains in Northeast Bangladesh can be attributed to the increase in the southwesterly flow from the Bay of Bengal towards the region.

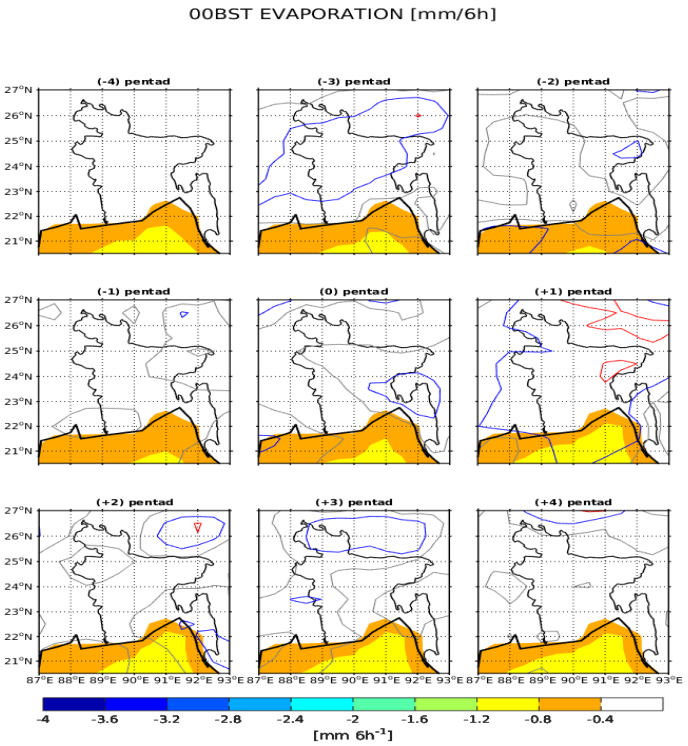

Figure 4.44: As in Figure 4.43, but for Evaporation [mm/6h] at 0000 BST.

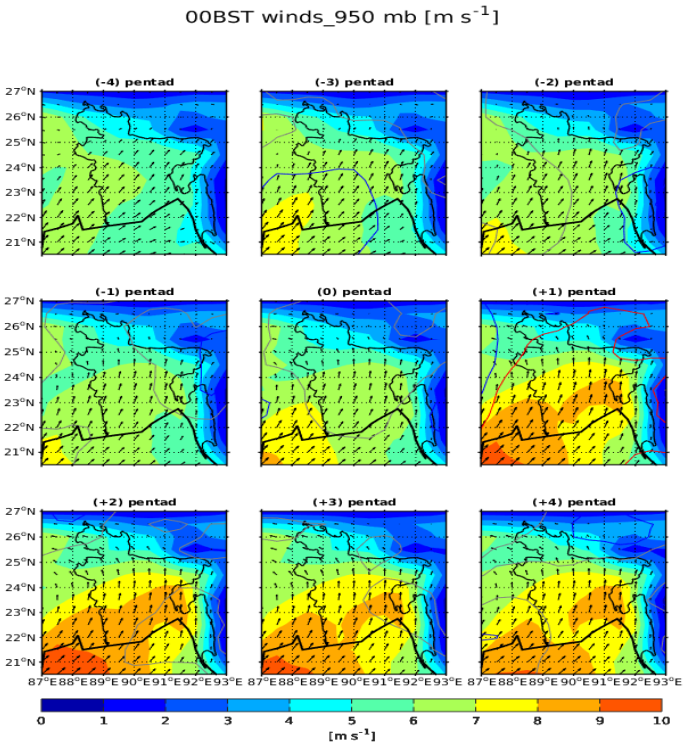

Figure 4.45: As in Figure 4.43, but for 950 hPa winds [m/s] at 0000 BST.

Figure 4.46 reveals that the moisture flux over Northeast Bangladesh increases from pentad (-4) to pentad (-2) and then decreases by about 100 kg/m/s from pentad (-1) up to onset.

The decrease in moisture flux prior to the onset is followed by a drastic increase of about 150 kg/m/s at pentad (+1) immediately after the onset. On the other hand, the water convergence increases from pentad (-4) to pentad (+4), showing a sudden increase of about 4 - 6 mm over the past 6 hours from pentad (+1) over Northeast Bangladesh [Figure 4.52]. The increase in water convergence over Northeast Bangladesh can be linked to the increase in moisture transport from the Bay of Bengal by the strong southwesterly winds and the insignificant evaporation during this time.

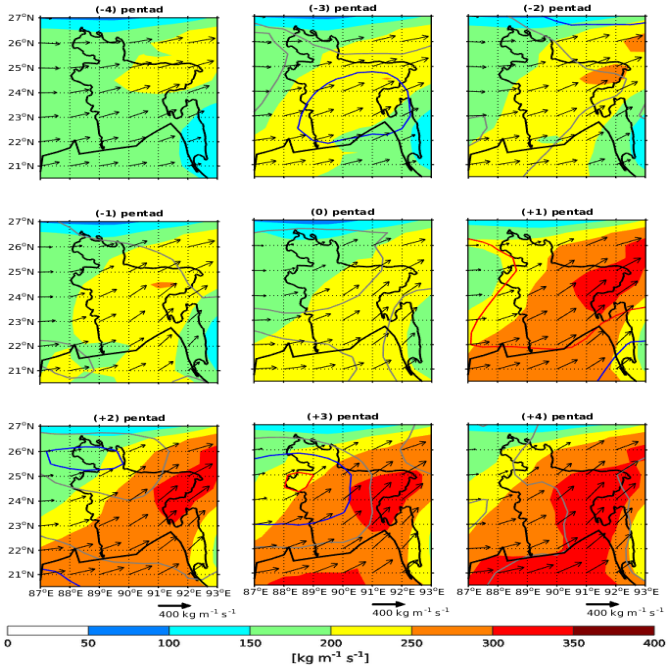

Figure 4.46: As in Figure 4.43, but for Vertically integrated moisture flux [kg/m/s] at 0000 BST.

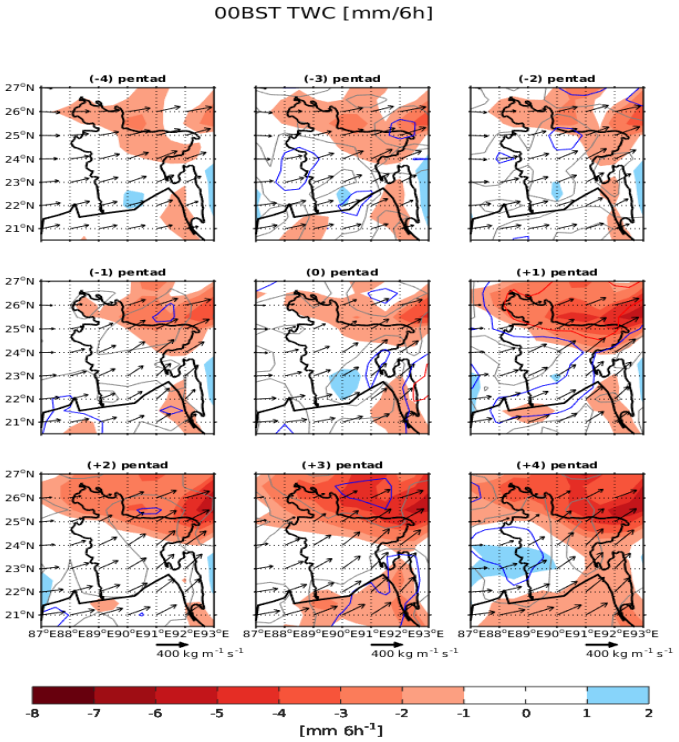

Figure 4.47: As in Figure 4.43, but for total water convergence [mm/6h] at 0000 BST.

4.4.3 Precipitation, evaporation, wind, moisture flux and water convergence at 0600 BST

Figure 4.48 shows a more increased intensity in the accumulated amount of rainfall recorded at 0600 BST with 2 - 3 mm over the past 6 hours in the pentads before the onset, and 5 - 7 mm in the pentads after the onset. The much more increase in precipitation amount recorded at this time confirms that the peak in rainfall intensity is achieved during the past 6 hours (i.e., 0000 - 0600 BST). Again, the much more increased rainfall intensity particularly at pentad (+1) just after the onset, indicates a strong and clear transition from onset (pentad(0)) to pentad (+1), [Figure 4.48]. Then from pentad (+1) onwards, precipitation shows a steady increase in intensity as the season progresses.

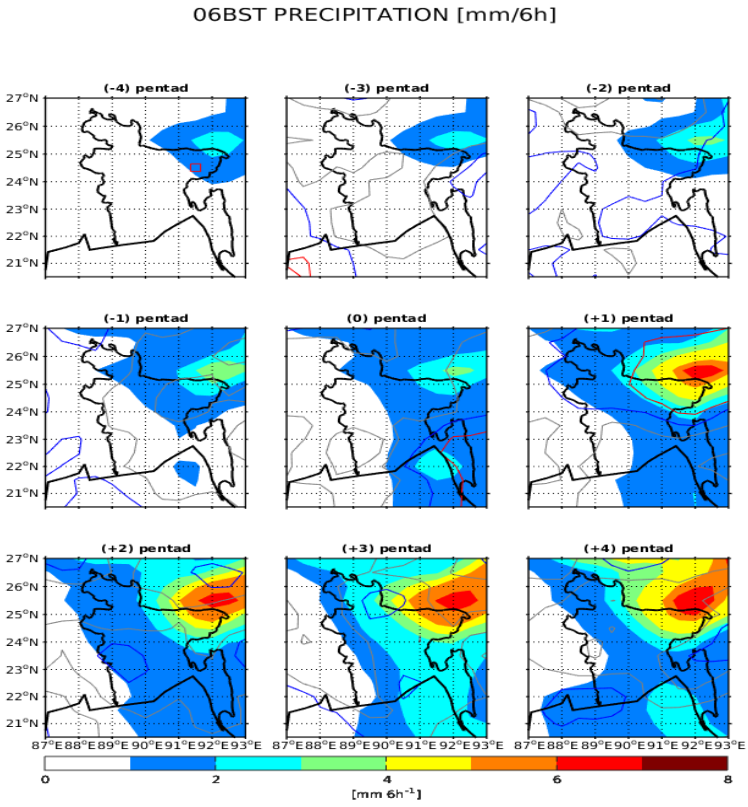

Figure 4.48: Lead-lag composites for precipitation [mm/6h] at 0600 BST. The red, blue, and gray contours represent the 0-25%, 25-50%, and 50-75% PDF overlaps, respectively. The red, blue and gray contours in this figure further show a clear, moderate, and weak regime transition over those areas.

The evaporation rate at 0600 BST is almost constant at 0.4 - 0.8 mm over the previous 6 hours before the onset, and then suddenly decreases to almost 0 mm from pentad (+1) onwards in Northeast Bangladesh [Figure 4.49]. The sudden decrease in evaporation rate after onset corresponds with the much more increase in precipitation from the onset of summer rains in Northeast Bangladesh which cools the region. The low-level winds at 0600 BST also increase in their acceleration speed before and after onset, with a drastic increase in wind speed acceleration across the entire Bangladesh at pentad (+1) followed by a gradual increase in wind speed as the season progresses [Figure 4.50]. By comparing

the wind speeds at 0000 BST and 0600 BST, it is evident that the winds also attain their maximum between 0000 BST and 0600 BST.

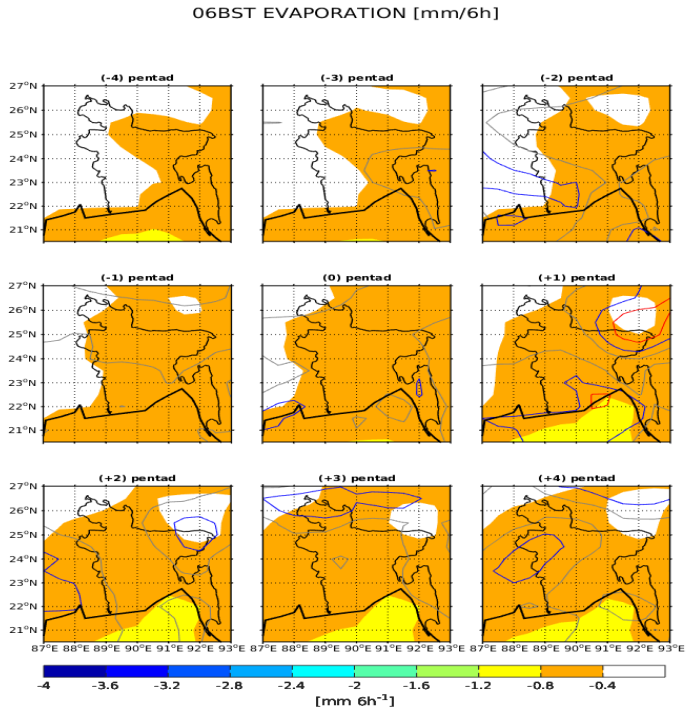

Figure 4.49: As in Figure 4.48, but for Evaporation at 0600 BST

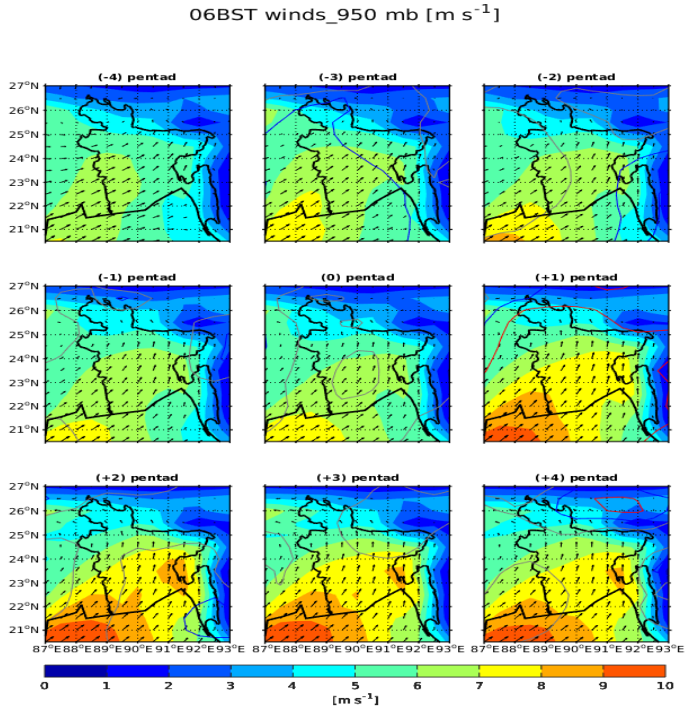

Figure 4.50: As in Figure 4.48, but for 950 hPa winds [m/s] at 0600 BST.

The moisture flux [Figure 4.51] and total water convergence [Figure 4.57] at 0600 BST both show a much more increased intensity around Northeast Bangladesh before and after the onset of summer rains. The moisture flux increases from 200 kg/m/s before the onset

to 350 kg/m/s after the onset, while the water convergence over Northeast Bangladesh increases from 1 - 3 mm before the onset to 4 - 8 mm after the onset. The much more increase in the intensity of both moisture flux and water convergence observed at this time over Northeast Bangladesh can be attached to the heavy nocturnal precipitation between 0000 and 0600 BST [Figure 4.48] and the strong nocturnal low-level southwesterly winds which transport huge moisture amounts from the Bay of Bengal towards the region [Figure 4.50], accompanied by the high elevated Meghalaya Plateau which blocks the strong moist southwesterly flow from proceeding to other places, and hence strong moisture convergence around Northeast Bangladesh.

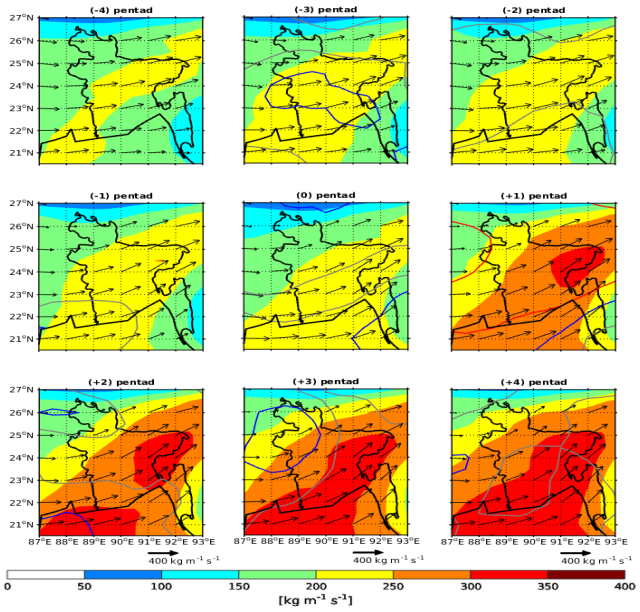

Figure 4.51: As in Figure 4.48, but for Vertically integrated moisture flux [kg/m/s] at 0600 BST.

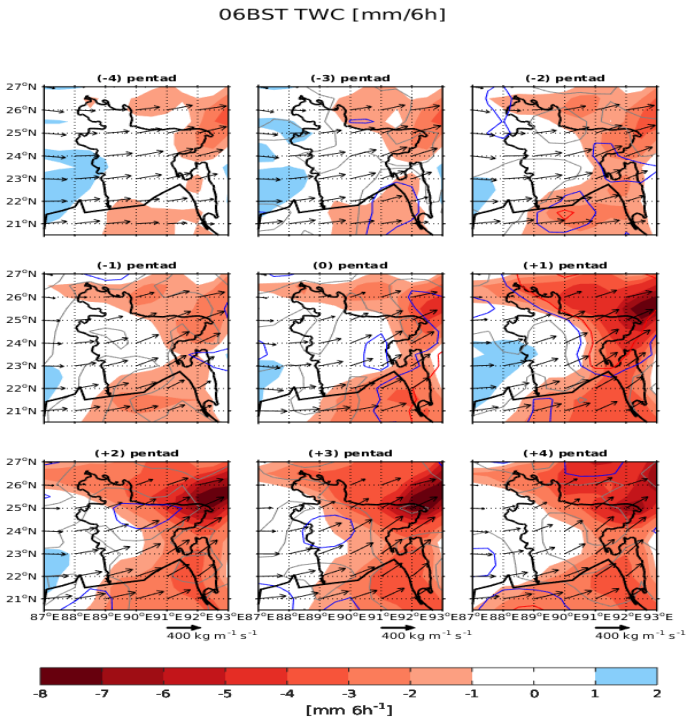

Figure 4.52: As in Figure 4.48, but for total water convergence [mm/6h] at 0600 BST.

4.4.4 Precipitation, evaporation, wind, moisture flux and water convergence at 1200 BST

The lead-lag composites of accumulated rainfall at 1200 BST [Figure 4.53] show some persistence of the rain that has been falling in the previous hours. The accumulated rainfall amount over the past 6 hours is in the range of 2 - 4 mm before onset, and 5 - 6 mm after the onset in Northeast Bangladesh. In Figure 4.53, we see that the rainfall increases in intensity at onset around Northeast Bangladesh and the surrounding areas in all directions. Still pentad (+1) shows a clear transition with an abrupt increment in the rainfall intensity with 0 - 25% overlap of the PDFs in Northeast Bangladesh, and then followed by a gradual increase in rainfall intensity within the season. From the same figure, we can also see that the rains spread over the whole country after the onset and even further to the coast of the Bay of Bengal with greater intensity. Figure 4.53 further reveals that the heavy rainfall may continue for some hours after 0600 BST or can even go up to mid-day (1200 BST) in Northeast Bangladesh and other parts of the country receive a wide spread of rainfall of less intensity.

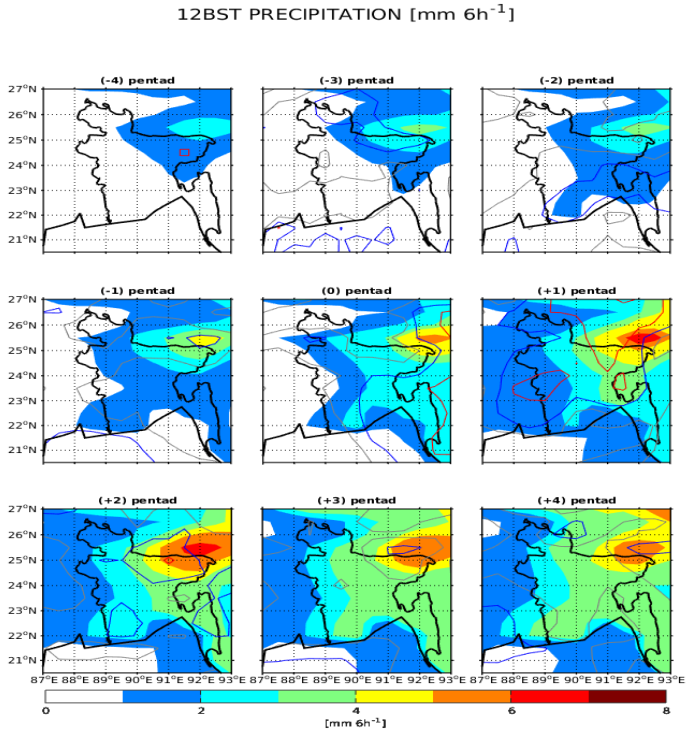

Figure 4.53: Lead-lag composites for precipitation [mm/6h] at 1200 BST. The red, blue, and gray contours represent the 0-25%, 25-50%, and 50-75% PDF overlaps, respectively.

Figure 4.54 shows that evaporation at 1200 BST is much more vigorous compared to that at 0000 and 0600 BST, with its rate increasing to about 2.4 - 2.8 mm before the onset and then reduces to about 2.0 - 2.4 mm over Northeast Bangladesh immediately after onset of the summer rains in the region. The increase in evaporation rate before the onset can be attached to less precipitation at this time [see Figure 4.53] and strong daytime summer solar heating at 1200 BST, while the sudden decrease immediately after the onset can be

attached to the precipitation from the onset of the summer rains. Figure 4.55 shows a much more decrease in low-level wind speed at 1200 BST in the pentads, compared to the wind speeds at 0600 BST. The much more decrease in wind speed indicates that the low-level winds over Northeast Bangladesh and entire Bangladesh experience their minimum speeds between 0600 BST and 1200 BST.

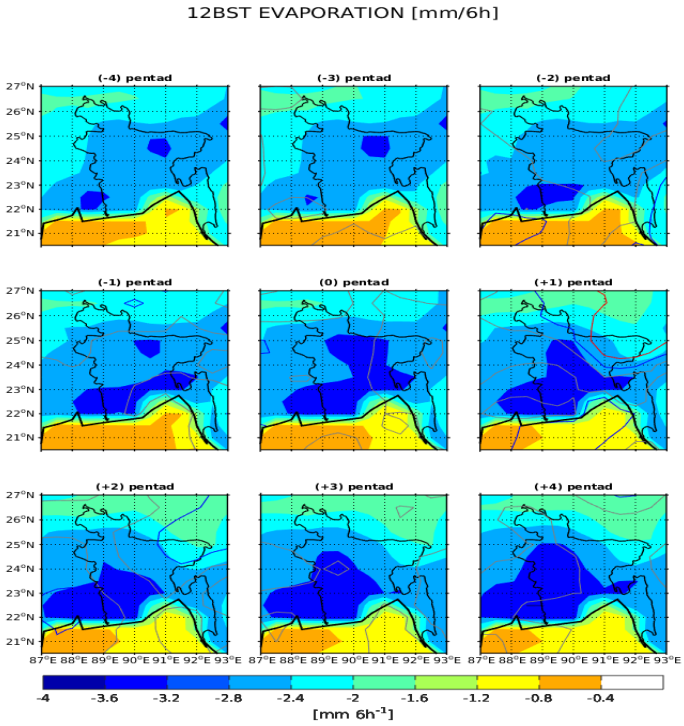

Figure 4.54: As in Figure 4.53, but for Evaporation [mm/6h] at 1200 BST

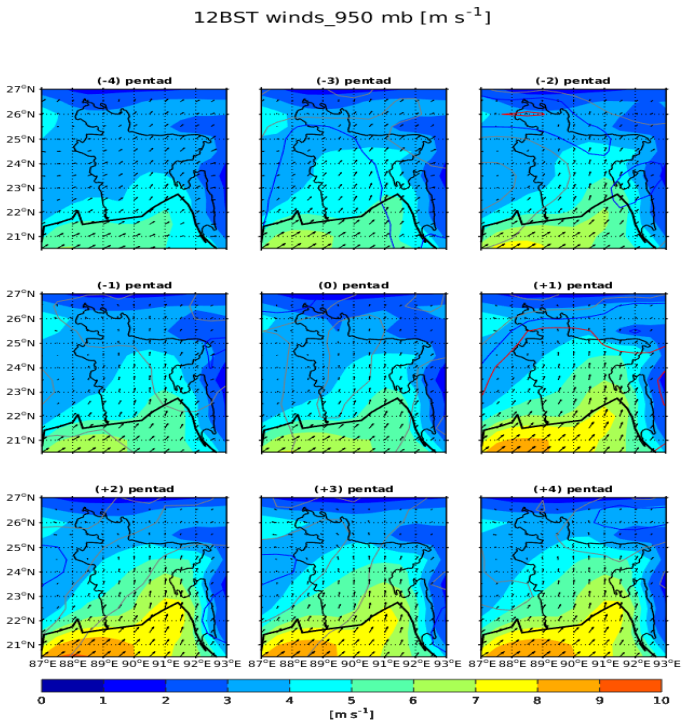

Figure 4.55: As in Figure 4.53, but for 950 hPa winds at 1200 BST

The moisture flux over Northeast Bangladesh at 1200 BST show similar character with that at 0600 BST before the onset with it values between 200 - 250 kg/m/s and then suddenly increases to values between 250 - 350 kg/m/s after the onset [Figure 4.56]. Figure 4.57 reveals that less water (moisture) converges around Northeast Bangladesh at 1200 BST before and after the onset, compared to the more vigorous water convergence at 0600 BST [see Figure 4.52]. This much decrease in water convergence at 1200 BST could be due to the vigorous evaporation caused by the much solar heating at this time, which means that much of the moisture evaporates instead of converging in the region.

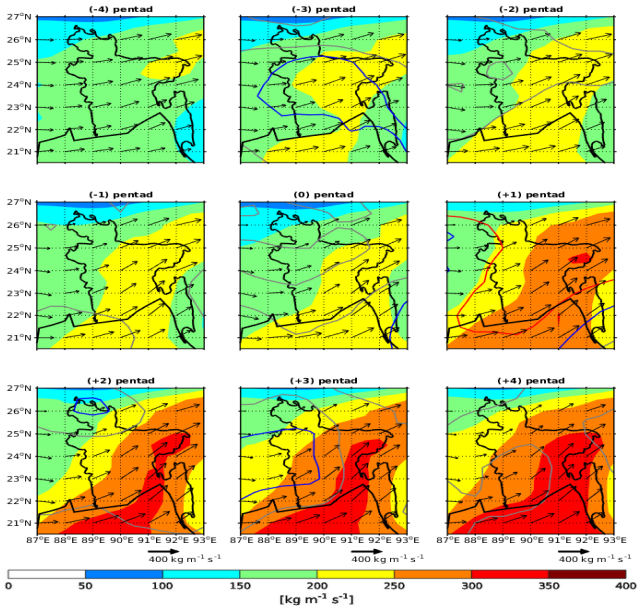

Figure 4.56: As in Figure 4.53, but for Vertically integrated moisture flux [kg/m/s] at 1200 BST

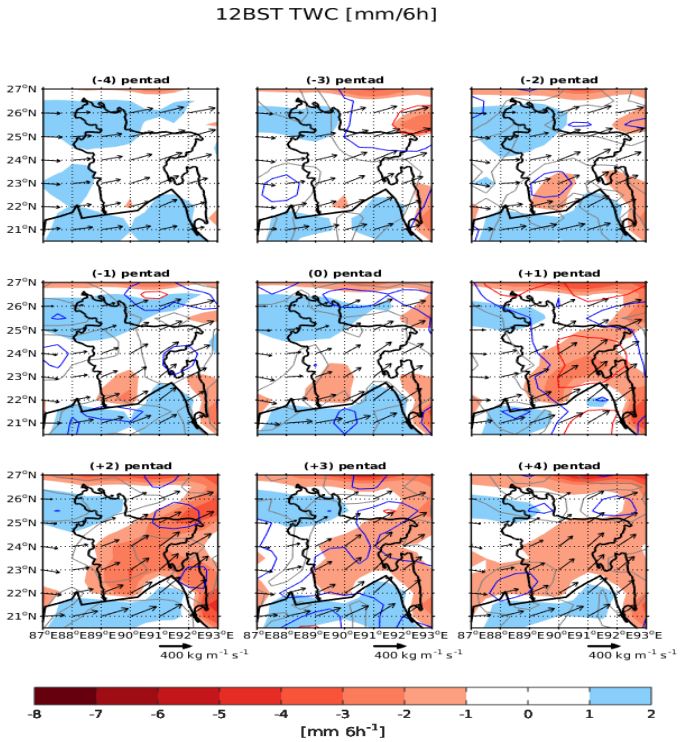

Figure 4.57: As in Figure 4.53, but for total water convergence [mm/6h] at 1200 BST

To summarize the diurnal variations of precipitation, low-level wind, evaporation, moisture flux and water convergence, Figures 4.58 - 4.62 give a more clear view of the diurnal cycles of precipitation, evaporation, low-level wind, moisture flux and water convergence over Northeast Bangladesh prior to, and after the onset of the summer rains in this region. The figures show a clear distinction of the behaviour of the diurnal cycles of these different parameters before and after the onset of the summer rains in Northeast Bangladesh. The figures also show a distinct regime transition in all the parameters, with the pentads prior to the onset [dashed lines in these figures] revealing that precipitation, low-level wind, moisture flux and water convergence show less activity before the onset [think solid black line], apart from evaporation [Figure 4.59] which is more vigorous before the onset of the summer rains.

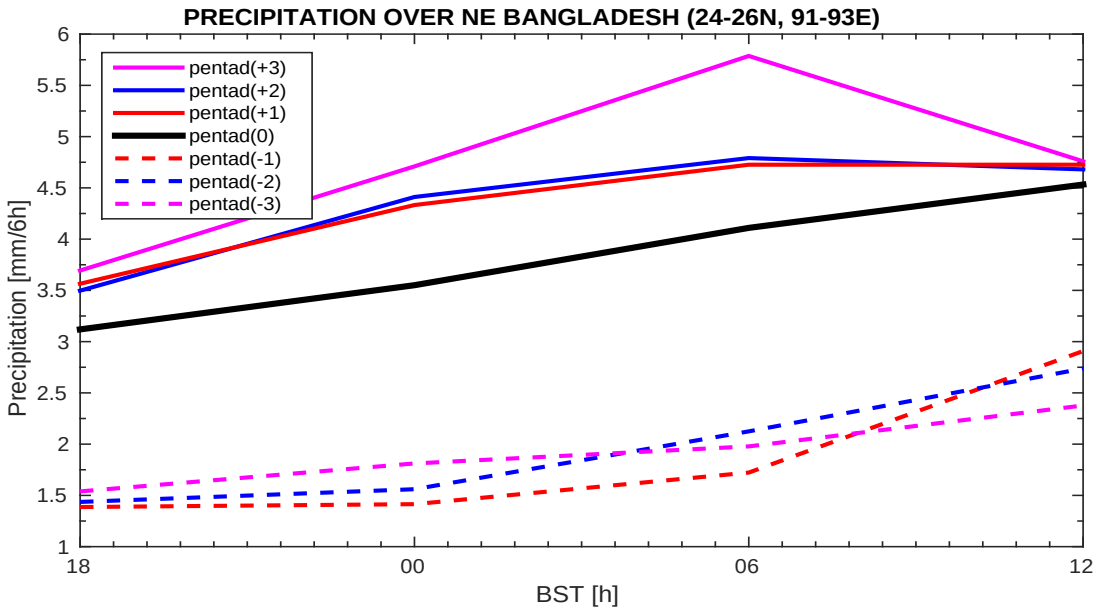

Figure 4.58: Lead-lag diurnal variations of precipitation over Northeast Bangladesh (24-26N, 91-93E). The black thick solid line indicates the onset pentad, while the other solid, and dashed lines indicate pentads after, and prior to the onset, respectively. Time used in this figure is Bangladesh Standard Time (BST) in hours.

The pentads after the onset [solid lines in Figures 4.58 - 4.62] show a drastic increase in precipitation, low-level wind, moisture flux and water convergence immediately after the onset of the summer rains in Northeast Bangladesh, except evaporation which shows a sudden decrease its rate after the onset. The sudden decrease in evaporation rate after of the onset of the summer rains can be strongly attached to the drastic increase in precipitation from onset onwards, which cools the region, while the drastic increase in moisture flux and water convergence over Northeast Bangladesh can be attributed to the drastic increase in strength of the moist southwesterly flow coming from the Bay of Bengal to the region and the strong blocking of moist flow by the Meghalaya Plateau. The diurnal cycles of precipitation, low-level wind, and water convergence over Northeast Bangladesh reveal that they all increase from 1800 BST to 0600 BST, attaining their maximum between 0000 BST and 0600 BST after the onset of the summer rains in the region [Figures 4.58, 4.60, and 4.62, respectively].

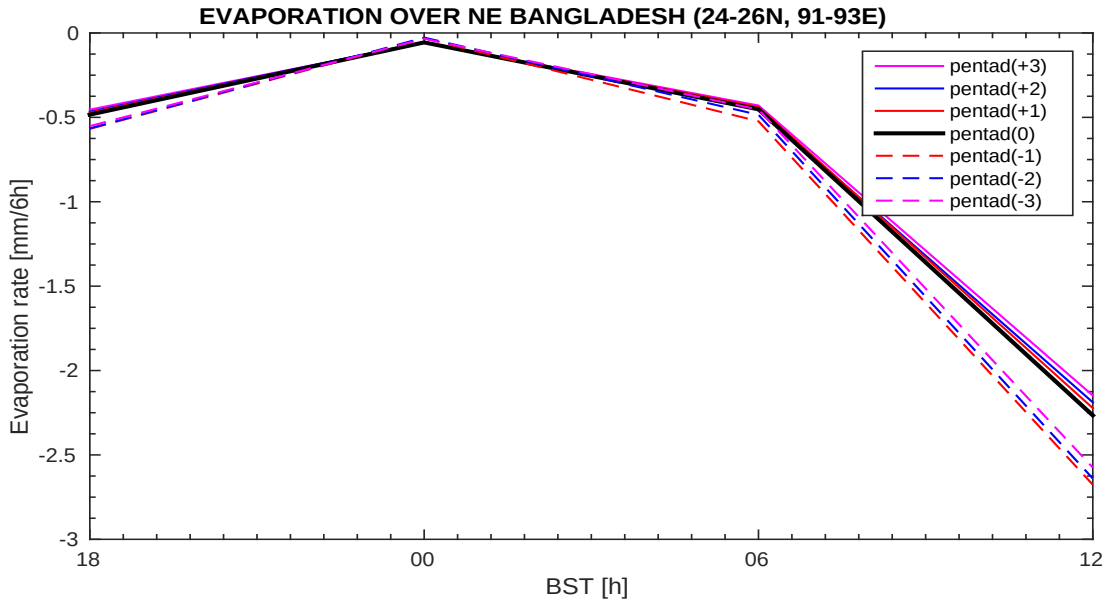

Figure 4.59: As in Figure 4.58, but for Evaporation.

Then from 0600 BST, the precipitation intensity, low-level wind speeds, and moisture convergence decrease steadily until 1200 BST, attaining their minimums in between. Both precipitation and low-level wind at night are termed as nocturnal rains and nocturnal low-level winds, respectively, with the maximum in nocturnal rains between 0000 BST (midnight) and 0600 (morning) being referred to as the late night-early morning rainfall maximum. Thus, Figure 4.58 clearly reveals that precipitation after the onset exhibit a distinctly remarkable late night-early morning rainfall maximum in Northeast Bangladesh. Despite the differences in the data sets used, Ohsawa et al. [2000, 2001]; Islam and Uyeda [2005]; Kataoka and Satomura [2005]; Terao et al. [2006] and Sato [2013] in their studies also found this distinct characteristic of precipitation over Northeast Bangladesh during this period.

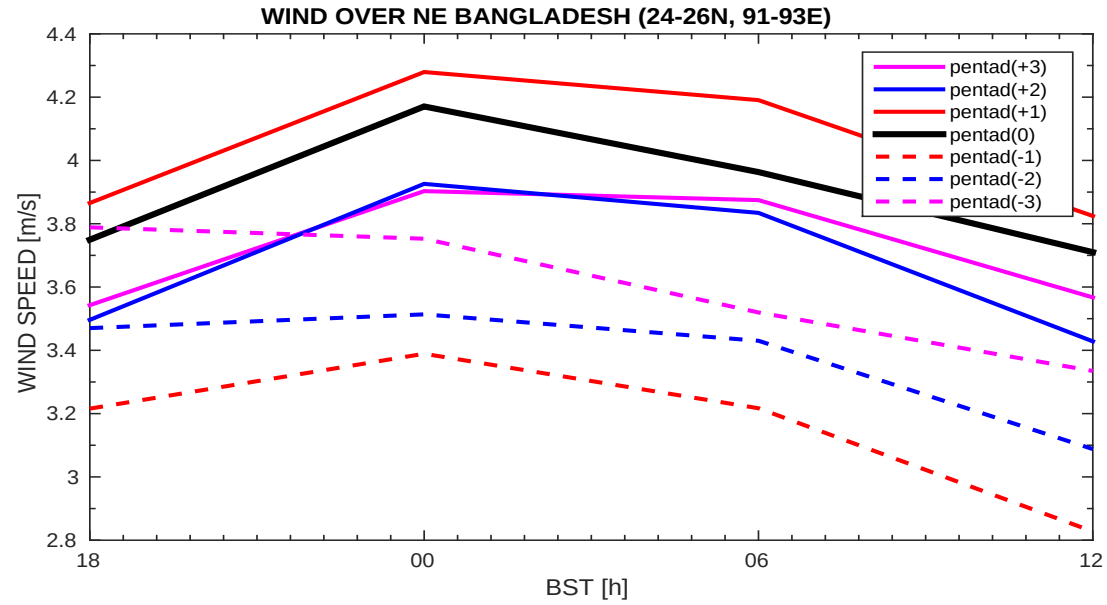

Figure 4.60: As in Figure 4.58, but for 950 hPa winds.

Although the winds at lower levels such as 950 hPa are usually weaker as opposed to the strength of the winds at upper levels, the increase in wind speed from 1800 BST to past midnight points to the presence of a nocturnal low-level jet during the onset of the summer rains in Northeast Bangladesh. Interestingly, it is worthy to note that the increase in acceleration of the low-level tropospheric winds over Northeast Bangladesh coincides with the increase in the precipitation intensity over the same region [Figure 4.58], both attaining their peaks between late night and early morning. Basing on this association, we can hypothesize that when these nocturnal low-level winds interact with mesoscale convective vortices and other outflow boundaries around Northeast Bangladesh, they can lead to the development of the convective systems that cause late night-early morning rainfall maximum in Northeast Bangladesh. This is because both nocturnal low-level wind acceleration and precipitation intensity increase/decrease concurrently over Northeast Bangladesh, and hence suggesting that nocturnal low-level winds have a strong effect to the cause of the late night-early morning rainfall maxium over this region. Similar association between nocturnal low-level wind maximum and late night-early morning rainfall maximum over Northeast Bangladesh was confirmed by Terao et al. [2006] during their study about the effects of nocturnal jet on early morning rainfall peak over northeastern Bangladesh in the summer monsoon season. Similarly, Sato [2013] associated the late night-early morning rainfall maximum to the low-level jet maxima that happens on the windward side of the Meghalaya Plateau during the late night-early morning hours. Notwithstanding the difference in context, Fujinami et al. [2014] also confirmed the linkage between the nocturnal low-level jet and the late night-early morning rainfall maximum during the active phase of intraseasonal oscillation (ISO) in summer monsoon rainfall.

The presence of the stronger southwesterly winds over the Bay of Bengal at 950 hPa level from pentad (+1) onwards at both 1200 BST [Figure 4.55] and 1800 BST [Figure 4.40], also suggests a possibility of having sea breeze circulations during these hours. This because we expect to have a strong temperature contrast between the coastal land and the Bay of Bengal surface since the boundary layer heating over land is at its maximum, which when it combines with the prevailing southwesterly winds, can produce conditions that are favourable for the development of the afternoon sea breeze circulation. This sea breeze is also expected to be most intense during the afternoon, suggests that it can penetrate several kilometres inland. As the sea breeze propagates inland during the nighttime, it could trigger convection at night.

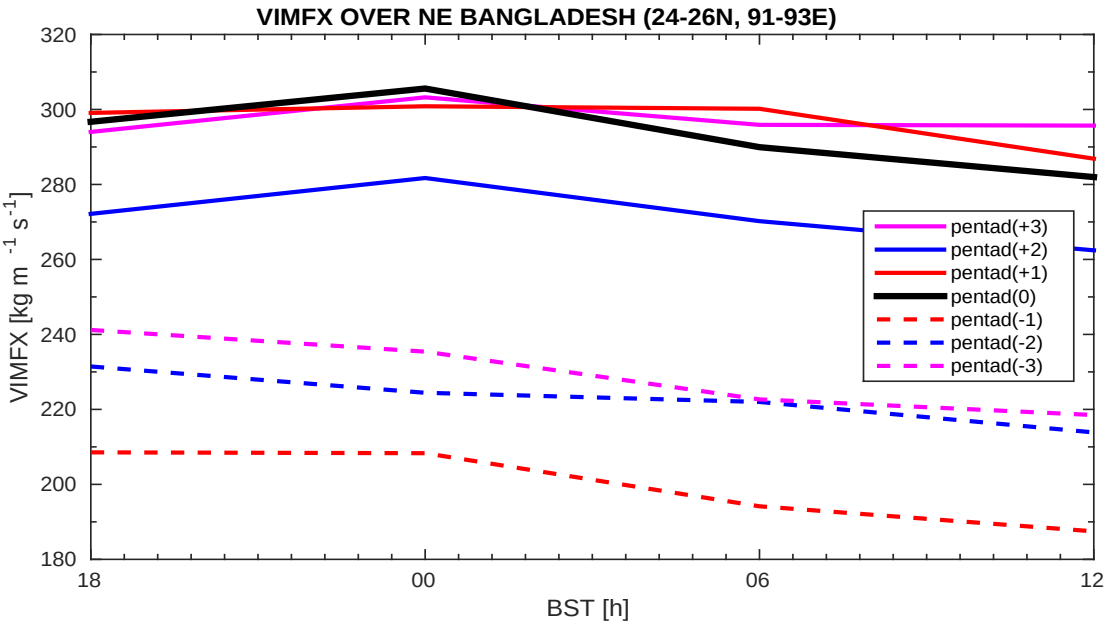

Figure 4.61: As in Figure 4.58, but for Vertically integrated moisture flux.

Figure 4.59 reveals that evaporation rate before and after the onset of summer rains exhibit a similar trend in the diurnal variation, decreasing to minimum from 1800 BST to 0000 BST and thereafter starting to increase steadily from 0000 BST to 0600 BST. From 0600 BST to 1200 BST, evaporation rate increases rapidly, attaining its maximum in between. The diurnal cycle of moisture flux reveals that moisture flux start to increase steadily from 1800 BST to 0000 BST before and after the onset of the summer rains, attaining its maximum in between, before it starts to decrease from 0000 BST [Figure 4.61].

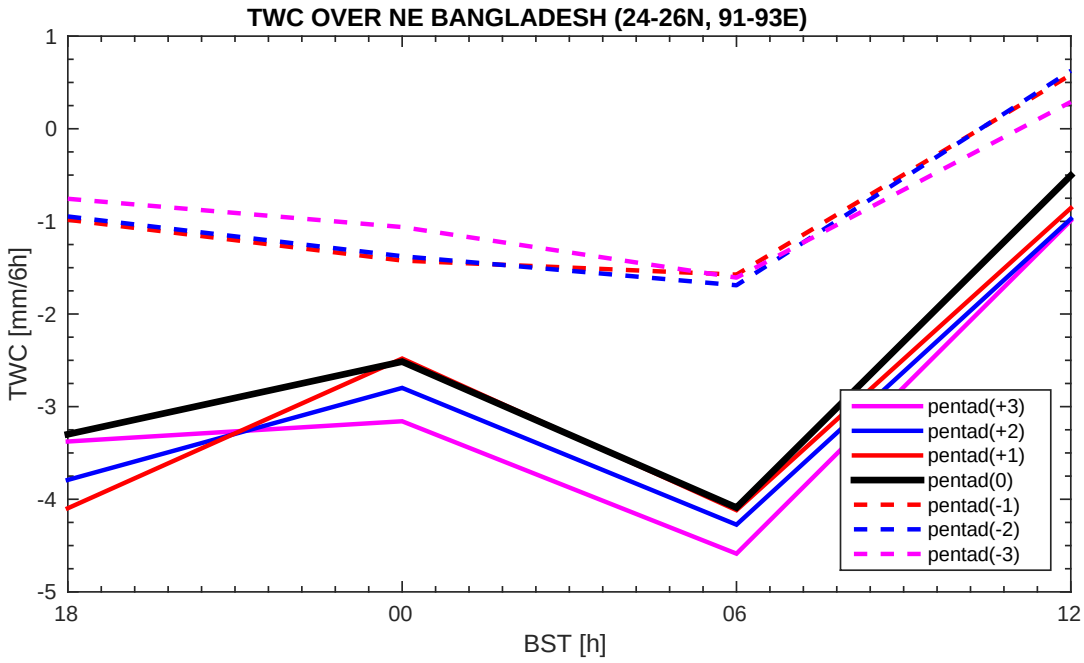

Figure 4.62: As in Figure 4.58, but for total water convergence.

As seen in Figures 4.43 and 4.48, the maximum rainfall in Northeast Bangladesh is received between 0000 BST and 0600 BST, which further attests that late night-early morning rain-

fall maximum happens during this time. The figures also reveal that these late night-early morning rains occur on the windward side of the Meghalaya Plateau which is north of Northeast Bangladesh. This suggests that the late night-early morning rainfall maximum received in Northeast Bangladesh is strongly associated with the topographic effect of the Meghalaya Plateau which acts as a barrier to the southwesterly flow of the warm moist winds from the Bay of Bengal [see Figures 4.45, 4.46, 4.50, and 4.51]. This late night-early morning rainfall maximum in Northeast Bangladesh and its associated cause is consistent with the findings of Ohsawa et al. [2001], who showed its occurrence on the windward side of the Meghalaya Plateau, which is located north of Northeast Bangladesh [see Figure 1.1]. Similarly, Kataoka and Satomura [2005] and Hatsuzuka et al. [2014] found a strong association between the late night-early morning rainfall maximum over Northeast Bangladesh and the precipitation systems triggered around the southern slope of the Meghalaya Plateau, and later propagating southward. The fact that these rains occur on the windward side of Meghalaya Plateau signifies their association with the topographic effect of the Meghalaya Plateau which blocks and uplifts the strong southerly/southwesterly moist winds from the Bay of Bengal. Thus, we can strongly agree with Ohsawa et al. [2001]; Fujinami et al. [2014]; Hatsuzuka et al. [2014] that the rainfall received over Northeast Bangladesh is as a result of orographic uplift of the southerly/southwesterly inflow of low-level moist winds from the Bay of Bengal.

Since the prevailing southerly/southwesterly nocturnal low-level winds are blowing towards the Meghalaya Plateau and the other elevated topography to the east of Northeast Bangladesh [Figures 4.45 and 4.50], we hypothesize that there is a possibility of the mountain breezes or katabatic winds from these mountains during the night that converge with nocturnal low-level winds to cause convection around Northeast Bangladesh during the late night-early morning hours. This hypothesis is in line with Ohsawa et al. [2001]'s suggestion that the mountain breeze from Meghalaya Plateau is sufficient to cause the low-level convergence during the nighttime especially when the prevailing winds are blowing against the mountain breeze, and thus triggering nighttime convection. However, Kataoka and Satomura [2005] discovered that the katabatic winds from these mountains around Northeast Bangladesh are not pivotal in the diurnal cycle of precipitation over Northeast Bangladesh.

Chapter 5

Summary and Concluding Remarks

This chapter provides a summary of the main results obtained using the various methods to achieve the study objectives. It also provides the conclusions, and further recommendations of the study.

5.1 Summary

The main aim of this study was to shed light on the convective triggering mechanisms influencing the summer rainfall in Northeast Bangladesh, while its other objectives included: 1) Understanding the climatology of summer rains using observation and reanalysis data; 2) Using large-scale composites to see if a conclusion can be drawn about the mechanism causing the summer rainfall; and 3) Understanding the diurnal cycle of precipitation and its effects on summer rainfall in Northeast Bangladesh.

The general climatology basing on rainfall observation data revealed that the heaviest rain in Northeast Bangladesh falls during the March - May period, which is the termed as the Bangladesh summer. We use the term summer rains to refer to the heavy precipitation that is received in Northeast Bangladesh during the summer months of March to May, before the large-scale monsoon begins in June. Further analysis on rainfall observation data showed that about 1.0%, 25.3%,67.6% and 6.1% of the total precipitation received annually in Northeast Bangladesh falls in DJF, MAM, JJAS, and ON periods, respectively. It was also revealed that heaviest rainfall in Northeast Bangladesh falls in April and May on average [Figure 4.2], and that over the past decades, the number of heavy rainfall events in May have increased to nearly the same number of heavy rainfall events in June [Figure 4.3(f)]. Furthermore, the wettest year basing on the wettest summer was 2010, while 1971 was the driest year in the period 1956 - 2010.

To determine the onset of the summer rains for every year over Northeast Bangladesh, Sylhet station rainfall observation data for the period from 1979 - 2010 was used with a 11

mm/day pentad rainfall mean threshold and a 6-pentad moving algorithm developed by Stiller-Reeve et al. [2015]. These onset pentads were later used to construct the lead-lag composites from the ERA-Interim reanalysis data to assess the large-scale situation prior to and after the onset. The composites were then tested for statistical significance using both the Monte Carlo (MC) and the Overlap Coefficient (OVC) method.

The lead-lag composites and the OVC results revealed a large transition in precipitation amount over Northeast Bangladesh at the first pentad immediately after the onset of summer rains. The results also showed that prior to the onset, the low-level winds change from westerly/northwesterly to strong southerly/southwesterly, leading to the well-marked shallow inflow of moisture from the Bay of Bengal directed towards Northeast Bangladesh, while the mid-upper tropospheric winds exhibit a purely moderate to strong westerly flow that is associated with the westerly jet across the Indian subcontinent. This implies that the typical characteristics of the large-scale monsoon in this region are not completely fulfilled, suggesting that the these rains are a result of local circulation around this region. It was noted that after the onset, the stronger low-level southwesterly winds over the Bay of Bengal manifested at pentad (+1). These winds can intensify the local convective activity over Northeast Bangladesh when they are blocked and forced to rise by the Meghalaya Plateau and the other mountains to the east of Northeast Bangladesh. They can also combine with the strong surface temperature gradient to produce conditions that are favourable for the development of the daytime sea breeze circulation. The analysis further showed that the atmosphere is unstable to vertical motions over Northeast Bangladesh at lower to mid-troposphere during the onset period due to the presence of abundance moisture in the lower troposphere over Northeast Bangladesh [Figure 4.37], which implies that even a small perturbation can be enough to produce rain-bearing clouds. These low-level environmental conditions are conducive for the development of convective systems during this period, and hence, the resultant summer rains.

Our analysis revealed the existence of both the thermal low over India and the dry-line at lower levels below 600 hPa, extending inwards of western Bangladesh around the onset of the summer rains in Northeast Bangladesh. The heat low greatly influences both the low-level circulation pattern and the dry-line. This is because we observed that the circulation pattern changes from moderate northwesterlies to strong southwesterlies over the heat low or just at eastern edge of the heat low, while the dry-line exists because of the hot and dry air mass (heat low) over India to the west and the warm moist air mass over Bangladesh to the east. The other fact that supports the great impact of the heat low on low-level circulation pattern is that the low pressure system deepened further when the heat low intensified. The confinement of the heat low to only lower levels below 600 hPa, renders the dry-line to be quite shallow, hence further confirming the great impact of the heat low on dry-line.

The temperature over Northeast Bangladesh at 925 hPa level dropped by 3 - 5 K immediately after the onset, making Northeast Bangladesh cooler than the surrounding areas to its west and south [Figure 4.20]. This cooling could be due to the evaporative cooling

from the intensive rain at onset of summer rains in Northeast Bangladesh. The resultant cool air was trapped in the region by the surrounding elevated topography, such as the Meghalaya Plateau and the other mountains to east of Northeast Bangladesh. We speculate that the warm moist southerly/southwesterly air mass on convergence with the cold air, it is forced to rise over the low-level cold pool before reaching the Meghalaya Plateau and possibly convect further, and hence triggering convection over Northeast Bangladesh.

A weak IMT was observed at both 600 and 700 hPa pressure levels in the the geopotential height field. This IMT is connected to the trough, which is seen to exist as a result of an elongation of the shallow low pressure system over India [Figure 4.16]. The IMT strongly influences the southwesterly flow, while the elongation of the low pressure system (trough) to cover the whole of Bangladesh, can result in the increase of rainfall over Northeast Bangladesh since it advects more moist air towards Northeast Bangladesh, where the local convective activity is much more vigorous during this period. It was also observed that precipitation over Northeast Bangladesh (east of the trough) increases as the IMT deepens further and shifts eastward.

The moisture flow pattern changed from moderate westerly/northwesterly before the onset to a purely strong southwesterly flow at onset, with a clear regime transition being exhibited by the meridional component of the moisture flux [Figure 4.8]. A bulk of the moisture that is contained in lower troposphere over Northeast Bangladesh comes from the Bay of Bengal, being transported by the low-level strong southwesterlies towards Northeast Bangladesh [Figure 4.9]. Furthermore, the analysis revealed that the upper-level troposphere contains little moisture, and the main transport mechanism for this moisture is the strong upper-level westerlies from India [Figure 4.10]. Much of the moisture converges around the Meghalaya Plateau and the other surrounding mountains before it converges over Northeast Bangladesh during the onset [Figure 4.11]. This is because these mountains block the warm moist southerly/southwesterly winds from their continuous horizontal flow, forcing them to converge over there before they are forced to rise. The analysis showed that areas around the Meghalaya Plateau with strong moisture convergence, are also the areas receiving much precipitation. In fact the water (moisture) convergence pattern is very similar to that of precipitation. Hence, this confirms the strong link between moisture convergence, precipitation and the orography around Northeast Bangladesh. At the same time, areas of high precipitation and moisture convergence have low evaporation rates [Figure 4.6], simply because the precipitation they receive reduces the temperature. As a consequence, these areas are moisture sinks since precipitation has a surplus over evaporation during this period.

The diurnal cycles of both precipitation and water/moisture convergence have revealed a steady increase in both rainfall intensity and water convergence over Northeast Bangladesh after the onset from 1800 BST to 0000 BST, and thereafter both precipitation and water convergence attaining their maximum intensities between 0000 BST and 0600 BST. We use the term late night-early morning rainfall maximum to refer to this distinct feature of the precipitation over Northeast Bangladesh because the rainfall maximum intensity is

achieved between 0000 BST to 0600 BST. The analysis also revealed that heavy precipitation over Northeast Bangladesh may go past 0600 BST for some hours of the morning.

To further examine the mechanisms responsible for the diurnal cycle of precipitation, analysis on the diurnal cycle of low-level winds over Northeast Bangladesh was also carried out as suggested by Terao et al. [2006]. The results from the analysis of the diurnal cycle of low-level wind revealed that wind speeds accelerated from 1800 BST past midnight, peaking between 0000 - 0600 BST. This peak in the low-level wind acceleration corresponded with the peak in precipitation over Northeast Bangladesh, which suggests a link between the nocturnal precipitation and the nocturnal low-level wind acceleration.

In the advent to somehow close up the water budget equation, the diurnal cycle of evaporation over Northeast Bangladesh was also considered. The results revealed that the diurnal behaviour of evaporation before and after the onset of the summer rains is similar, with evaporation decreasing to its minimum between 1800 BST and 0000 BST, while its maximum is between 0600 BST and 1200 BST [Figure 4.59].

5.2 Conclusion

The study focused on summer rainfall in Northeast Bangladesh with the aim of shedding light on the triggering mechanisms that are at play during the onset of summer rains in this region. While a number of plausible theories were linked to the cause of summer convection in Northeast Bangladesh, a lot of ambiguities and disagreements about which mechanism(s) trigger(s) this convection still existed among the research community. It was from these much ambiguities and disagreements surrounding the convective triggering mechanisms of summer rainfall that the study derived its motivation.

The results from this study revealed that the summer rains in Northeast Bangladesh are not part of the large-scale monsoon, but rather a result of local circulations around this region. The results also revealed the stronger low-level southwesterly winds over the Bay of Bengal at the first pentad after the onset of summer rains. The presence of these stronger winds during the onset period points to a possible mechanism of the sea breeze circulations. Despite the fact that the mechanism of sea breeze circulations is not yet discussed in literature, we plausibly believe that the sea breeze circulations play part in triggering summer convection over Northeast Bangladesh. Furthermore, our results from this study show that the previously discussed theories are plausible causes of the summer rainfall in Northeast Bangladesh as highlighted below;

1. Orographic uplifting of low-level southerly/southwesterly moist wind inflow by the Meghalaya Plateau. This is due to the fact that during this period, the warm moist southwesterlies from the Bay of Bengal are blowing towards the Meghalaya Plateau and their meridional components are enhanced, and hence the heavy precipitation is probably triggered as a result of orographic uplifting of the moist air. The other

fact that supports this theory is that the heavy rainfall is limitedly found on the windward side of the Meghalaya Plateau, and that the areas further away from the Megalaya Plateau are found to have less moisture convergence and at the same time receiving less or no rainfall at all.

2. Nocturnal low-level jet interacting with other air masses and the orography around Northeast Bangladesh seems to be a viable triggering factor of the late night-early morning rainfall maximum. This is because much of rainfall in Northeast Bangladesh is received at night when the low-level southwesterly winds become stronger. The fact that the peak in low-level wind acceleration from midnight to early morning corresponds with the peak in rainfall intensity during the same time, confirms a strong affection of the nocturnal low-level jet with the heavy precipitation over Northeast Bangladesh.

3. The presence of a cold pool of air over Northeast Bangladesh at 925 hPa immediately after the onset also echoes at a possibility of having convection over Northeast Bangladesh being triggered by uplifting the warm moist southwesterly air mass on convergence with this cold air mass before reaching Meghalaya Plateau as suggested by Kataoka and Satomura [2005].

4. Although the dry-line observed during this period is quite shallow due to its confinement only to the lower troposphere, we anticipate that it can still cause convective instabilities even at higher levels that may lead to the development of convective systems which can be blown eastward towards Northeast Bangladesh by the strong mid-upper tropospheric westerly jet present during this period.

Subjectively, we can not rule out the theory of katabatic wind converging with the strong warm moist low-level southwesterly winds to trigger the late night-early morning rainfall maximum since the prevailing low-level southwesterlies are blowing against the mountain breeze during the night and the fact that the heavy precipitation happens after midnight when the southwesterly nocturnal low-level wind blowing towards Meghalaya Plateau is also strongest.

5.3 Recommendations

The present study has been able to confirm some of the mechanisms triggering convection during the onset of the summer rains in Northeast Bangladesh. However, the study has left some unanswered questions and gaps, and thus points to the possible extensions of the results obtained. For example, ERA-interim reanalysis data used in the study is produced at a coarse resolution which cannot reproduce small-scale local features that may be at play during the early onset in Northeast Bangladesh, and the fact that it is only available at most in 6 hour's interval, hinders proper elucidation of the nature of the diurnal cycle over the study region. We therefore suggest a further look at some of the research findings, such as the nature of the diurnal cycle of precipitation, should be done using high resolution data

with short time intervals to fully explicate nature of the diurnal variation of precipitation over Northeast Bangladesh. Numerical modeling is also needed in the future to investigate the mechanisms influencing the late night-early morning rainfall maximum in relation to the local circulation (e.g., katabatic winds). Another interesting study in the future should be to investigate the possibilities of how the sea breeze circulations can influence/trigger convection in Northeast Bangladesh during the summer months. All in all, the findings of this study should be extended to numerical modeling to test the mechanisms influencing summer rains over Northeast Bangladesh.

Appendix A

Winds at 200 hPa

The winds at 200 hPa level show a strong westerly flow across the entire domain prior to and after the onset of the summer rains, Figure A.1.

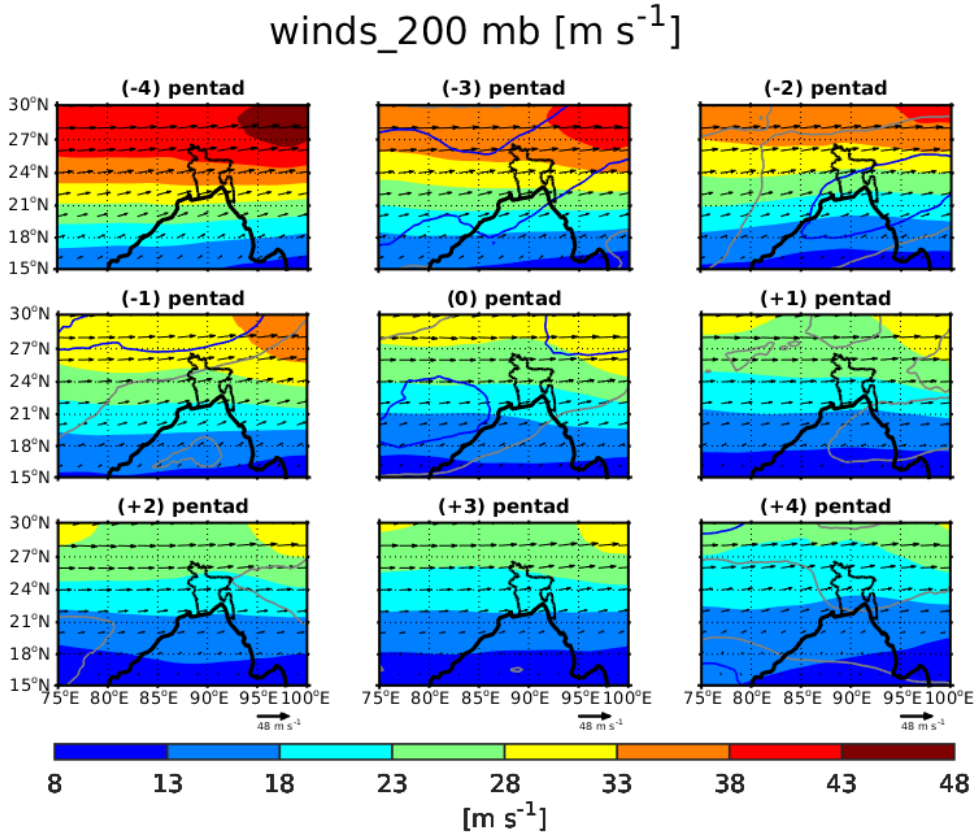

Figure A.1: Winds at 200 hPa level with wind speed overlap. The red contour, blue contours and the grey contours show 0-25%, 25-50%, and 50-75% overlap of the PDFs with the neighbouring pentads at the same grid points, respectively.

Appendix B

Winds at PV2000 level

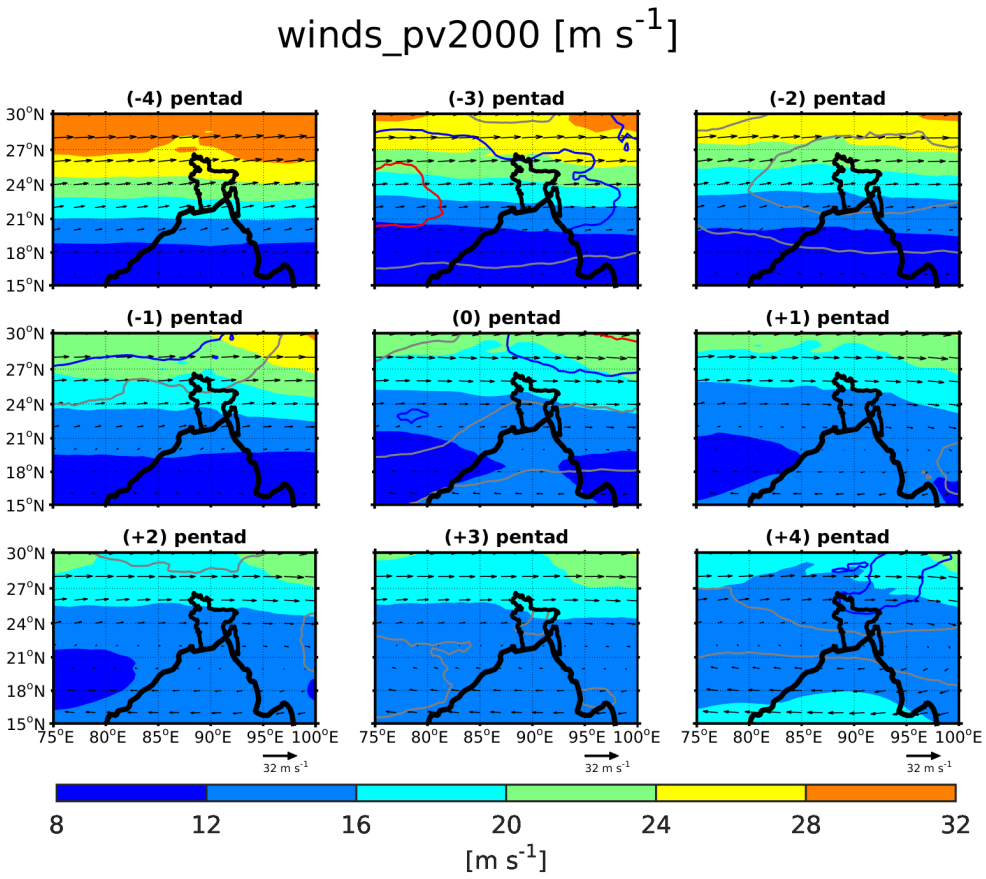

Figure B.1: Lead-lag composites for winds at PV2000 level with wind speed overlap. The red contour, blue contours and the grey contours show 0-25%, 25-50%, and 50-75% overlap of the PDFs with the neighbouring pentads at the same grid points, respectively.

The winds at PV2000 surface (Figure B.1) show a westerly flow of winds across the entire domain. The winds at this level show a clear transition towards the onset and after the onset in Northeast Bangladesh. The shift from strong westerly winds of 24 ms^{-1} to less than 16 ms^{-1} signifies the shift of the tropospheric jet stream.

Appendix C

The Clausius-Clapeyron Equation

The Clausius-Clapeyron equation is used to describe the relationship between saturation vapour pressure (e_s) and temperature (T).

The Clausius–Clapeyron equation is given below as stated by Markowski and Richardson [2010];

$$\frac{de_s}{dT} = \frac{L_v(T)e_s}{R_v T^2} \tag{C.1}$$

where ;

$L_v(T)$ is the specific latent heat of vaporisation, which is a function of temperature (T); L_v = 2.50 x 10^6 J/kg at 0°C, and R_v is the gas constant of water vapour; R_v = 8.314 J/Kmol.

Rearranging the above equation yields;

$$\frac{de_s}{e_s} = \frac{L_v(T)}{R_v}\frac{dT}{T^2} \tag{C.2}$$

Eq.C.2 implies that lowering (increasing) temperature reduces (increases) saturation vapour pressure, respectively.

Bibliography

Adamson, G. C. and Nash, D. J. (2013). Long-term variability in the date of monsoon onset over western india. *Clim. Dyn.*, 40(11-12):2589–2603.

Ahmed, R. and Kim, I.-K. (2003). Patterns of daily rainfall in bangladesh during the summer monsoon season: case studies at three stations. *Phys. Geogr.*, 24(4):295–318.

Alestalo, M. (1983). The atmospheric water vapour budget over europe. In *Variations in the global water budget*, pages 67–79. Springer.

Allcock, M. M. and Ackerley, D. (2015). Representing the australian heat low in a gcm using different surface and cloud schemes. *Adv. Meteorol.*, 2016.

Alonso, S., Portela, A., and Ramis, C. (1994). First considerations on the structure and development of the iberian thermal low-pressure system. In *Annales Geophysicae*, volume 12, pages 457–468. Springer.

Ashfaq, M., Shi, Y., Tung, W.-w., Trapp, R. J., Gao, X., Pal, J. S., and Diffenbaugh, N. S. (2009). Suppression of south asian summer monsoon precipitation in the 21st century. *Geophys. Res. Lett.*, 36(1).

Basu, B. (2007). Diurnal variation in precipitation over india during the summer monsoon season: observed and model predicted. *Mon. Wea. Rev.*, 135(6):2155–2167.

Berrisford, P., Dee, D., Poli, P., Brugge, R., Fielding, K., Fuentes, M., Kallberg, P., Kobayashi, S., Uppala, S., and Simmons, A. (2011). The era-interim archive version 2.0, era report series 1, ecmwf, shinfield park. *Reading, UK*, 13177.

Boer, G. (1986). A comparison of mass and energy budgets from two fgge datasets and a gcm. *Mon. Wea. Rev.*, 114(5):885–902.

Boer, G. and Sargent, N. E. (1985). Vertically integrated budgets of mass and energy for the globe. *J. Atmos. Sci*, 42(15):1592–1613.

Corfidi, S. F. (2003). Cold pools and mcs propagation: Forecasting the motion of downwind-developing mcss. *Weather and forecasting*, 18(6):997–1017.

Dee, D., Uppala, S., Simmons, A., Berrisford, P., Poli, P., Kobayashi, S., Andrae, U., Balmaseda, M., Balsamo, G., Bauer, P., et al. (2011). The era-interim reanalysis: Configuration and performance of the data assimilation system. *Q. J. R. Meteorol. Soc.*, 137(656):553–597.

Fujinami, H., Yasunari, T., and Morimoto, A. (2014). Dynamics of distinct intraseasonal oscillation in summer monsoon rainfall over the meghalaya–bangladesh–western myanmar region: covariability between the tropics and mid-latitudes. *Clim. Dyn.*, 43(7-8):2147–2166.

Gadgil, S. (2003). The indian monsoon and its variability. *Ann. Rev. Earth Planet. Sci.*, 31(1):429–467.

Ghosh, A., Lohar, D., and Das, J. (2008). Initiation of nor'wester in relation to mid-upper and low-level water vapor patterns on meteosat-5 images. *Atmos. Res.*, 87(2):116–135.

Hahn, D. G. and Manabe, S. (1975). The role of mountains in the south asian monsoon circulation. *J. Atmos. Sci.*, 32(8):1515–1541.

Hatsuzuka, D., Yasunari, T., and Fujinami, H. (2014). Characteristics of low pressure systems associated with intraseasonal oscillation of rainfall over bangladesh during boreal summer. *Mon. Wea. Rev.*, 142(12):4758–4774.

He, H., McGinnis, J. W., Song, Z., and Yanai, M. (1987). Onset of the asian summer monsoon in 1979 and the effect of the tibetan plateau. *Mon. Wea. Rev.*, 115(9):1966–1995.

Islam, M. N. and Uyeda, H. (2007). Use of trmm in determining the climatic characteristics of rainfall over bangladesh. *Remote Sens. Environ.*, 108(3):264–276.

Islam, N. and Uyeda, H. (2005). Comparison of trmm 3b42 products with surface rainfall over bangladesh. In *IGARSS*, pages 4112–4115.

Islam, S. (2003). *Banglapedia: National Encyclopedia of Bangladesh*. Number v. 2. Asiatic Society of Bangladesh.

Kataoka, A. and Satomura, T. (2005). Numerical simulation on the diurnal variation of precipitation over northeastern bangladesh: A case study of an active period 14-21 june 1995. *Sola*, 1:205–208.

Kripalani, R., Inamdar, S., and Sontakke, N. (1996). Rainfall variability over bangladesh and nepal: Comparison and connections with features over india. *Int. J. Climatol.*, 16(6):689–703.

Kutzbach, J., Guetter, P., Ruddiman, W., and Prell, W. (1989). Sensitivity of climate to late cenozoic uplift in southern asia and the american west: Numerical experiments. *J. Geophys. Res.*, 94(D15):18393–18407.

Laken, B. A. and Čalogović, J. (2013). Composite analysis with monte carlo methods: an example with cosmic rays and clouds. *J. Space Weather and Space Climate*, 3:A29.

Lau, K. and Yang, S. (1997). Climatology and interannual variability of the southeast asian summer monsoon. *Adv. Atmos. Sci.*, 14(2):141–162.

Lawrence, D. M. (1999). *Intraseasonal variability of the south Asian monsoon*. PhD thesis, University of Colorado.

Lefort, T. (2013). Dry-line, nor'westers and tornadic storms over east india and bangladesh: an operational perspective through synergie, the new imd forecaster's workstation. *Mausam*, 64:517–530.

Li, C. and Yanai, M. (1996). The onset and interannual variability of the asian summer monsoon in relation to land-sea thermal contrast. *J. Clim.*, 9(2):358–375.

Markowski, P. and Richardson, Y. (2010). *Mesoscale Meteorology in Midlatitudes*. Wiley-Blackwell.

Matsumoto, J. (1989). Synoptic features of heavy monsoon rainfall in 1987 related to the severe flood in bangladesh. *Japanese progress in climatology*, pages 35–48.

Matsumoto, J. (1997). Seasonal transition of summer rainy season over indochina and adjacent monsoon region. *Adv. Atmos. Sci*, 14:231–245.

Matsumoto, J. et al. (2007). Seasonal transition features of large-scale moisture transport in the asian-australian monsoon region. *Adv. AtmoS. Sci.*, 24(1):1–14.

Matsumoto, J., Rahman, M. R., Hayashi, T., and Monji, N. (1996). Rainfall distribution over the indian subcontinent during the 1987 and 1988 severe floods in bangladesh. *Japanese progress in climatology*, pages 34–53.

Murakami, T. and Matsumoto, J. (1994). Summer monsoon over the asian continent and western north pacific. *Japanese progress in climatology*, pages 3–29.

Murata, F., Terao, T., Hayashi, T., Asada, H., and Matsumoto, J. (2008). Relationship between atmospheric conditions at dhaka, bangladesh, and rainfall at cherrapunjee, india. *Nat. Hazards*, 44(3):399–410.

Murata, F., Terao, T., Kiguchi, M., Fukushima, A., Takahashi, K., Hayashi, T., Habib, A., BHUIYAN, S. H., and Choudhury, S. A. (2011). Daytime thermodynamic and airflow structures over northeast bangladesh during the pre-monsoon season: a case study on 25 april 2010. *J. Meteor. Soc. Japan*, 89:167–179.

Ogwang, B., Guirong, T., and Haishan, C. (2012). Diagnosis of september-november drought and the associated circulation anomalies over uganda. *Pakistan J. Meteor. Vol*, 9(17).

Ohsawa, T., Hayashi, T., Mitsuta, Y., and Matsumoto, J. (2000). Intraseasonal variation of monsoon activities associated with the rainfall over bangladesh during the 1995 summer monsoon season. *J. Geophys. Res.*, 105(D24):29445–29459.

Ohsawa, T., Ueda, H., Hayashi, T., Watanabe, A., and Matsumoto, J. (2001). Diurnal variations of convective activity and rainfall in tropical asia. *J. Meteor. Soc. Japan*, 79(1B):333–352.

Okoola, R. E. (1999). A diagnostic study of the eastern africa monsoon circulation during the northern hemisphere spring season. *Int. J. Climatol.*, 19(2):143–168.

Pant, G. B. and Kumar, K. R. (1997). *Climates of south Asia*. John Wiley & Sons.

Peixoto, J. P. (1973). *Atmospheric vapour flux computations for hydrological purposes*. Number 20. Secretariat of the World Meteorological Organization.

Peixoto, J. P. and Oort, A. H. (1992). Physics of climate.

Prasad, B. (1974). Diurnal variation of rainfall in brahmaputra valley. *Indian J. Meteor. and Geophys.*, 25(2).

Rácz, Z. and Smith, R. K. (1999). The dynamics of heat lows. *Quart. J. Roy. Meteor. Soc.*, 125(553):225–252.

Rafiuddin, M., Uyeda, H., and Islam, M. N. (2010). Characteristics of monsoon precipitation systems in and around bangladesh. *Int. J. Climatol.*, 30(7):1042–1055.

Rafiuddin, M., Uyeda, H., and Kato, M. (2013). Development of an arc-shaped precipitation system during the pre-monsoon period in bangladesh. *Meteorol. Atmos. Phys.*, 120(3-4):165–176.

Ramage, c. s. (1971). *Monsoon Meteorology*. Academic Press.

Ramage, C. S. (1995). Forecasters guide to tropical meteorology. aws tr 240 updated. Technical report, DTIC Document.

Reeve, M. A. (2014). *Monsoon Onset in Bangladesh: Reconciling scientific and societal perspectives*. PhD thesis, University of Bergen, Norway.

Reeve, M. A. and Kolstad, E. W. (2011). The spitsbergen south cape tip jet. *Quart. J. R. Meteor. Soc.*, 137(660):1739–1748.

Ruddiman, W. and Kutzbach, J. (1989). Forcing of late cenozoic northern hemisphere climate by plateau uplift in southern asia and the american west. *J. Geophys. Res.*, 94(D15):18409–18427.

Saeed, S., Müller, W. A., Hagemann, S., Jacob, D., Mujumdar, M., and Krishnan, R. (2011). Precipitation variability over the south asian monsoon heat low and associated teleconnections. *Geophys. Res. Lett.*, 38(8).

Sanderson, M. and Ahmed, R. (1979). Pre-monsoon rainfall and its variability in bangladesh: a trend surface analysis/chute des pluis de la pré-mousson et sa variabilité au bangladesh: Tendance d'analyse en superficie. *Hydrol. Sci. J.*, 24(3):277–287.

Sato, T. (2013). Mechanism of orographic precipitation around the meghalaya plateau associated with intraseasonal oscillation and the diurnal cycle. *Mon. Wea. Rev.*, 141(7):2451–2466.

Shahid, S. (2010). Rainfall variability and the trends of wet and dry periods in bangladesh. *Int. J. Climatol*, 30(15):2299–2313.

Simmonds, I., Bi, D., and Hope, P. (1999). Atmospheric water vapor flux and its association with rainfall overchina in summer. *J. Clim.*, 12(5):1353–1367.

Simpson, M., Warrior, H., Raman, S., Aswathanarayana, P., Mohanty, U., and Suresh, R. (2007). Sea-breeze-initiated rainfall over the east coast of india during the indian southwest monsoon. *Nat. Hazards*, 42(2):401–413.

Spengler, T., Reeder, M., and Smith, R. (2005). The dynamics of heat lows in simple background flows. *Quart. J. R. Meteor. Soc.*, 131(612):3147–3166.

Spengler, T. and Smith, R. K. (2008). The dynamics of heat lows over flat terrain. *Quart. J. R. Meteor. Soc.*, 134(637):2157–2172.

Stiller-Reeve, M. A., Spengler, T., and Chu, P.-S. (2014). Testing a flexible method to reduce false monsoon onsets. *PloS one*, 9(8):e104386.

Stiller-Reeve, M. A., Syed, M. A., Spengler, T., Spinney, J. A., and Hossain, R. (2015). Complementing scientific monsoon definitions with social perception in bangladesh. *Bull. Amer. Meteor. Soc.*, 96(1):49–57.

Strong, G., Proctor, B., Wang, M., Soulis, E., Smith, C., Seglenieks, F., and Snelgrove, K. (2002). Closing the mackenzie basin water budget, water years 1994/95 to 1996/97. *Atmosphere-Ocean*, 40(2):113–124.

Terao, T., Islam, M., Hayashi, T., Oka, T., et al. (2006). Nocturnal jet and its effects on early morning rainfall peak over northeastern bangladesh during the summer monsoon season. *Geophys. Res. lett.*, 33(18).

Terao, T., Islam, M. N., Murata, F., and Hayashi, T. (2008). High temporal and spatial resolution observations of meso-scale features of pre-and mature summer monsoon cloud systems over bangladesh. *Nat. Hazards*, 44(3):341–351.

Trenberth, K. E. (1991). Climate diagnostics from global analyses: Conservation of mass in ecmwf analyses. *J. Clim.*, 4(7):707–722.

Trenberth, K. E. (2011). Changes in precipitation with climate change. *Clim. Res.*, 47(1):123.

Trenberth, K. E., Hurrell, J. W., and Stepaniak, D. P. (2006). The asian monsoon: global perspectives. In *The Asian Monsoon*, pages 67–87. Springer.

Trenberth, K. E., Stepaniak, D. P., and Caron, J. M. (2000). The global monsoon as seen through the divergent atmospheric circulation. *J. Clim.*, 13(22):3969–3993.

Turner, A. G. and Annamalai, H. (2012). Climate change and the south asian summer monsoon. *Nat. Clim. Chang.*, 2(8):587–595.

Wang, B. (2002). Rainy season of the asian-pacific summer monsoon*. *J. Clim.*, 15(4):386–398.

Wang, T., G. W. and Wan, R. (2008). Influences of the thermal and dynamical forcing of the tibetan plateau on the circulation over the asian monsoon region (in chinese). *Plateau Meteorol.*, 27:1–9.

Wang, T., Yang, S., Wen, Z., Wu, R., and Zhao, P. (2011). Variations of the winter india-burma trough and their links to climate anomalies over southern and eastern asia. *J. Geophys. Res.*, 116(D23).

Webster, P. J., Magana, V. O., Palmer, T., Shukla, J., Tomas, R., Yanai, M., and Yasunari, T. (1998). Monsoons: Processes, predictability, and the prospects for prediction. *J. Geophys. Res.*, 103(C7):14451–14510.

Weston, K. (1972). The dry-line of northern india and its role in cumulonimbus convection. *Quart. J. R. Meteor. Soc.*, 98(417):519–531.

Xie, S.-P., Xu, H., Saji, N., Wang, Y., and Liu, W. T. (2006). Role of narrow mountains in large-scale organization of asian monsoon convection*. *J. Clim.*, 19(14):3420–3429.

Xu, W., Zipser, E. J., and Liu, C. (2009). Rainfall characteristics and convective properties of mei-yu precipitation systems over south china, taiwan, and the south china sea. part i: Trmm observations. *Mon. Wea. Rev.*, 137(12):4261–4275.

Yanai, M. and Li, C. (1994). Mechanism of heating and the boundary layer over the tibetan plateau. *Mon. Wea. Rev.*, 122(2):305–323.

Zhang, S. and Wang, B. (2008). Global summer monsoon rainy seasons. *Int. J. Climatol.*, 28(12):1563–1578.

Zhang, Y., Li, T., Wang, B., and Wu, G. (2002). Onset of the summer monsoon over the indochina peninsula: Climatology and interannual variations*. *J. Clim.*, 15(22):3206–3221.

Zhang, Z., Chan, J. C., and Ding, Y. (2004). Characteristics, evolution and mechanisms of the summer monsoon onset over southeast asia. *Int. J. Climatol.*, 24(12):1461–1482.

Zheng, Q. and Liou, K.-N. (1986). Dynamic and thermodynamic influences of the tibetan plateau on the atmosphere in a general circulation model. *J. Atmos. Sci.*, 43(13):1340–1355.